

Organic Mixed Valence

Jihane Hankache and Oliver S. Wenger*

Institut für Anorganische Chemie, Georg-August-Universität Göttingen, Tammannstrasse 4, D-37077 Göttingen, Germany

CONTENTS

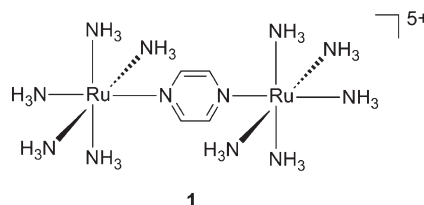
1. Introduction	5138
1.1. Scope of the Review	5138
1.2. General Introduction to Mixed Valence	5138
1.3. Brief Historical Survey of Organic Mixed Valence	5139
1.4. Survey over the Main Types of Organic Mixed Valence Systems	5141
2. Phenylenediamine Derivatives and Closely Related Systems	5143
3. Electronic Coupling in Covalent Systems: Importance of the Molecular Bridge between the Two Redox Centers	5146
3.1. Distance Dependence	5146
3.2. Influence of Bridge Structure, Connectivity, Topology, and Conformation	5154
3.3. Influence of the Bridge Redox States	5159
4. Multidimensional Organic Mixed Valence	5163
5. Intervalence Charge Transfer across Noncovalent Pathways	5167
6. Use of EPR Spectroscopy as a Direct Test for Hush Theory	5170
7. Solvent and Ion Pairing Effects	5171
8. Crystallographic Studies	5173
9. Concluding Remarks	5175
Author Information	5175
Biographies	5175
Acknowledgment	5176
References	5176

1. INTRODUCTION

1.1. Scope of the Review

Mixed valence is a phenomenon that many chemists spontaneously associate with coordination compounds. The prototype of a designed mixed valence species, the so-called Creutz–Taube ion (**1**, Chart 1),^{1,2} is indeed a coordination complex with an electronic structure that has been under debate for more than 30 years.³ By now, there exists a large body of literature on experimental and theoretical work, including several excellent reviews, on the subject of mixed valence in coordination complexes.^{3–11} By definition, mixed valence compounds contain an element which, at least formally, is present in more than one oxidation state. This element does not necessarily have to be

Chart 1



metallic; indeed, purely organic mixed valence compounds have been known since the early days of investigations in this research field.¹² In this paper, we review work that has been specifically geared at exploring the electronic structures of mixed valence compounds with purely organic redox sites.

1.2. General Introduction to Mixed Valence

The question of charge localization or delocalization is paramount in mixed valence chemistry. For one-electron mixed valence compounds comprised of two redox sites R connected by a bridging unit b, two extreme forms described by R^{n+} –b– $R^{(n+1)+}$ (complete localization), and $R^{(n+0.5)+}$ –b– $R^{(n+0.5)+}$ (full delocalization) as well as anything in between is possible.¹³ Robin and Day introduced a useful classification scheme for these different forms that has been generally adopted by the scientific community.¹⁴ Completely localized systems belong to class I, fully delocalized molecules are class III, and systems in between belong to class II. The transitions between these regimes are not abrupt, and an additional class of “almost delocalized” systems at the borderline between classes II and III has later been considered useful.^{3,6,15} Two key factors (and their interplay) determine to which class a mixed valence compound belongs, namely, the electronic coupling (H_{AB}) between the two redox sites, and the reorganization energy (λ) associated with electron transfer between them.¹⁶ In the extreme case of $H_{AB} = 0$ (Figure 1a), the odd electron may find itself in either one of two harmonic potential energy wells with equal force constants (corresponding to 2λ). On the dimensionless reaction coordinate X, which represents an antisymmetric combination of the R–b and solvent stretching vibrations, the equilibrium positions are at $X = 0$ and at $X = 1$. When $H_{AB} = 0$, the system belongs to class I, and vertical electronic transitions from one potential well to the other are not observed. The situation changes fundamentally when $H_{AB} \neq 0$, because mixing between the wave functions that define the two potential wells removes their degeneracy at $X = 0.5$. This gives rise to new adiabatic potential energy surfaces

Received: December 20, 2010

Published: May 16, 2011

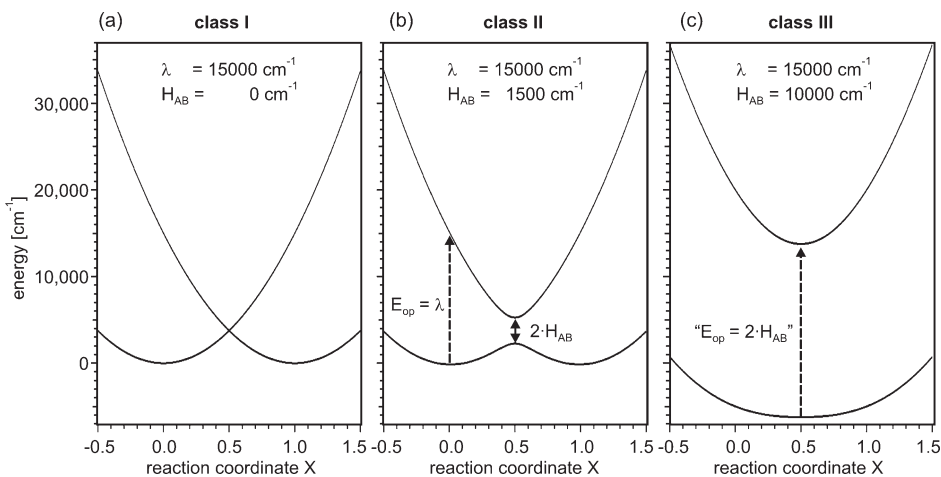


Figure 1. Potential energy surfaces for electron transfer in mixed valence systems with (a) negligible, (b) weak, and (c) strong electronic coupling (H_{AB}). λ is the total reorganization energy accompanying the electron transfer.

(Figure 1b) with their energy splitting at $X = 0.5$ corresponding to $2H_{AB}$. Vertical electronic transitions from the minimum of one potential well to a vibrationally excited state of the second potential energy surface are now possible. In the regime of relatively weak electronic coupling in which there are two clear minima in the lower potential well near $X = 0$ and $X = 1$ (class II), the Franck–Condon transitions occur to a steeply sloping region of the higher potential well, and hence, given a Gaussian distribution of energies in the ground-state centered near $X = 0$, nearly Gaussian shaped (and usually structureless) broad intervalence absorption bands are the result. In this case the energetic position of the intervalence absorption band maximum (E_{op}) corresponds to the total reorganization energy (λ). When $H_{AB} \geq 1/2\lambda$, there are no longer two minima in the lower potential energy well, but instead there occurs a single minimum at $X = 0.5$ (Figure 1c), and the limit of strong coupling (class III) is attained. In this case the resulting intervalence absorption band is comparatively narrow (and frequently exhibits vibrational fine structure) because it occurs to a weakly sloping region of the upper potential well. While the terms “intervalence transition” and “mixed valence” are also used for class III systems, the transitions in this limit do not involve net charge transfer, and the two redox centers have an averaged valence state. In the simple two-state model E_{op} now measures the magnitude of the electronic coupling. However, Nelsen and Zink pointed out that there is a serious problem with this picture:¹⁷ Fully delocalized systems are symmetrical, and hence their intervalence transition can be symmetry forbidden and vanishingly weak.^{18,19} The important conclusion from Nelsen’s and Zink’s work is that the two-state model cannot apply to the strong intervalence bands that are experimentally observable for many class III systems. Instead, a so-called neighboring orbital model was found to provide a significantly more accurate description of the electronic structure of fully delocalized systems.¹⁸

Even for class II systems, the use of more complicated theoretical models is frequently unavoidable. A three-state model represents an extension to the two-state model by including a third electronic state formed by charge transfer to or from the molecular bridge that connects the two redox centers.⁶ The mediating state “C” has its potential energy minimum at $X = 0.5$ above the intersection of the reactant (“A”) and product (“B”) diabatic states. In this case, bridge-mediated electronic coupling

is described by a superexchange formalism,^{7,20,21} and the overall electronic coupling (H_{AB}) becomes a function of the individual couplings between the redox sites and the bridge (H_{AC}, H_{CB}) and the vertical energy gap ($\Delta\varepsilon$) at $X = 0.5$ between the reactant/product intersection and the minimum of the bridge potential energy surface.^{22,23}

As far as the reorganization energy (λ) is concerned, a partitioning into inner- (λ_{in}) and outer-sphere (λ_{out}) contributions is useful.²⁴ λ_{in} represents the energy that is required for reorganization of bond lengths and angles in the course of the electron-transfer process, whereas λ_{out} quantifies the energy required for solvent reorganization. The solvent is frequently treated as a dielectric medium that has no specific interactions with the redox sites and the bridge.²⁵

More detailed descriptions of physical models describing the mixed valence phenomenon are found in several reviews on this subject.^{3,6–8}

1.3. Brief Historical Survey of Organic Mixed Valence

One of the earliest instances in which a purely organic compound was brought into connection with the concept of mixed valence was an investigation of the electrical conductivity of tetrathiafulvalene (TTF) and its one-electron oxidized form (TTF^+).²⁶ Initial investigations suggested that neutral TTF is a photoconducting molecule, but the photocurrent spectrum led to the conclusion that trace amounts of TTF^+ were responsible for this phenomenon. When neat TTF^+ was investigated in the form of its chloride salt (2, Chart 2), it was found to be an excellent organic semiconductor with a room-temperature resistivity that is 12 orders of magnitude below that of neutral TTF. Wudl and co-workers pointed out that this observation is similar to one previously made for a mixed valence biferrocenium picrate salt (3),²⁶ which has a room-temperature resistivity that is 4–6 orders of magnitude lower than that of charge-neutral ferrocene.²⁷ Yet, at that point, the issue of charge delocalization within a given TTF molecule was not further addressed and the two five-rings of the TTF^+ cation were simply designated as “oxidized half” and “reduced half”.²⁶ Only 1 year later, Cowan and co-workers pointed out in a review that TTF^+ may be considered a class III mixed valence compound.¹²

A comparative study of the flexibility of alkane and poly(ethylene glycol) chains represents a noteworthy early example

Chart 2

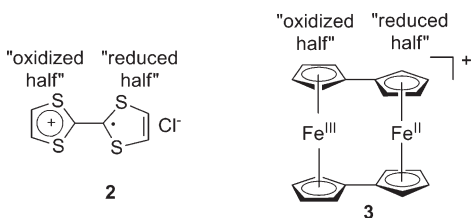


Chart 3

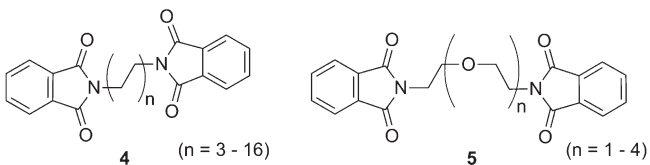
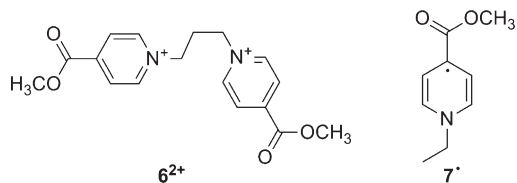


Chart 4



in which the dynamics of *thermal* intramolecular electron transfer between two organic moieties in different redox states was investigated by electron paramagnetic resonance (EPR) spectroscopy.²⁸ Depending on temperature and the chain length *n* of the flexible spacer between two phthalimide (PI) units in a series of PI-(CH₂)_{*n*}-PI (**4**, Chart 3) and PI-(CH₂CH₂-O)_{*n*}CH₂CH₂-PI (**5**) molecules, the one-electron reduced forms of these species either exhibited EPR spectra that were consistent with localization of the excess electron at one single PI unit or with electron delocalization over both PI redox centers.

Shortly after the Cowan review,¹² Kosower and Teuerstein reported on optically detected intramolecular electron transfer in an organic mixed valence compound that is structurally related to 4.²⁹ Their titration of the alkane-bridged bis(pyridinium) dication (6^{2+} , Chart 4) with a pyridinyl radical (7^\bullet) in acetonitrile solution led to the formation of a species that exhibited a weak ($\epsilon_{\max} \sim 1500 \text{ M}^{-1}\text{cm}^{-1}$) and broad absorption band peaking at 1360 nm. On the basis of a series of control experiments, this species was identified as a complex formed between the two pyridinium rings of 6^{2+} and a pyridinyl radical 7^\bullet sandwiched in between, and the near-infrared absorption band was termed “intervalence absorption”.²⁹ It was noted that similar near-infrared absorption bands had previously been observed for radical anions of tetracyanoquinodimethane (TCNQ). Indeed, the infrared spectrum of $\text{Et}_3\text{NH}^+\text{TCNQ}^-$ had been reported already in 1962 to exhibit a broad featureless band between 1000 and 1500 nm that was ascribed to an electronic rather than vibrational absorption.³⁰

An investigation of the one-electron reduced form of diketone 8 (Chart 5) represents one of the first studies that was specifically geared toward a detailed understanding of charge delocalization

in an organic mixed valence compound.³¹ The key question that Mazur and co-workers tackled is whether the molecular structure of the radical anion of **8** is best described by rapidly equilibrating species **8a**⁻ and **8b**⁻ or whether the fully symmetrical structure **8c**⁻ would be more appropriate. In other words, it was attempted to elucidate whether **8**⁻ belongs to class II or class III of the Robin–Day classification scheme,¹⁴ although this terminology was not used in this work. The intriguing experimental observation was that the infrared spectrum of **8**⁻ showed no evidence for the typical ketone ($\sim 1700 \text{ cm}^{-1}$) or ketyl ($\sim 1550 \text{ cm}^{-1}$) stretching modes but instead exhibited three intense infrared absorption bands at significantly lower frequencies, which were absent in a reference molecule (**9**) that basically corresponds to half of molecule **8**. Schroeder and Mazur pointed out that if **8**⁻ was merely a composite of noninteracting ketone and ketyl (**8a**⁻, **8b**⁻), then infrared absorptions at ~ 1700 and 1550 cm^{-1} would be expected.³² Conversely, for full charge delocalization (**8c**⁻) an infrared absorption at some intermediate frequency should result. The fact that the experimental infrared spectrum did not correspond to either of the two intuitive expectations was explained by low-energetic vibronic transitions that are not simply vibrational but contain some electronic contribution. A very detailed study including investigation of solvent and counterion effects finally lead to the conclusion that **8**⁻ is a weakly coupled system with an electronic coupling matrix element $H_{AB} = 450 \text{ cm}^{-1}$ in dimethyl sulfoxide.³²

An increasing interest in long-range electron transfer in the 1980s also stimulated investigations of charge delocalization between organic redox centers which are separated over distances that are considerably greater than the sum of their van der Waals radii.³³ One illustrative example is the radical anion of molecule **10** (Chart 6), which is comprised of two biphenyl units connected by a rigid spacer, separating these moieties by six C–C single bonds and holding them at an edge-to-edge distance larger than 7 Å.³⁴ The rate of intramolecular (thermal) electron transfer between the two biphenyl units of **10⁻** was found to exceed 10^7 s^{-1} in polar solvents, but for lower polarity solvents EPR experiments indicated slower rates. This observation was attributed to the formation of tight ion pairs in the less polar solvents. Thereby rapid electron movement is impeded, and the electron-transfer rate becomes governed by the rate for counter-ion migration.

These findings shed a new light on a prior study of charge delocalization in the syn- and anti-conformers of the radical anion **11⁻** (Chart 7). EPR spectroscopy indicated the simultaneous presence of spin-localized and spin-delocalized species in a mixture comprised of the two conformers.³⁵ The spin-localized species was originally thought to be the anti-conformer because the two biphenyls are somewhat further apart from each other than in the syn-conformer. The new study agreed with this assignment but offered a different explanation:³⁴ The radical anion of the anti-conformer may be a localized system because electron transfer between the two biphenyl units is associated with cation migration over a significantly greater distance than in the syn-conformer. The latter is U-shaped, and in the course of intramolecular electron transfer between the two biphenyls, the cation can always stay more or less in the middle of the cavity between them.

One of the first systematic investigations of the distance dependence of intervalence charge transfer in organic mixed valence compounds was made by Miller and co-workers using diquinone radical anions. In their initial studies,^{36,37} these researchers

Chart 5

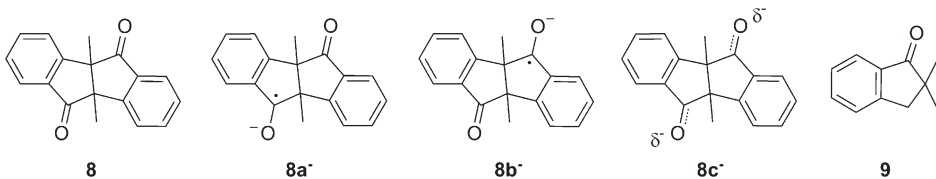


Chart 6

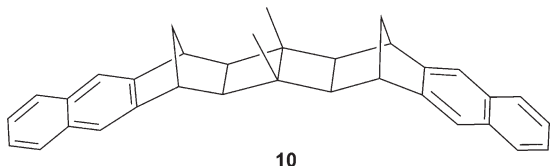
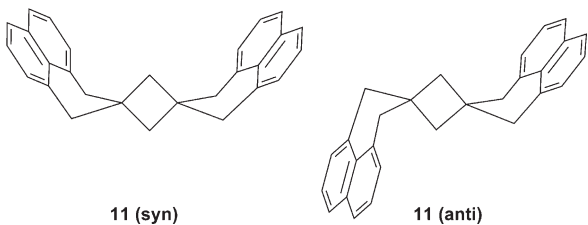


Chart 7



report on an unordinary near-infrared absorption band for the radical anion of molecule **12** (Chart 8).

Because neither monoquinone radical anions nor the neutral diquinone exhibited this long-wavelength band, it was concluded that diquinone radical anions, formally comprised of a quinone and a semiquinone site, can in fact be regarded as mixed valence species. Due to a lack of solvent dependence of the near-infrared absorption band, it was further concluded that **12**^{·-} belongs to Robin–Day class III, and infrared absorption experiments monitoring the carbonyl C–O stretching bands were in line with this assignment.³⁸ The radical anions of **13** and **14** did also exhibit near-infrared absorption bands, but when compared to that of **12**^{·-}, they were much broader, contained no vibrational fine structure, and occurred at longer wavelengths.³⁹ From this it was hypothesized that **13**^{·-} and **14**^{·-} adopt a mixed valence structure which tends to temporarily localize the anion radical on one quinone moiety.

Nelsen and co-workers aimed at a direct comparison of electron-transfer rates estimated on the basis of analyses of intervalence absorption bands (following Hush's theory)¹⁶ with the electron-transfer rates measured directly by EPR spectroscopy. It was noted that certain organic mixed valence compounds exhibit much slower electron-transfer rates than commonly observed for metal-based mixed valence systems, and hence the charge-transfer dynamics become measurable on an EPR time scale, while the electronic coupling between the two redox centers remains strong enough for uncomplicated detection of intervalence absorption bands.⁴⁰ The key to this favorable situation is the large inner-sphere reorganization energy (λ_{in}) associated with electron transfer in carefully selected organic mixed valence systems. Hydrazine redox units were identified as

particularly interesting in this respect since they undergo unusually large geometry changes upon electron loss. Oxidation of bis(hydrazine) molecule **15** (Chart 9) gives a mixed valence species that formally contains a paramagnetic (neutral) hydrazine unit and a diamagnetic (cationic) dinitrogen unit. Intramolecular charge transfer between these two moieties is associated with $\lambda_{\text{in}} = 45.8 \text{ kcal/mol}$,⁴¹ a value that is far larger than those reported for example for an organometallic bis(ferrocene) mixed valence compound (2.0 kcal/mol) or a mixed valence diruthenium complex (4.7 kcal/mol).

1.4. Survey over the Main Types of Organic Mixed Valence Systems

The foregoing brief historical review introduced already several different types of purely organic mixed valence compounds, but with the exception of the exemplary system from Nelsen (**15**⁺), the molecules presented so far do not belong to the most thoroughly investigated families of such compounds. The most popular redox active centers in organic mixed valence compounds in recent years are tertiary amines, particularly para-substituted triarylamines. This is largely due to the stability of their radical cation forms and the synthetic possibilities that resulted from relatively recent developments in palladium-catalyzed N–C coupling reactions. There exists a fairly large body of literature on systems of the general type described by molecular structure **16** (Chart 10) in which the substituent R is usually either a methoxyl or methyl group. Many specific examples of this type will be described in the following sections of this review. An important subgroup of organic mixed valence species based on tertiary amines are radical cations of *p*-phenylenediamines (**17**) in which the two nitrogen centers are particularly close to one another. The question of charge localization and delocalization in these systems has received much attention in several alkyl- and aryl-substituted molecules, but the radical cation of *N,N,N',N'*-tetramethyl-*p*-phenylenediamine (TMPD) is the most thoroughly studied example. TMPD⁺ is the prototype of a fully delocalized (class III) organic mixed valence species,⁴² and it will serve as an exemplary system on which some of the basic principles of organic mixed valence chemistry will be illustrated in the next chapter.

The *p*-phenylene bridge motif plays an important role in a variety of different types of organic mixed valence compounds. It is a good coupling unit not only between amino groups but also for many other functional groups that lead to redox active compounds. One important example is *p*-dinitrobenzene (**18**, Chart 11), the radical anion of which is the prototype for a series of dinitro compounds that qualify as organic mixed valence species and that have received significant attention in recent years.⁴³ In terms of stability, the reduced dinitro compounds are substantially less well behaved than oxidized diamines and hence represent a much less popular choice for investigations of organic mixed valence. More exotic examples of *p*-phenylene bridged

Chart 8

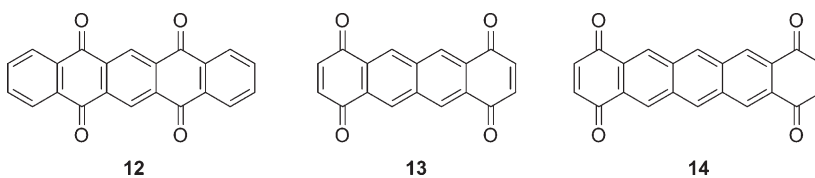


Chart 9

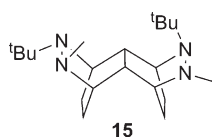
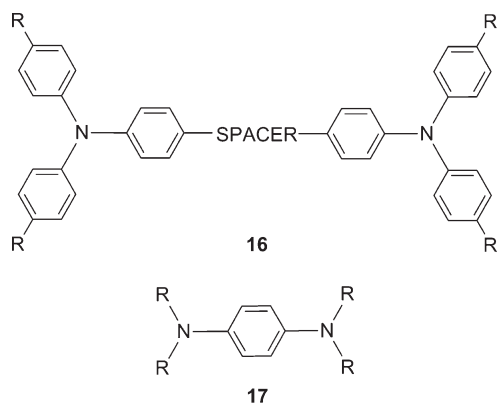


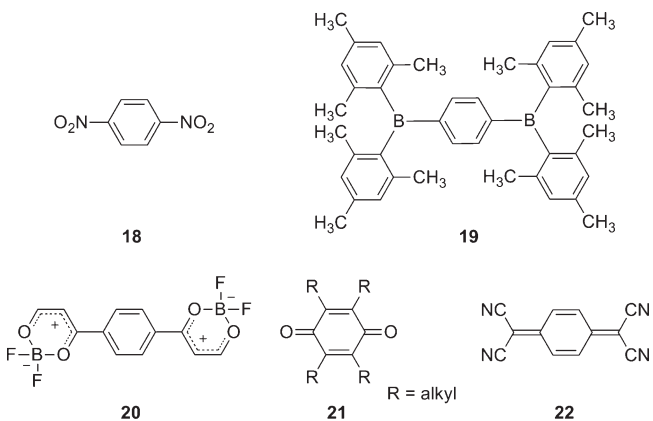
Chart 10



systems are diboranes (19) or bis(dioxaborines) (20).^{44–46} Kaim and Schulz found that *p*-phenylenediboranes are essentially mirror images of *p*-phenylenediamines in that the strongly electron accepting boryl groups represent counterparts to the strongly electron donating amino groups.⁴⁴

The charge-neutral forms of molecules 17–20 are benzenoid; that is, they are para-disubstituted benzene derivatives with single bonds between the 1,4-carbons and their substituents. In their radical ion forms, however, they adopt quinonoid electronic structures in which the bonds between the 1,4-carbons and their substituents adopt some double bond character. Similar quinonoid radical ion structures are accessible upon reduction of *p*-benzoquinone (21) and tetracyanoquinodimethane (22), which represent the prototypes for two other prominent classes of organic mixed valence compounds.^{47,48} Indeed, the close electronic relationship between *p*-phenylenediamine radical cations and quinone radical anions was pointed out already more than 85 years ago.⁴⁹ Due to their instability in air, the quinone radical anions are considerably more difficult to handle experimentally than intervalence radical cations. The stability is markedly increased for quinones that are alkyl-substituted in the ortho position to the carbonyl functional group, and a variety of such alkylated quinone radical anions with bridges much longer than a single benzene unit have been investigated in recent years.⁴⁷ This family of systems is structurally markedly different from the diquinone molecules (12–14) studied in the early work by Miller and co-workers.^{36,37,39,50}

Chart 11



Polychlorinated triphenylmethyl radicals typically have high thermal and chemical stability and therefore have received considerable attention in the context of organic mixed valence.⁵¹ Steric reasons demand for a bridging unit somewhat larger than *p*-phenylene in order to obtain significant electronic coupling between two such centers; an all-trans *p*-divinylbenzene bridge leads to the prototype system (23, Chart 12) for this class of compounds. Combination of polychlorinated triphenylmethyl redox centers with tertiary amines has recently allowed the preparation of charge-neutral organic mixed valence compounds, the prototype of which is represented by molecule 24.⁵² The vast majority of organic mixed valence systems are charged species, a fact that often severely limits their solubility in less polar solvents. The recent development of neutral mixed valence compounds like 24 is therefore particularly valuable for investigations of the solvent dependence of intervalence transitions. Unchlorinated triphenylmethyl radicals and their anions are substantially less stable than their chlorinated counterparts and consequently have received relatively little attention in mixed valence chemistry.⁵³

Given the important role played by methylviologen and its numerous derivatives in bimolecular electron-transfer chemistry, there are surprisingly few studies that specifically aimed at a detailed understanding of the mixed valence electronic structure of the one-electron reduced forms of such compounds. Methylviologen radical monocation itself is a fully delocalized mixed valence system,^{54,55} and also the half-reduced forms of a series of so-called extended viologens (25^+ , Chart 13) were found to be class III mixed valence molecules.⁵⁶ In light of the increasing interest in diimide electron acceptors,⁵⁷ it is also somewhat surprising to note that there are comparatively few studies that discuss the radical monoanions of these species as mixed valence systems.^{50,58}

Bis(tetrathiafulvalene) compounds represent a last important family of organic mixed valence systems that is to be mentioned

Chart 12

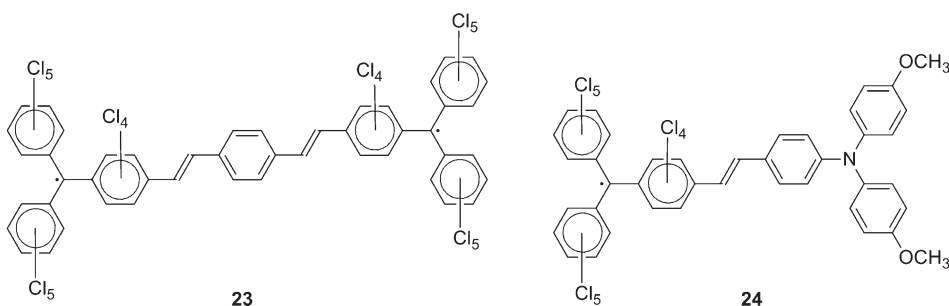
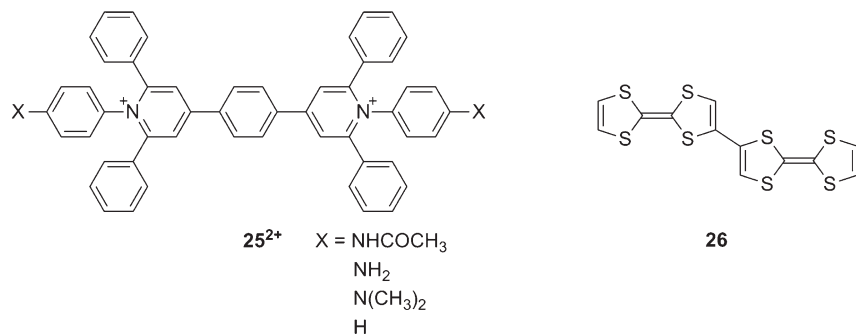


Chart 13

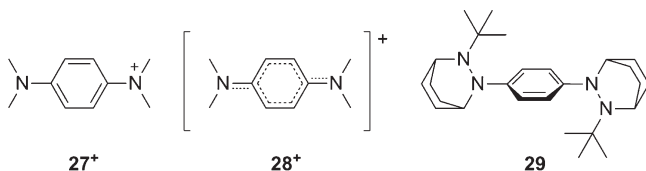


in this Introduction. As discussed in section 1.3, the tetrathiafulvalene radical cation itself can be considered a class III mixed valence system, but when two TTF units are connected to one another, new mixed valence phenomena arise as a consequence of electronic interactions between the two TTF redox centers.⁵⁹ The prototype given here is the radical cation of molecule **26**,³ but there exists a fairly broad variety of bis(tetrathiafulvalene) compounds that are rather badly represented by this particular molecular structure. This includes for example fused TTFs in which the two TTF moieties are connected by a planar conjugated π -system.⁵⁹ Mixed valence systems from this family of compounds were already part of a comprehensive review on bis(tetrathiafulvalene) molecules.⁶⁰

2. PHENYLEDIAMINE DERIVATIVES AND CLOSELY RELATED SYSTEMS

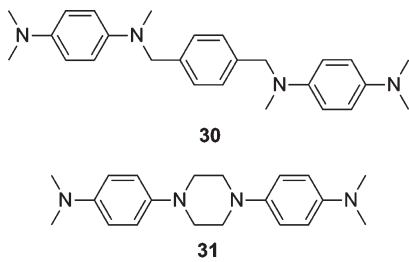
Derivatives of *p*-phenylenediamine were the first organic radical cations ever isolated.⁶¹ Wurster prepared the blue TMPD⁺ in 1879,⁶² and Weitz recognized its true chemical nature in 1928, designating it “Kationradikal”.⁶³ In early applications of electron-transfer theory to organic compounds the TMPD⁺ molecule played an eminent role, and the rate for electron self-exchange between TMPD and TMPD⁺ was one of the first measured.⁶⁴ In principle, two extreme cases of different electronic structures are conceivable for TMPD⁺, namely, a structure (**27**⁺, Chart 14) with one planar dimethylamino group that bears the positive charge, while the other dimethylamino group is neutral and has pyramidal geometry, and, as an alternative, a structure (**28**⁺) which has equivalent nitrogen atoms and charge delocalized over the eight atom π system, corresponding to a class III system according to Robin and Day.⁴² In structure **27**⁺ the positive

Chart 14



charge is localized, but a rapid intramolecular electron transfer could interchange the role of the two nitrogens, in which case TMPD⁺ would be a class II mixed valence system. Spectroscopic,^{42,43,65} structural,⁶⁶ and theoretical studies^{43,67} are consistent with TMPD⁺ being a completely delocalized class III system; i.e., structure **28**⁺ represents a reasonable description of this organic radical cation. One of the spectroscopic arguments to assign it to class III comes from the observation of vibrational fine structure in the intervalence absorption band.^{43,68} Generally, vibrational fine structure in an optical absorption spectrum occurs when a Franck–Condon transition results in a wavepacket on the excited-state surface that can return to its origin within about a picosecond.⁶⁹ This is only possible when the excited-state surface has its minimum near the equilibrium geometry of the ground state, a situation that is encountered exclusively for class III intervalence compounds (Figure 1c).⁷⁰ A balance of reorganization and delocalization energies is decisive for the fully delocalized electronic structure of TMPD⁺: Formation of structure **27**⁺ requires a geometry change from pyramidal to planar at one single nitrogen center, whereas in structure **28**⁺ both nitrogens have to be reorganized while at the same time delocalization energy is gained. Obviously, for TMPD⁺ this energy gain outweighs the price to be paid by reorganizing two (instead of one) nitrogen centers.⁴²

Chart 15

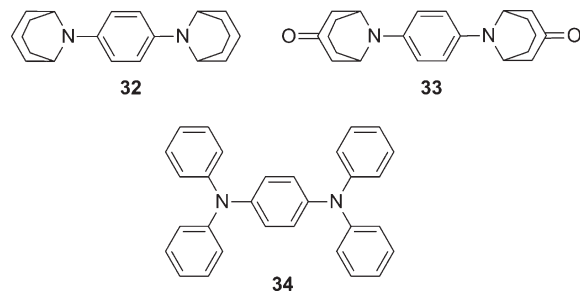


Nelsen and co-workers have demonstrated that upon increase of the reorganization energy in a bis(hydrazine) analogue of TMPD^+ (29^+) the situation changes, and a charge-localized radical cation structure becomes energetically more favorable.⁴² While the room-temperature EPR spectrum of 29^+ exhibits the nine-line pattern expected for four equivalent nitrogens in a fully delocalized electronic structure, a five-line pattern indicative of spin localization was observed at -105°C . The intervalence charge-transfer band is solvent dependent, consistent with class II behavior, and a reorganization energy (λ) of ~ 38 kcal/mol was estimated from the energetic position of the intervalence band maximum. This compares to a reorganization energy of ~ 30 kcal/mol for TMPD^+ .⁷¹ Thus, the 27% increase in λ when going from 28^+ to 29^+ is associated with a transition from a charge-delocalized to a charge-localized electronic structure. The reason for the large reorganization energy associated with electron transfer in 29^+ becomes evident from its X-ray crystal structure, which reveals that very large structural changes are associated with oxidation/reduction chemistry of the hydrazine units.⁴² In 29^+BPh_4^- , the formally charge-neutral hydrazine unit has a nitrogen–nitrogen distance of 1.454 Å, while in its oxidized counterpart the distance between the two nitrogens is only 1.359 Å. Moreover, there are important differences in the twist angles between the phenyl plane and the neutral and oxidized hydrazine units. This latter fact also accounts for the large difference in electronic coupling matrix elements between 28^+ ($H_{AB} \approx 23.3$ kcal/mol) and 29^+ ($H_{AB} \approx 5.8$ kcal/mol).

As becomes obvious from this discussion, accurate estimates of the reorganization energies are important for proper understanding of the electronic structures of mixed valence compounds. Grampp and Jaenicke attempted to determine λ for electron self-exchange between TMPD and TMPD^+ through EPR line broadening experiments.⁷² By this method, estimates of λ are only available by making a number of assumptions, and therefore it was deemed desirable to determine λ directly by observing the intervalence band associated with electron transfer from a neutral TMPD unit to a TMPD^+ cation in a molecule that links the two moieties together covalently. Molecules 30 (Chart 15) and 31 were made for this purpose, but an intervalence absorption band could only be detected for 31⁺.⁷¹ This is because the intensity of the intervalence absorption is proportional to H_{AB}^2 , and H_{AB} must be significantly smaller in 30⁺ than in 31⁺ due to the larger distance between the two individual phenylenediamine units (7 versus 3 σ -bonds between the closest N atoms). Analysis of the intervalence absorption band of 31⁺ produced $\lambda \approx 30$ kcal/mol, a value that is far larger than that obtained from prior EPR studies of $\text{TMPD}/\text{TMPD}^+$ self-exchange.

Replacement of the methyl groups of TMPD^+ by other alkyl or aryl substituents was found to have a nonnegligible impact on

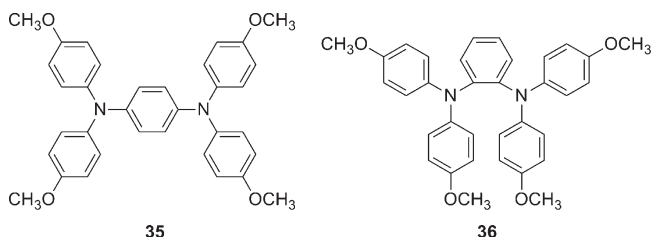
Chart 16



the energetic position of the intervalence absorption band (E_{op}), which is a direct measure for the electronic coupling in class III systems (Figure 1c).⁶⁵ For TMPD^+ , $E_{op} = 46.6$ kcal/mol, whereas for 32^+ (Chart 16) and 33^+ the E_{op} -values are 45.5 and 46.2 kcal/mol. The bicyclooctyl substituents of 32^+ permit somewhat more effective delocalization of the partially oxidized nitrogen p lone pairs than the methyl groups of TMPD^+ ; hence, E_{op} decreases by 1.1 kcal/mol. On the other hand, γ -keto substitution of the bicyclooctyl rings in 33^+ decreases their ability to stabilize the positive charge, and this results in an E_{op} -value practically on par with that of TMPD^+ . While these changes in E_{op} are relatively minor, the radical cation of N,N,N',N' -tetraphenyl-p-phenylenediamine (TPPD⁺, 34⁺) yields $E_{op} = 34.7$ kcal/mol.⁶⁵ Thus, quite rightfully it has been asked how delocalized the electronic structure of the TPPD⁺ radical cation might be.⁷³

TPPD⁺ has been crystallized as a hexachloroantimonate salt, and X-ray structure analysis indicates that the TPPD⁺ cation is centrosymmetric, exhibits a quinoidal distortion, and has aryl rings arranged in propeller form around the nitrogen centers.⁷³ All of these structural features can be reproduced by density functional theory (DFT) calculations, yet assignment of TPPD⁺ to class III based only on these grounds is not justified for several reasons: The crystallographic symmetry might be due to static or dynamic disorder of molecules that are actually slightly asymmetric, and the gas-phase calculations are only of limited relevance to solution where solvent and counterions may introduce a certain degree of asymmetry. Therefore, a detailed optical spectroscopic and vibrational study of TPPD⁺ was undertaken.⁷³ Unfortunately, the selection rules for IR and Raman vibrations in microsymmetries corresponding to localized or delocalized structures of the central p-phenylenediamine unit of TPPD⁺ are similar, and hence the comparison of infrared and Raman spectra alone was not particularly insightful. Yet, from the fact that solution and solid-state IR spectra are very similar to one another, in conjunction with the determination of a centrosymmetric crystal structure and an excellent agreement of experimental vibrational spectra with those calculated for a delocalized structure, TPPD⁺ was finally assigned to class III. Resonance Raman spectroscopy revealed that no less than eight vibrational modes are strongly coupled to the intervalence band, indicating that the charge-transfer excited-state potential energy surface is displaced along a multitude of normal coordinates relative to the ground-state potential energy surface. Application of time-dependent theory⁶⁹ allowed determination of the dimensionless (Huang–Rhys) displacement parameters for the individual resonance enhanced vibrational modes. Particularly large Huang–Rhys factors were found for a symmetrical N–aryl–N stretch as well as twisting and wagging motions of the phenyl groups. All of

Chart 17

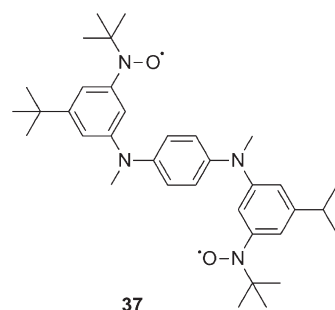


these are modes involving important distortions of the axial C–N bonds. From a fit of the resonance Raman and optical absorption cross-sections it was possible to estimate the inner- (λ_{in}) and outer-sphere (λ_{out}) reorganization energies, the sum of which (3480 cm^{-1}) compares favorably to the total reorganization energy obtained from application of Hush theory to the intervalence absorption band (4080 cm^{-1}). The finding of a λ_{out} -value almost five times smaller than λ_{in} is in line with a small influence of the solvent on the intramolecular charge-transfer process and consequently supports the assignment of TPPD^+ to Robin–Day class III.

The tetraalkyl-*p*-phenylenediamine radical cation 33^+ has been subjected to similarly detailed investigations by resonance Raman spectroscopy and analyses by time-dependent theory of electronic transitions.⁷⁴ Contrary to that of 34^+ , the intervalence absorption band of 33^+ exhibits vibrational fine structure, featuring a vibrational progression in a mode with a frequency of 1324 cm^{-1} . However, such a mode is absent in the resonance Raman spectrum of 33^+ . Instead, nine modes with other frequencies are found to be resonance enhanced. The atomic motions associated with these nine modes were identified by using Gaussian 98 calculations, and it was found that the most resonance-enhanced mode is the symmetric aromatic C–C and C–N stretch at 1620 cm^{-1} leading to a quinonoid distortion of the molecule. The vibrational mode leading to the largest Huang–Rhys factor is an out-of-plane $\text{R}_2\text{N}-\text{aryl}-\text{NR}_2$ bend (405 cm^{-1}) involving a large amplitude phenyl ring tilt. The absence of a 1324 cm^{-1} mode corresponding to the vibrational progression in the intervalence absorption spectrum was attributed to the missing-mode effect (MIME), which is not an uncommon phenomenon for large molecules.⁷⁵ Analysis in terms of the time-dependent picture of electronic transitions gave an almost perfect fit to the experimental absorption spectrum⁷⁵ and led to the conclusion that 33^+ is a true class III system.

The radical cation of *N,N,N',N'*-tetraanisyl-*p*-phenylenediamine (TAPD⁺, 35^+ , Chart 17) differs from TPPD^+ (34^+) only in the presence of additional methoxyl groups in the para positions of the aryl substituents. In general, this prevents electrochemical dimerization upon oxidation of tertiary amines and hence ensures reversible oxidation.⁷⁶ There have been two independent studies of the electronic structure of TAPD⁺.^{77,78} The outcome of the experimental and theoretical work by Lambert and Nöll is that the electronic spectrum of 35^+ can be interpreted adequately in terms of a localized (class II) structure just at the border to class III.⁷⁷ Brédas and co-workers reinterpreted their results in the framework of a dynamic vibronic model and arrived also at the conclusion that 35^+ is at the borderline of class II and class III.⁷⁸ An important point that emerged from this vibronic coupling analysis is that the shape of the intervalence charge-transfer band alone does not necessarily provide a good indication whether a mixed valence system

Chart 18



belongs to class II or class III.⁷⁸ If there are strong interactions with symmetric vibrations, the shape of the intervalence band can be broad and unstructured even in the case of class III systems, a fact that has also been noted by Nelsen.¹⁵ Thus, even though the intervalence band of 35^+ is broad and unstructured, unlike those of 32^+ or 33^+ , it is still close to being a class III system. Particularly noteworthy in this context is the fact that Lambert and Nöll found the intervalence band of 35^+ to be strongly asymmetric.⁷⁷ Gaussian fits to the experimental spectrum are poor due to a cutoff on the low-energy side, as predicted by theory for systems that are close to the class II/class III borderline.¹⁵ Because strong electronic couplings usually give rise to rates for electron transfer (k_{ET}) that are much faster than what can be measured by magnetic resonance techniques ($k_{\text{ET}} \propto H_{\text{AB}}^2$),²⁴ the possibility of obtaining experimental values for electronic couplings from photoelectron spectroscopy was explored.⁷⁹ Work on 27^+ , 35^+ , and four other bis(triarylamine) radical cations demonstrated the feasibility of this approach to obtaining experimental values for H_{AB} that can be used to verify those extracted from intervalence absorption band analysis.⁷⁹

A study of the ortho-isomer of TAPD⁺ (36^+) led to the same classification as that for 35^+ .⁸⁰ The electronic coupling matrix element is estimated to be on the order of 2000 cm^{-1} for the ortho-isomer and 3240 cm^{-1} for the para-isomer. In phenylene-bridged systems, complete planarization is usually most favorable for charge transfer because of effective π -delocalization pathways,^{81,82} but in the ortho-isomer this geometry is not possible due to steric constraints. Therefore it has been speculated that the relatively large electronic coupling in 36^+ might be caused (at least partially) by through-space interaction between the two nitrogen lone-pair orbitals.⁸⁰

Ito et al. investigated a *p*-phenylenediamine derivative (37, Chart 18), with two attached nitroxide units that both carry an unpaired spin.⁸³ In the charge-neutral form of 37, the two nitroxide spins are antiferromagnetically coupled with an exchange constant of only 4 cm^{-1} ; i.e., the two spins are essentially uncorrelated. After oxidation of the central *p*-phenylenediamine unit, a third unpaired electron is present. Pulsed EPR measurements on 37^+ show that, at 5 K, there is predominant population of a spin quartet state, indicating ferromagnetic coupling between the three spins. The intervalence absorption of the oxidized *p*-phenylenediamine unit remains unaffected by this. The tri-radical cation 37^+ is an unusual species in that there coexist two localized (nitroxide) spins and a delocalized spin (on the *p*-phenylenediamine), with the latter mediating spin alignment.

Recently, a series of papers on macrocyclic compounds (38, 39, and 40, Chart 19) containing two TMPD units was published.^{84–86} In their dicationic forms, some of these molecules

Chart 19

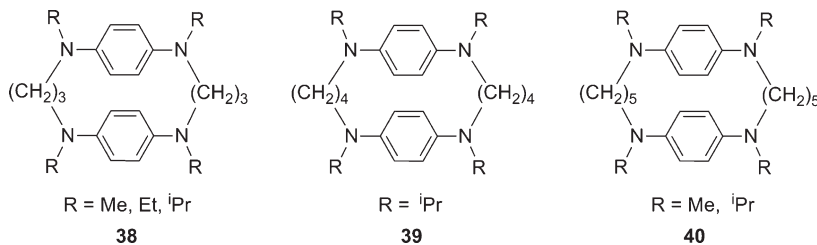


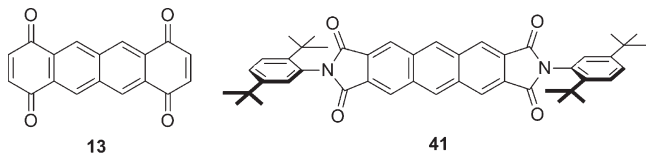
exhibit close intramolecular contacts between the two singly oxidized TMPD units, and the macrocyclic compounds display topologies resembling those found in cyclophane molecules.⁸⁵ Although the focus of this research appears to be on such face-to-face π -stacking geometries in doubly oxidized bis(TMPD) macrocycles, there have been some interesting observations on the singly oxidized species that are relevant in the context of organic mixed valence. For example, methyl-substituted **38**⁺ exhibits a near-infrared absorption band at \sim 5800 cm⁻¹ that has been attributed to an intervalence transition that is caused by intramolecular electron transfer from the neutral TMPD moiety to the oxidized TMPD⁺ partner. In isopropyl-substituted **38**⁺, the same band occurs at \sim 10 000 cm⁻¹, i.e., at substantially higher energy. X-ray crystallographic studies indicate where this large difference comes from, albeit structures for the mixed valence forms (**38**⁺) are not available. However, the X-ray crystal structures of the charge-neutral and dicationic forms of both methyl- and isopropyl-substituted **38** have been determined,^{84,86} and the important finding is that, for the methyl-substituted version of **38**²⁺, the two *p*-phenylenediamine units are essentially coplanar, whereas in the analogous isopropyl-substituted system, they are twisted considerably relative to one another.⁸⁶ The reason for this appears to be the bulkier nature of the isopropyl groups, and therefore it is likely that similar structural differences occur between the methyl- and isopropyl-substituted monocations. Molecular mechanics calculations on the neutral forms of **39** and **40** suggest that the alkane spacers of these macrocycles are too long in order to force the two *p*-phenylenediamine units into coplanar arrangement,⁸⁶ and intervalence absorption bands for the monocationic forms of these molecules were not reported.

3. ELECTRONIC COUPLING IN COVALENT SYSTEMS: IMPORTANCE OF THE MOLECULAR BRIDGE BETWEEN THE TWO REDOX CENTERS

3.1. Distance Dependence

Work by Miller and co-workers on the diquinone systems **12–14** mentioned in section 1.3 represents one of the earliest investigations of the distance dependence of charge transfer in organic mixed valence molecules.^{39,87} Much of this research focused on the question, at what distance between the two redox active units would a transition occur from a fully delocalized class III structure (as observed for **12**[–]) to a charge-localized class II system? For the diquinones, this turned out to be the case already for the naphthalene-bridged system **13**[–]. Interestingly, the anthracene-bridged diimide radical anion **41**[–] (Chart 20) was found to be a class III system, despite even greater spatial separation of its two redox sites.⁵⁰ It was assumed that this arises

Chart 20



because diimide π^* orbitals are higher in energy than quinone π^* orbitals, which leads to smaller energy gaps ($\Delta\epsilon$, section 1.2) to the π^* orbitals of the bridging units. A systematic investigation of the distance dependence of the electronic coupling matrix element or the reorganization energy was not performed.

As part of an in-depth study of distance, connectivity, and conformation effects on intramolecular electron transfer in organic mixed valence systems, Kochi and co-workers investigated molecules **42–46** (Chart 21) in which two redox active 2,5-dimethoxy-4-methylphenyl units are connected to one another either directly or by variable-length oligo-*p*-phenylene spacers.^{88–90} The 2,5-dimethoxy-4-methylphenyl (DMP) unit is easy to oxidize ($E_{\text{ox}} \approx 1.1$ V vs SCE) and undergoes relatively large geometrical changes during oxidation due to an energetically favorable quinonoidal resonance form.⁹⁰ Intervalence absorption bands caused by intramolecular electron transfer from neutral DMP to oxidized DMP⁺ were observed for the radical cations of **42–45**. Complementary temperature-dependent EPR studies and investigations by X-ray crystallography indicate that **42**⁺ is a class III system and **43**⁺ is at the class II–class III borderline, whereas **44**⁺ and **45**⁺ are “clean” class II systems.^{88,89} The near-infrared absorption bands of **42**⁺–**45**⁺ were analyzed in the framework of Hush’s theory,¹⁶ whereby electronic coupling matrix elements ranging from 2330 cm⁻¹ (for **42**⁺) to 217 cm⁻¹ (for **45**⁺) were determined. The distance (*d*) between the DMP units increases from 4.3 Å in **42**⁺ to 21.5 Å in **46**⁺, and a plot of $\log(H_{AB})$ against *d* (Figure 2a) is linear, as predicted by superexchange theory.²⁰

From temperature-dependent EPR line broadening experiments, electron-transfer rate constants (k_{ET}) were determined for molecules **43**⁺–**46**⁺. At a temperature of 20 °C, k_{ET} was estimated to decrease from 10^{10} s⁻¹ for the molecule with a single *p*-phenylene spacer (**43**⁺) to a value of 3×10^7 s⁻¹ for the tetra-*p*-phenylene-bridged system (**46**⁺). A plot of $\log(k_{\text{ET}})$ versus DMB–DMB⁺ distance (Figure 2b) is less clearly linear, and the exponential distance dependence of the electron-transfer rate is less obvious than for the electronic coupling matrix element. Yet, linear regression fits to the two sets of data in Figure 2 yield slopes that roughly differ by the factor of 2 (-0.18 Å for H_{AB} compared to -0.44 Å for k_{ET}) that would be expected on the basis of the relationship $k_{\text{ET}} \propto H_{AB}^2$ predicted by

Chart 21

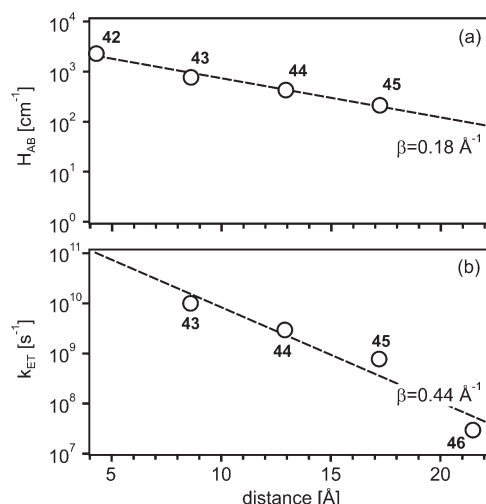
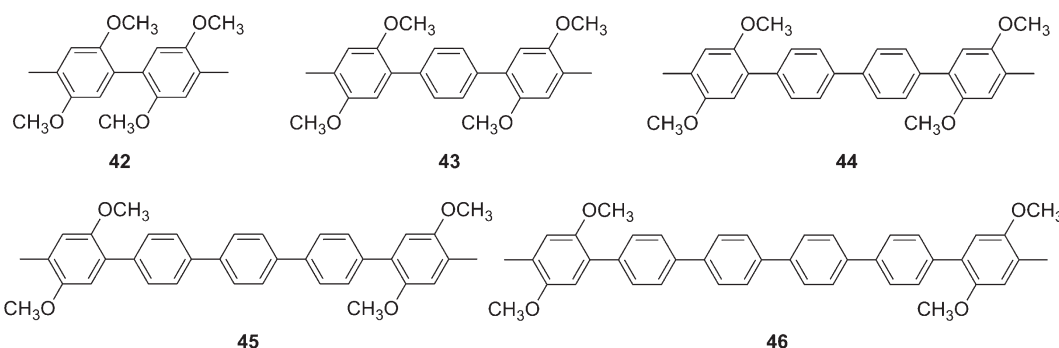
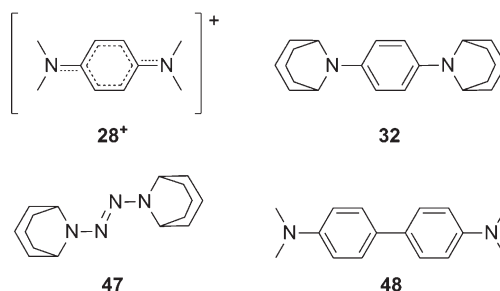


Figure 2. (a) Distance dependence of the electronic coupling matrix element (H_{AB}) in mixed valence radicals of molecules with terminal *p*-dimethoxytolyl redox sites and *p*-phenylene bridges. The number of intervening phenylene bridging units increases from 0 (42^+) to 3 (45^+); (b) distance dependence of the rate for intramolecular electron transfer (k_{ET}) in the same type of radicals as determined by EPR spectroscopy. The number of phenylene spacers increases from 1 (43^+) to 4 (46^+).^{88–90} The dashed lines are linear regression fits yielding distance decay constants of $\beta = 0.18 \text{ \AA}^{-1}$ (for H_{AB}) and $\beta = 0.44 \text{ \AA}^{-1}$ (for k_{ET}).

semiclassical electron-transfer theory.²⁴ The absolute value of the slope determined from the k_{ET} data (0.44 \AA) is a distance decay constant (β) that can be compared to β -values extracted from investigations of photoinduced long-range electron transfer in donor–acceptor systems with oligo-*p*-phenylene bridges. Literature values for β for such bridges range from 0.21 to 0.77 \AA^{-1} ,²³ with values around 0.4 \AA^{-1} being observed most frequently.⁹¹ All subsequent β -values in this review describe the distance dependence of k_{ET} and hence are exactly twice as large as the slopes extracted from plots of $\ln(H_{AB})$ versus distance.

Nelsen and co-workers investigated the distance dependence of the electronic coupling in a series of violene molecules which have $2n + 3$ π electrons on $2n + 2$ sp^2 hybridized atoms.⁹² The most prominent member of the series is the TMPD⁺ radical cation (28^+).⁶⁵ The other members were the TMPD⁺ analogue 32^+ with two bicyclooctyl rings at the place of the four methyl substituents, then a molecule in which the same two amines are connected by an azo group (47^+ , Chart 22), and last the biphenyl

Chart 22



analogue of TMPD⁺ (48^+). The radical cations of all four molecules are class III systems, and H_{AB} can be extracted directly from their intervalence absorption band maxima (Figure 1c). Given the fully delocalized electronic structure of these systems, their N–N distance was judged a poor measure of the electron-transfer distance. Therefore, the lengths of the overall systems were simply expressed in terms of the number (n) of connecting σ -bonds between the two amine nitrogen atoms. The dependence of H_{AB} on n (ranging from $n = 3$ for 47^+ to $n = 9$ for 48^+) turned out to be nearly perfectly exponential, and a (dimensionless) distance decay constant (β_n) of 0.3 was obtained.⁶⁵ This is significantly lower than what is typically observed for saturated alkane bridges ($\beta_n \approx 1.0$),⁹³ and reflects the fact that the molecules considered here are π -conjugated. An investigation of pyridylethylene-bridged pentaaamineruthenium mixed valence systems yielded $\beta_n \approx 0.34$.^{65,94} The good agreement between the diamine β_n -value (0.3) with that from the ruthenium study (0.34) is reassuring, because the inorganic systems belong to class II and have much better defined electron-transfer distances.⁶⁵

Lambert and Nöll studied an entire series of bis(triarylamine) molecules that are based on the *N,N,N',N'*-tetraanisyl-*p*-phenylenediamine prototype molecule (35).⁷⁷ Instead of a single *p*-phenylene spacer between the two nitrogens, the longer analogues have naphthalene (49), biphenyl (50), tolane (51), or even longer bridges (52 , 53) (Chart 23).

The N–N distance increases from 5.6 to 19.3 \AA along this series, and a near-infrared absorption band due to intramolecular electron transfer is observable for all radical cationic forms. Compounds $49^+–53^+$ are class II systems with H_{AB} -values decreasing from 2240 to 500 cm^{-1} . The dependence of H_{AB} on the number of σ -bonds (n) connecting the two nitrogens was found to be exponential (Figure 3a), despite the fact that $49–53$

Chart 23

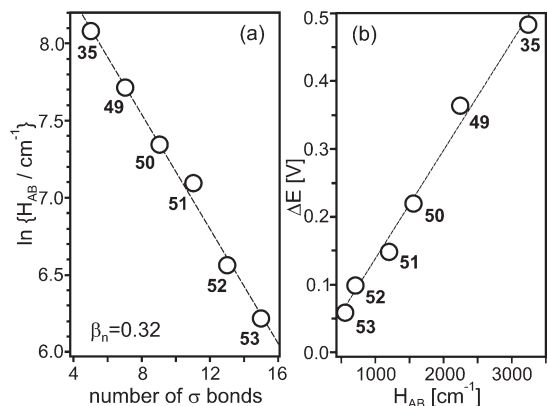
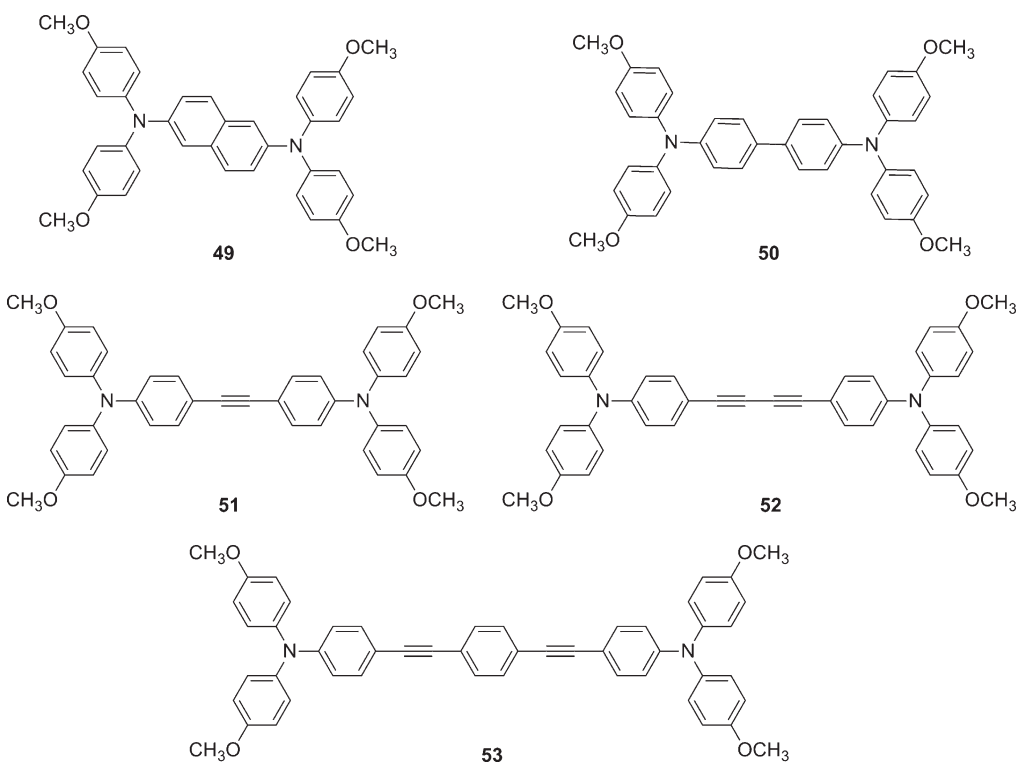


Figure 3. (a) Semilogarithmic representation of H_{AB} versus the number of σ -bonds between nitrogen atoms in a series of bis(triarylamine) radical cations. A linear regression fit to the data (dashed line) yields a dimensionless distance decay constant of $\beta_n = 0.32$.⁷⁷ (b) Difference in electrochemical potential (ΔE) between the first two oxidations for the same series of bis(triarylamine) molecules as a function of the electronic coupling (H_{AB}) determined for their mixed valence radical cations.⁷⁷ Adapted with permission from ref 77. Copyright 1999 American Chemical Society.

do not represent a true homologous series of molecules. The distance decay constant in this case is 0.32 (including the data point for 35^+),⁷⁷ in excellent agreement with Nelsen's β_n value of 0.3 for the class III violenes from above.⁶⁵ Furthermore, there is a linear correlation of the redox potential splitting (ΔE) between the first two oxidation waves of these bis(triarylamine) molecules and the electronic coupling matrix elements (H_{AB}) of their mixed valence forms (Figure 3b). For the shortest member of the series

(35) $\Delta E = 485$ mV, whereas in the longest member (53) ΔE has dropped to 60 mV. It is primarily the first oxidation process that occurs at increasingly negative potentials, while the second oxidation stays relatively constant at an electrochemical potential of 340 mV versus the ferrocene/ferrocenium couple.⁷⁷ This observation is similar to that made by Miller and co-workers in their investigations of the diquinone and diimide molecules (12–14 and 41).⁸⁷

Computational work by Brédas and co-workers on 35^+ and $50^+ - 52^+$ yielded complementary insight into the geometrical and electronic structures of these bis(triarylamine) systems from Lambert and Nöll.⁷⁸ Specifically, DFT calculations were used to investigate the geometrical changes that are associated with oxidation of the neutral molecules to their radical cation forms. Throughout the series the central N–C bonds shorten by ~ 0.025 Å, the central phenylene rings undergo a quinonoidal distortion, and the twist angles between the amino groups decrease. In the alkyne systems 51^+ and 52^+ , the lengths of the triple bonds increase by ~ 0.010 Å, while the central single bond in 52^+ shortens by roughly the same amount.⁷⁸ Analysis of the molecular frontier orbitals suggests that the intramolecular charge transfer in these radicals involves a shift of electron density from the terminal anisyl rings toward the central part of the molecules. It has been pointed out that this may contribute significantly to the solvent dependence of the intervalence absorptions of these systems. The effect of temperature on the charge-transfer transitions in 50^+ and 51^+ was also explored.⁹⁵

Investigations of photoinduced long-range electron transfer in donor–bridge–acceptor molecules revealed far weaker distance dependences for charge transfer across oligo-*p*-phenylene vinylene (OPV) wires than for oligo-*p*-phenylenes, due to the activation of a hopping mechanism that is more weakly

Chart 24

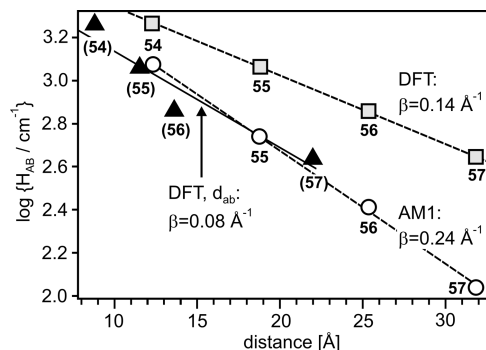
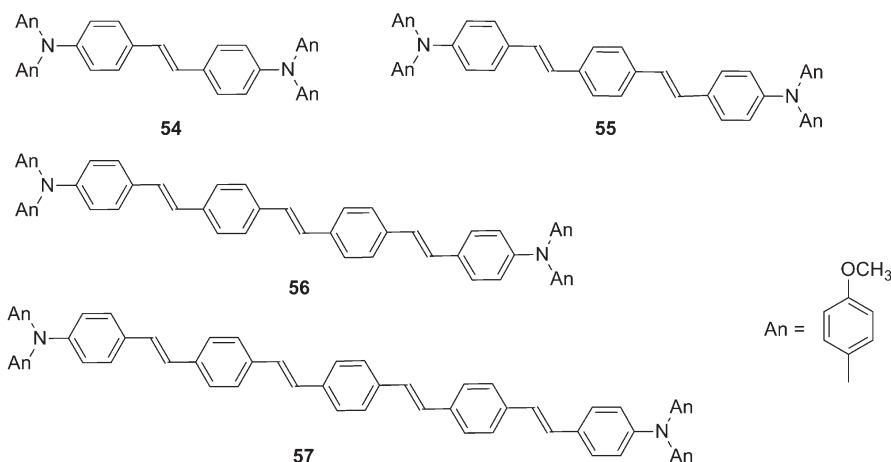


Figure 4. Semilogarithmic representation of the distance dependence of H_{AB} in vinylene-bridged bis(triarylamine) radical cations $54^+ - 57^+$ as obtained by various computational methods: by DFT calculations (gray filled squares), by AM1 calculations (open circles), and by DFT calculations based on effective donor–acceptor separations (d_{ab}) rather than N–N distances (black triangles).

dependent on distance than the superexchange tunneling process.^{96,97} In this context, the study by Barlow et al. on OPV-bridged tertiary amines $54 - 57$ (Chart 24),⁹⁸ represents an important extension of the work by Lambert and Nöll on molecules $49 - 53$.⁷⁷

The shortest member of the Barlow series (54^+) is found to exhibit a strongly asymmetric near-infrared absorption band that is only a weakly solvatochromic (930 cm^{-1} blue shift between CH_2Cl_2 and CH_3CN). By contrast, the intervalence absorption band of 55^+ has a symmetrical Gaussian shape and is a more strongly solvent-dependent (2070 cm^{-1} blue shift between CH_2Cl_2 and CH_3CN), and hence it appears plausible to assign 54^+ to class III and 55^+ to class II.^{6,8} The longer congeners (56^+ and 57^+) did also exhibit intense absorption bands around 9000 cm^{-1} , but similar absorptions with approximately twice the absorptivity were observed for the 56^{2+} and 57^{2+} dication, indicating that these bands are due to charge transfer from the highest occupied bridge-localized orbital to the oxidized tertiary amines. With intervalence bands in 56^+ and 57^+ being masked by other absorptions, experimental values for the electronic coupling matrix elements of these longer congeners remained elusive, and consequently the distance dependence of H_{AB} in

$54^+ - 57^+$ was explored only with computational methods. AM1 and DFT calculations gave results that significantly deviate from each other (Figure 4). DFT-computed values for H_{AB} (gray filled squares) were consistently greater than those estimated by AM1 calculations (open circles), and the distance decay constants of the two sets of calculated H_{AB} data are 0.14 \AA^{-1} (DFT) and 0.24 \AA^{-1} (AM1). Both values are substantially greater than those previously reported for photoinduced charge transfer across OPV wires (0.01 \AA^{-1}).^{96,97} Barlow et al. note that the N–N distance is quite simply a bad measure of the electron-transfer distance in these highly π -conjugated molecules. When the effective separation (d_{ab}) between donor and acceptor sites is estimated on the basis of calculated transition dipole moments, values between 8.78 \AA (54^+) and 21.98 \AA (57^+) are found. These effective electron-transfer distances are between 28 and 46% smaller than the N–N distances. A plot of $\ln(H_{AB})$ versus d_{ab} yields $\beta = 0.08 \text{ \AA}^{-1}$ (black triangles in Figure 4), in somewhat better agreement with the values obtained for OPV wires in donor–bridge–acceptor molecules.

The comparison between stilbene-bridged 54^+ and tolane-bridged 51^+ is exemplary for the stronger electronic coupling mediated by double bonds with respect to triple bonds:⁹⁹ The intervalence absorption band of 54^+ exhibits the above-mentioned weak solvatochromism, and the crystallographic structure of this cation is consistent with class III behavior. The near-infrared absorption of 51^+ is strongly solvatochromic, and consequently this species was allocated to class II. Thus, despite identical numbers of connecting σ bonds between the two redox units, the alkene and alkyne species 54^+ and 51^+ fall into very different regimes of delocalization.⁹⁹

For increasingly long mixed valence systems the intervalence absorption bands become more and more difficult to detect, because the intensity of these bands is proportional to H_{AB}^2 .⁶ In some of the above-mentioned examples ($56^+, 57^+$) such bands have remained undetected, not only because of their weakness but also because of electronic transitions from the bridge to the oxidized redox centers that superpose the intervalence bands. One clever approach to circumvent this latter problem involves the use of electron-deficient bridges. Lambert and co-workers reported on a comparative study of 58^+ (Chart 25) and 59^+ , which differ only by two cyano groups attached to the bridge.¹⁰⁰ In 58^+ , an intense ($\epsilon \sim 25\,000 \text{ M}^{-1} \text{ cm}^{-1}$) band due to hole

Chart 25

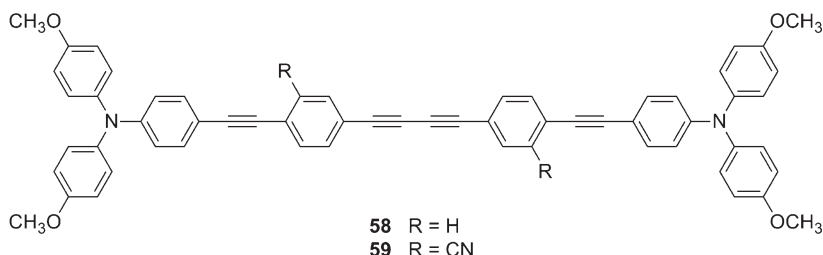
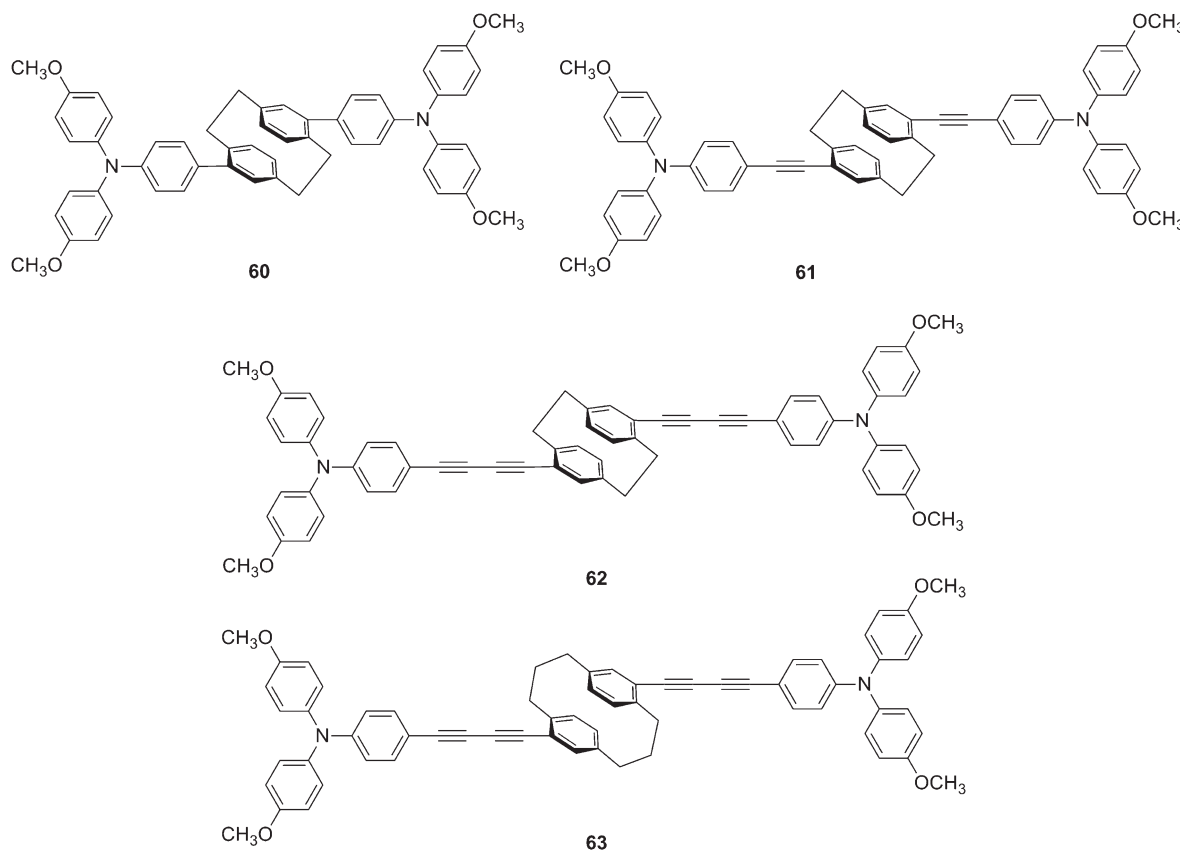


Chart 26



transfer from the oxidized amine to the bridge is observed around $11\,000\text{ cm}^{-1}$. In $\mathbf{59}^+$, the analogous transition occurs at $\sim 14\,200\text{ cm}^{-1}$, and a weak ($\epsilon < 1000\text{ M}^{-1}\text{ cm}^{-1}$) intervalence absorption band becomes observable at $\sim 11\,800\text{ cm}^{-1}$. Its analysis in terms of Mulliken–Hush theory yielded $H_{AB} = 190\text{ cm}^{-1}$.

Lambert and Amthor explored the distance dependence of H_{AB} in bis(triarylamine) systems that incorporate [2.2]paracyclophane as a bridging unit.¹⁰¹ The cations of **60**–**62** (Chart 26) are class II mixed valence systems with intervalence absorption band maxima between 6230 cm^{-1} (**60**⁺) and 7500 cm^{-1} (**62**⁺). These species exhibit optical absorption bands due to hole transfer from the oxidized triarylamine unit to the bridge around $11\,000\text{ cm}^{-1}$, which nearly mask the intervalence bands. Due to the close energetic proximity of these electronic transitions, a three-level model including the one-electron oxidized state of the bridge in addition to the two intervalence charge-transfer states

was used to describe the electronic structures of these species. Electronic couplings calculated in this manner are between 37 and 214% larger than those calculated on the basis of a simple two-level model that neglects the bridge states, with deviations becoming larger with increasing bridge length (Figure 5). Plots of $\ln(H_{AB})$ versus the number of σ bonds between the two nitrogens are essentially linear for both types of models, and the distance decay constants are $\beta_n = 0.36$ for the three-level model and $\beta_n = 0.56$ for the two-level model (Figure 5). The β_n -value from the three-level model differs only marginally from that extracted from analysis of the structurally similar radical cations of **35** and **49**–**53** (Figure 3, $\beta_n = 0.32$), indicating that the [2.2]paracyclophane unit is acting more like an unsaturated spacer than like a saturated bridge.¹⁰¹

In a collaboration between the groups of Grampp and Lambert, the distance dependence of barrier heights associated with thermal electron transfer was explored by comparing the

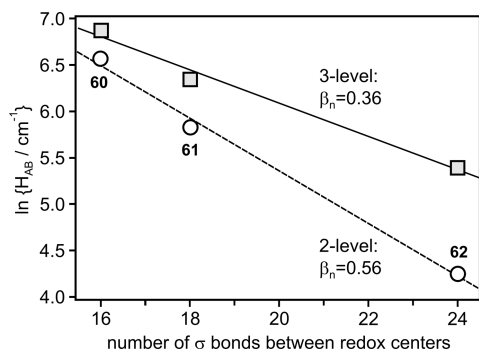


Figure 5. Dependence of $\ln(H_{AB})$ on the number of σ -bonds between nitrogen atoms in three [2.2]paracyclophane-bridged bis(triarylamine) cations as determined from intervalence absorption data using a two-state model (open circles) and a three-state model (gray filled squares).¹⁰¹ Adapted with permission from ref 101. Copyright 2006 American Chemical Society.

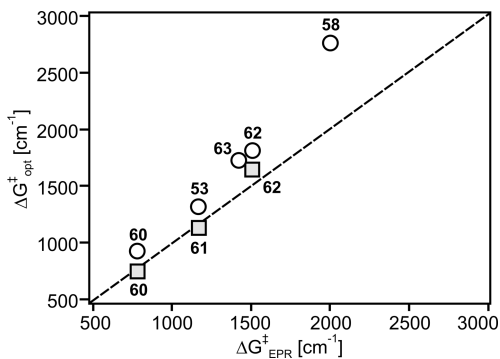
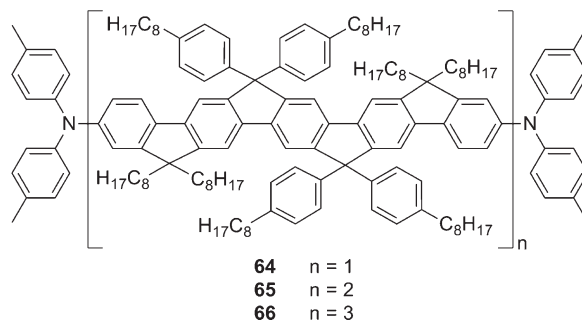


Figure 6. Correlation between the activation energy for thermal electron transfer determined by EPR spectroscopy ($\Delta G^{\ddagger}_{\text{EPR}}$) and the activation energy ($\Delta G^{\ddagger}_{\text{opt}}$) determined from analysis of the intervalence charge-transfer bands in various bis(triarylamine) radical cations.¹⁰² Data points represented by open circles were obtained using a two-state model; data points represented by gray filled squares were obtained using a three-level model. The dashed line has a slope of 1, while a fit to the experimental data points would yield a slope of 1.5.¹⁰² Adapted with permission from ref 102. Copyright 2009 American Chemical Society.

radical cations of 53, 58, and 60–63.¹⁰² These systems exhibit room-temperature electron-transfer rates between 3×10^7 and $1.6 \times 10^9 \text{ s}^{-1}$ and give rise to EPR spectra either consisting of three major lines (indicative of spin localization on a single nitrogen center with a nuclear spin of 1) or spectra consisting of five major lines that can be explained by interaction of the unpaired spin with two equivalent nitrogens. Variations in temperature induce a changeover between these slow and fast exchange limits, and Eyring analysis of the temperature-dependent data yields activation parameters for thermal electron transfer. The activation free energies ($\Delta G^{\ddagger}_{\text{EPR}}$) thus obtained for the thermal electron-transfer range from 780 cm^{-1} (for 60^+) to 2000 cm^{-1} (for 58^+) and correlate linearly with the activation energies determined from analyses of the intervalence charge-transfer bands using a three-level model ($\Delta G^{\ddagger}_{3\text{-level}}$) and a two-level model ($\Delta G^{\ddagger}_{2\text{-level}}$).¹⁰² However, the barriers extracted from these models systematically exceed those determined by EPR spectroscopy, and a plot of $\Delta G^{\ddagger}_{3\text{-level}}$ and $\Delta G^{\ddagger}_{2\text{-level}}$ versus $\Delta G^{\ddagger}_{\text{EPR}}$ yields a linear correlation with a slope of 1.5 (Figure 6).

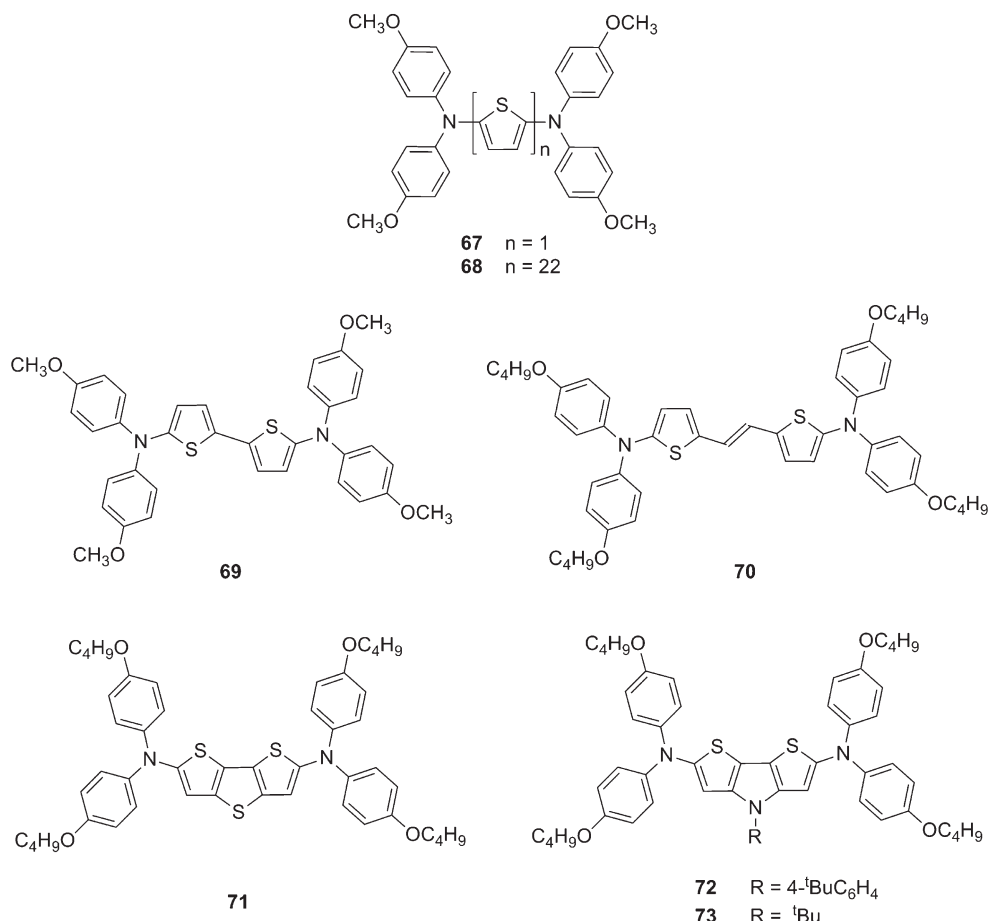
Chart 27



Müllen and co-workers noted that much of the prior research on organic mixed valence had involved conjugated bridges that were not completely planar due to torsion about formal single bonds, thereby leading to less than optimal π -conjugation. Therefore, they explored the length dependence of electronic coupling between two triarylamine units connected by ladder-type pentaphenylene bridging units, which are more planar and more conjugated than many of the previously used molecular wires.^{103,104} Terminal amino groups were connected by one (**64**, Chart 27), two (**65**), or three (**66**) pentaphenylene units, yielding N–N distances of 22, 43, and 63 Å. In molecule **64**, the first two electrons are removed successively with a potential difference of 100 mV, but for the longer molecules (**65**, **66**) the first two oxidations are unresolved, suggesting that the two electrons are removed simultaneously from both amines. Compound **64**⁺ exhibits a broad and unstructured absorption band peaking at 5280 cm^{-1} which has been attributed to intervalence charge transfer, but in this spectral region **65**⁺ and **66**⁺ only show absorptions that are identified as bridge-to-oxidized amine charge transfers. Thus, while **64**⁺ can be described as a class II system with $H_{AB} = 548 \text{ cm}^{-1}$, there is no evidence for any significant electronic interaction between the triarylamine redox centers in **65**⁺ and **66**⁺, and they have to be considered charge-localized systems.¹⁰³ It is possible that the torsional junctions occurring between neighboring pentaphenylene units are responsible for this.

Thiophene-based polymers are of interest for a variety of different (opto)electronic applications, and hence charge transfer in oligothiophenes has received considerable attention.¹⁰⁵ In this context, Lacroix and co-workers performed a computational study of charge delocalization in bis(triarylamine) radical cations with oligothiophene bridges ranging in length from one (**67**⁺, Chart 28) to 22 thiophene units (**68**⁺).¹⁰⁶ The computations mainly focused on bond length and charge density differences between neutral and cationic forms. For systems with only one or two bridging thiophene units, the calculated geometries of the radical cations are symmetrical, whereas for longer congeners they are consistent with the formation of a localized charge defect. This manifests itself in semiquinonoidal distortions on one side of the radical cation, while the other side stays structurally nearly identical to the geometry calculated for the charge-neutral form. In other words, a transition from class III to class II behavior upon bridge lengthening is calculated. The calculations also predict that, with increasing bridge length, electron transfer from the oligothiophene bridge to the oxidized amine becomes increasingly probable. This suggests that, upon bridge lengthening, long-range charge transfer between triarylamine units will

Chart 28



undergo a changeover in mechanism from superexchange tunneling to hopping.¹⁰⁶

Odom et al. performed an experimental study of the distance dependence of charge delocalization in thiophene-bridged bis(triarylamine) radical cations.¹⁰⁷ The asymmetric intervalence absorption band of **69⁺** indicates a fully delocalized electronic structure, in line with the computational work by Lacroix and co-workers discussed above.¹⁰⁶ The characteristics of the intervalence absorptions of **70⁺–73⁺** support their assignment to class III, and in the case of the dithienopyrrole-bridged species **72⁺/73⁺** an exceptionally large electronic coupling of $H_{AB} = 5790 \text{ cm}^{-1}$ was estimated.¹⁰⁷ This is one of the largest values reported yet for a bis(triarylamine) radical cation. The close energetic proximity of the one-electron oxidized states of thiophenes and triarylamines is likely to contribute to this large electronic coupling, and one may ask, to what extent can these radicals still be regarded as bis(triarylamine) mixed valence species rather than bridge-oxidized compounds? EPR spectroscopy on **69⁺–73⁺** indicates that most of the spin density is associated with the nitrogen atoms, but it is clear that the thiophene bridge units bear a larger amount of spin density than the bridges in other (non-thiophene-linked) bis(triarylamine) radical cations.¹⁰⁷

Lambert and co-workers performed a distance dependence study of intramolecular electron transfer in the radical cationic forms of molecules with two dimethylphenazine redox centers (**74–77**, Chart 29).¹⁰⁸ Electronic couplings for these class II

systems were found to be exponentially dependent on the number of σ -bonds connecting the two phenazines. $\beta_n = 0.34$,¹⁰⁸ in excellent agreement with the value extracted from the triarylamine systems **35⁺** and **49⁺–53⁺** (Figure 3a).⁷⁷ The diethynylanthracene bridge in **77⁺** appears to mediate somewhat weaker electronic coupling than the divinylanthracene bridge in **78⁺**, but direct comparison is difficult because the latter system uses methylphenothiazine redox centers instead of dimethylphenazines.¹⁰⁹

Recent work by Nelsen and co-workers provided detailed insight into the distance dependence of charge transfer in mixed valence dinitroaromatic radical anions.¹⁷ Such species had long been considered charge-localized species due to their tight interaction with alkali metal or even tetrabutylammonium counterions, but it has become clear that when reducing various dinitroaromatics with sodium in the presence of excess cryptand **79** (Chart 30), many of the resulting anionic species are in fact truly delocalized intervalence compounds. For investigation of the distance dependence of intervalence charge transfer in these systems, direct comparison between the radical anions of 1,4-dinitrobenzene (**80**), 2,6-dinitronaphthalene (**81**), and 2,6-dinitroanthracene (**82**) (Chart 31) is a good starting point.

These species exhibit highly structured near-infrared absorption spectra which are typical for fully delocalized (class III) systems. H_{AB} is found to decrease exponentially along the series with a distance decay constant of $\beta_n = 0.2$ (Figure 7).¹⁷ The deviation from the value obtained for class II bis(triaryamine) radical cations ($\beta_n = 0.32$, Figure 3a) is significant.⁶⁵ When

Chart 29

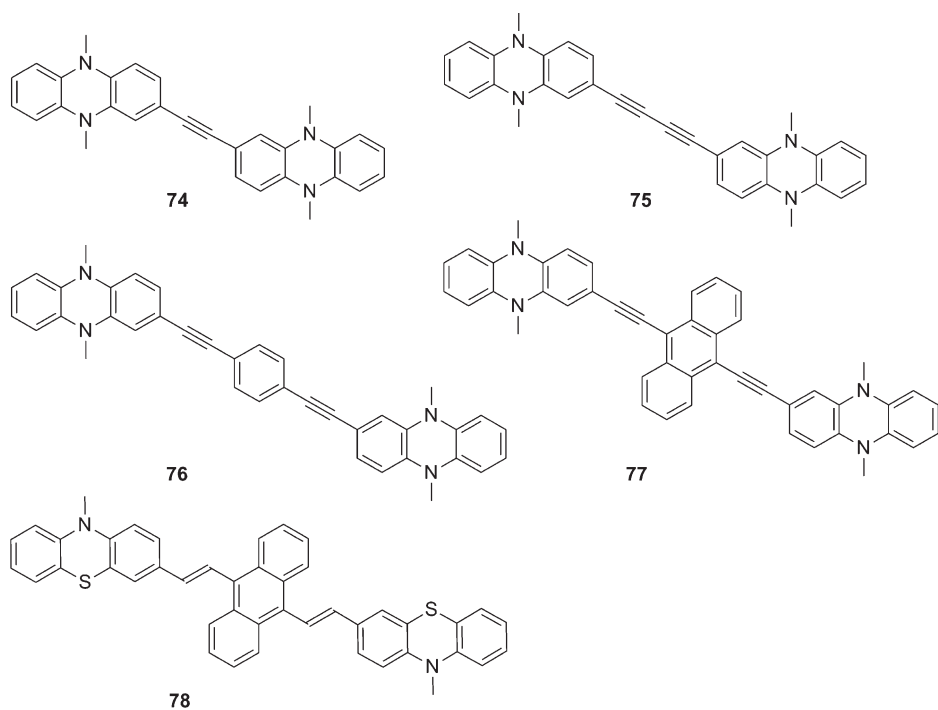
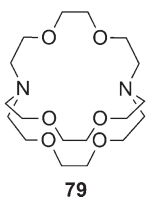


Chart 30



adding the H_{AB} -value for 1,5-dinitronaphthalene (83^-) to the distance dependence plot in Figure 7, this data point (gray filled square) does not fit at all into the picture of an exponential distance dependence. Indeed, H_{AB} is smaller in 83^- than in 81^- by 25%, and the rate for (thermal) intramolecular electron transfer at 215 K (as determined by EPR spectroscopy) is 2 orders of magnitude slower for 83^- than for 81^- , despite the fact that the two systems are constitutional isomers.¹¹⁰

The important fundamental difference between 2,6- and 1,5-substituted naphthalene is that the former has a so-called Kekulé substitution pattern, whereas the latter does not. What this means is that the 5- σ -bond shortest pathway for coupling between the two nitro groups is not functional for 83^- and instead has to be replaced by an 11- σ -bond pathway. This point is illustrated by the (simpler) examples of 2,6- and 1,5-naphthoquinones, 86 and 87 (Chart 32). When included as an 11- σ -bond compound, 83^- fits the exponential distance dependence in Figure 7 reasonably well. However, additional inclusion of two radical anions with biphenyl or fluorene spacers between the two nitro groups (84^- , 85^-) reveals a deviation from strictly exponential distance dependence for the series 80^- – 85^- . Such deviations are expected for systems in which the energy difference between the charge-bearing units and the bridge orbitals involved in superexchange decreases as a function of increasing

bridge length.²⁰ Similarly curved distance dependences were reported for photoinduced electron transfer in certain donor–bridge–acceptor molecules.^{22,112} Large differences in electronic couplings between Kekulé- and non-Kekulé-substituted isomers were also reported for naphthalene-bridged bis(hydrazine) molecules.^{110,113}

The x -axis in Figure 7 simply counts the number of σ -bonds between nitrogen atoms, but as seen above for the class II triarylamine systems, the N–N distance can actually be a rather poor measure of the electron-transfer distance. One would expect this to be an even greater problem for class III mixed valence systems such as the dinitroaromatics considered here. To explore this aspect, the transition dipole moments associated with the intervalence charge transfers in the dinitroaromatic systems 80^- – 85^- were calculated on the basis of optical absorption data and subsequently converted to electron-transfer distances (d_{ab}).¹⁷ The important finding is that the electron-transfer distance on the adiabatic surfaces is only between 26 and 40% of the N–N distance. Thus, the dinitro radical anions seem to exhibit much smaller d_{ab} at comparable electronic coupling than those of bis(triarylamine) radical cations. It has been noted that something may be wrong with the analysis of the radical anion intervalence data in the framework of a simple two-state model, and this suspicion has been substantiated by DFT calculations.¹⁸ The key conclusion was that the two-state model is inadequate for analysis of intervalence bands in strongly coupled class III systems in which the transition energies cannot be related to a single electronic coupling in the molecule.¹⁸

Quite remarkably, even the biphenyl- and fluorene-bridged systems 84^- and 85^- with 9 σ -bonds between nitro groups are fully delocalized class III systems. Thus, the question arises at which point the transition to partially localized class II systems will occur. To explore this frontier, three Kekulé-substituted

Chart 31

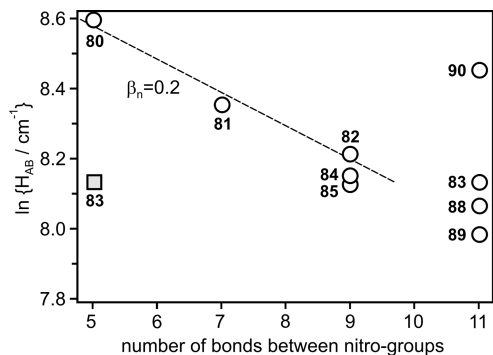
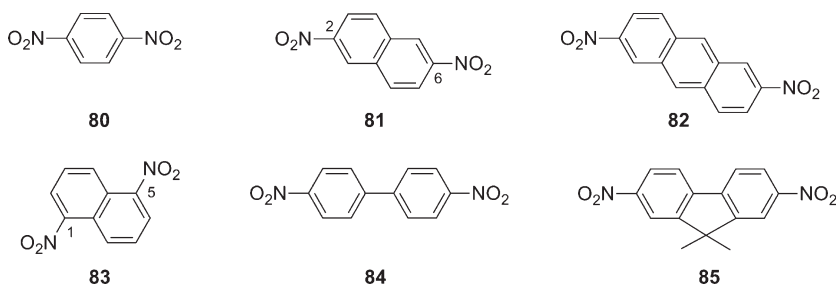
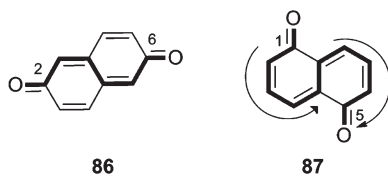


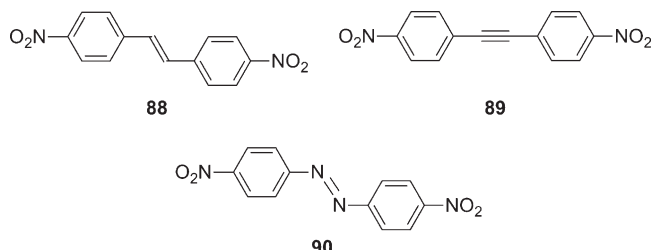
Figure 7. Distance dependence of the electronic coupling in various dinitroaromatic radical anions. The dashed line is a fit to the data points of the homologous series $80^- - 82^-$.^{17,111} Compound 83^- is represented twice: once with a non-Kekulé 5- σ -bond pathway (gray filled square) and once with its 11- σ -bond Kekulé coupling pathway (open circle).¹¹⁰ Adapted with permission from ref 17. Copyright 2003 American Chemical Society.

Chart 32



11- σ -bond bridged dinitroaromatic radical anions ($88^- - 90^-$, Chart 33) were investigated recently.¹¹¹ There is a pronounced solvent dependence of the intervalence absorption bands of 88^- and 89^- that will be discussed in section 7, and in most solvents these anions are class II species. However, 90^- remains a class III system in all solvents, and its H_{AB} -value (4700 cm^{-1}) is remarkably high. When included in the plot of Figure 7, this species stands out by an exceptionally large deviation from an exponential distance dependence of H_{AB} . Notably, the electronic coupling in this 11- σ -bond species is larger than that obtained for the 7- σ -bond compound 81^- , indicating once again that the distance between redox active groups is not the sole factor determining electronic couplings. The explanation for the remarkably large H_{AB} in 90^- comes from energetically low-lying one-electron reduced states on the azo bridge: The smaller the energy gap between the donor/acceptor states and the bridge state, the stronger superexchange coupling becomes (sections 1.2 and 3.3).^{20,22}

Chart 33



The close electronic relationship between *p*-phenylenediamine radical cations and quinone radical anions was noted more than 85 years ago.⁴⁹ Indeed, quinone radical anions are true mixed valence species, but, due to their instability in air, they are considerably more difficult to handle experimentally than intervalence radical cations. However, their stability is markedly improved when the positions ortho to the carbonyl groups are alkylated.¹¹⁴ The radical anions of molecules $91 - 95$ (Chart 34) all exhibit highly structured intervalence absorption bands indicative of class III behavior, while 96^- displays an unstructured Gaussian-shaped near-infrared absorption band that this is in line with class II behavior.⁴⁷ For the five fully delocalized systems, $\ln(E_{op})$ depends linearly on the number of bridging σ -bonds between the terminal oxygen atoms with $\beta_n = 0.3$ (Figure 8), but absolute values for H_{AB} were not reported, due to the prior observation that the simple two-state model is inadequate for estimation of electronic couplings in class III systems (see above). Be that as it may, the observation of a fully delocalized electronic structure for a 17-bond mixed valence radical anion (95^-) is quite remarkable.

3.2. Influence of Bridge Structure, Connectivity, Topology, and Conformation

There are numerous studies in which the electronic interaction between two nearly equidistant organic redox centers was investigated as a function of the chemical structure of the linker between them. A case in point is the comparison of the radical cations of 53 and 97 (Chart 35).¹¹⁵ Both of them are class II mixed valence species, and their H_{AB} -values are 350 cm^{-1} (53^+) and 450 cm^{-1} (97^+). The observation of stronger electronic coupling for the platinum–phenylacetylidyne bridge is in line with the previous finding that Pt-bridged phenylacetylide can have higher molecular conductivity than oligo-*p*-phenylene ethynlenes.¹¹⁶

Mayor et al. investigated intramolecular electron transfer between pentakis(thiophenyl)benzene subunits in 98^- , 99^- , and 100^- (Chart 36).¹¹⁷ The former two have similar

Chart 34

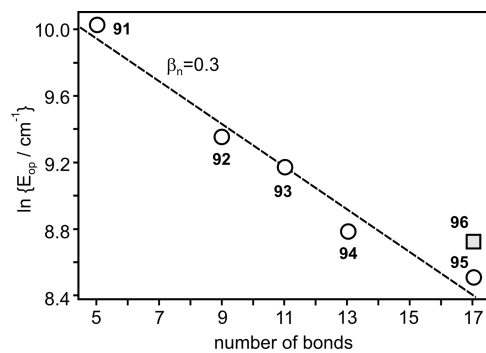
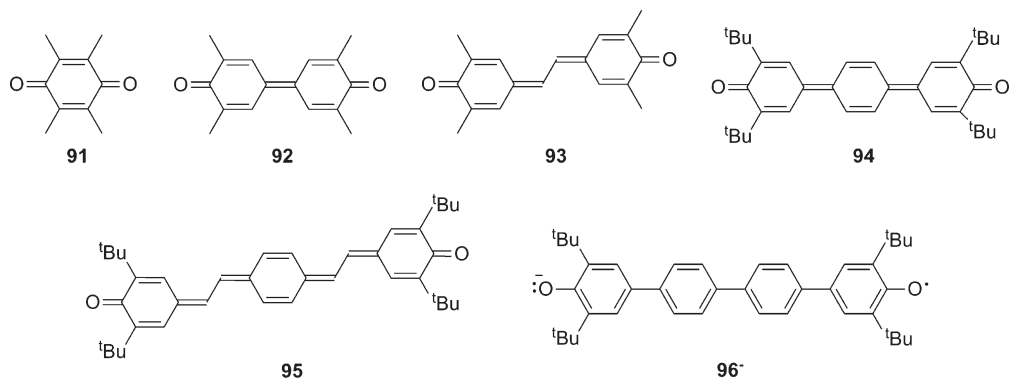
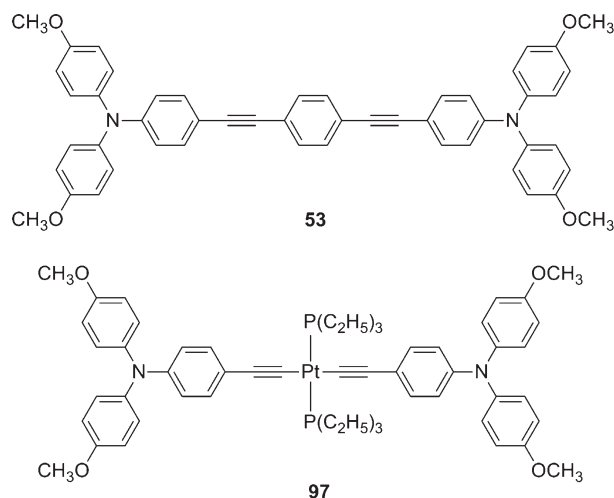


Figure 8. Plot of $\ln(E_{\text{op}})$ versus number of connecting σ -bonds between oxygen atoms in six diquinone radical anions.⁴⁷ The dashed line is a linear regression fit to the five data points representing class III species (open circles) and yields a slope of -0.15 . Consequently, the distance decay constant for electron-transfer rates is $\beta_n = 0.3$. Radical anion 96^- is a class II species (gray filled square) and was not included in the fit.⁴⁷ Adapted with permission from ref 47. Copyright 2007 American Chemical Society.

center-to-center distances between the two reducible subunits (9.4 \AA versus 8.7 \AA), but only the diacetylene bridge in 98^- mediates detectable electronic coupling. It manifests itself in a separation of the first two one-electron reduction waves by 260 mV and an intervalence absorption at a wavelength of 1310 nm . A crystal structure of 99 indicates why coupling is poor in its radical anion: There are torsion angles of 72° between the $\text{C}=\text{N}$ double bonds and the central benzene planes of the reducible subunits; hence, the system is likely to be poorly π -conjugated.¹¹⁷ The *p*-divinylbenzene bridge in 100^- was found to isolate completely the two redox centers, in clear contrast to the class II behavior observed for the *p*-divinylanthracene bridged methylphenoxythiazine system 78^+ .¹⁰⁹ The special role of anthracene as a bridging unit will be discussed in section 3.3.

A given aromatic bridging unit can mediate vastly different electronic couplings depending on the positions at which it is substituted. This phenomenon has already been illustrated by comparison of the 2,6- and 1,5-dinitro-substituted naphthalenes 81 and 83 .¹⁷ Like the latter, 2,7-dinitronaphthalene (101 , Chart 37) has a non-Kekulé substitution pattern, and its anion is a class II mixed valence system.¹¹⁸ Dinitro substitution of phenanthrene cores leads to similar differences between Kekulé- (102) and non-Kekulé-substituted (103) isomers: 103^- has a

Chart 35



somewhat shorter N–N distance, but with $H_{AB} = 445 \text{ cm}^{-1}$ an electronic coupling that is by a factor of 2 smaller than that of 102^- . The reason for this is that 102^- has a 9-bond conjugation pathway between nitro groups, whereas, in 103^- there is only an 11-bond pathway. On the other hand, as long as Kekulé-substituted molecules are compared to other Kekulé-substituted isomers, very similar mixed valence properties are observed. For example, the radical anions of *p*- and *o*-dinitrobenzene (80^- , 104^-) are both fully delocalized class III systems. Likewise, the radical anions of 2,7-dinitrobiphenylene (105) and 1,8-dinitrobiphenylene (106) have nearly identical electronic couplings.¹¹⁸

[2.2]Paracyclophane bridges can also give rise to isomerism that affects the extent of electron delocalization in organic mixed valence systems. The simplest examples are the pseudo-para (107) and pseudo-ortho (108) isomers of dinitro[2.2]paracyclophane. Compound 108^- is a class II system with a broad and unstructured intervalence absorption band in solvents of widely varying polarity. By contrast, 107^- is so close at the borderline that changing the solvent from acetonitrile to hexamethylphosphoramide tips it from class II to class III.¹¹⁹ Computational work explains where the difference in electronic coupling between the two isomers comes from: The nodal patterns for the singly occupied molecular orbital (SOMO) of 107^- and 108^- differ significantly: In 107^- there is positive overlap between the

Chart 36

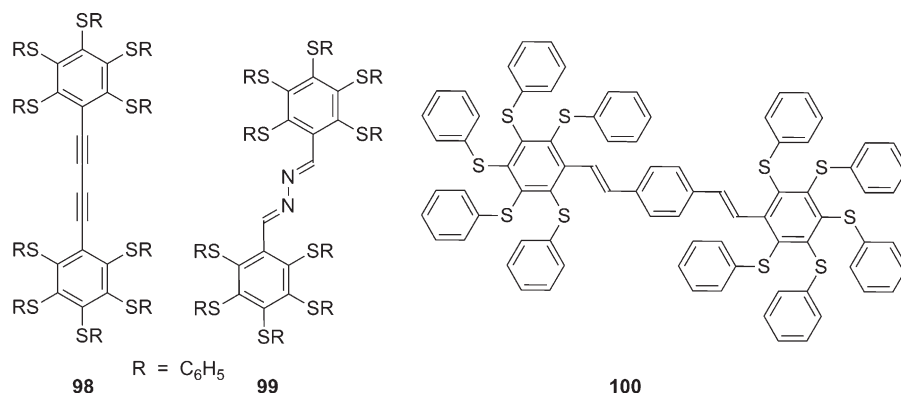
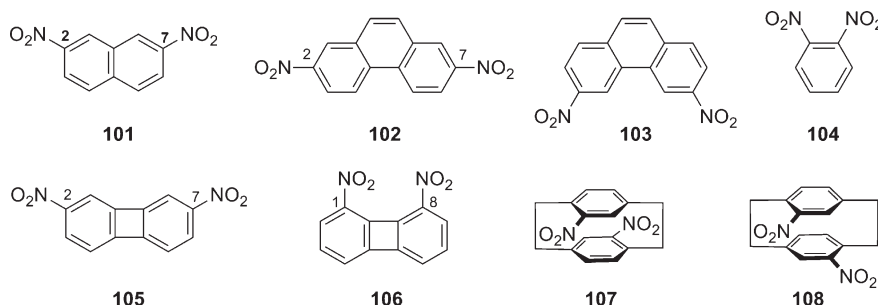


Chart 37



C–N bonds and the pseudo-geminal carbons on the opposite ring, while in **108⁻** this overlap is missing. Consequently, cross-ring communication is greater in the pseudo-para than in the pseudo-ortho isomer. The computations also indicate that in solvents which lead to small outer-sphere reorganization energies, the intervalence transition cannot simply be regarded as electron transfer between nitro groups.¹¹⁹

The same type of isomerism distinguishes the cyclophane-bridged bis(triarylamine) radical cations of **61** and **109** (Chart 38).¹⁰¹ Electronic couplings, calculated from intervalence absorption data using a three-state model, are 570 cm^{-1} for the pseudo-para isomer (**61⁺**) and 430 cm^{-1} for the pseudo-ortho isomer (**109⁺**). When compared to the dinitro systems **107⁻** and **108⁻**, this is a small difference which is due to the fact that the redox active triarylamine units are connected to the cyclophane through additional ethynyl groups that elongate the overall molecules. When the [2.2]paracyclophane spacer of **61** is replaced by a [3.3]paracyclophane unit (**63**), the electronic coupling between the two triarylamine moieties, as determined from intervalence absorption data, remains surprisingly constant. In line with this finding, temperature-dependent EPR measurements reveal very similar rates for intramolecular electron transfer in **61⁺** and **63⁺**.¹⁰² This is surprising because of the much shorter distance between π -faces in [2.2]paracyclophane with respect to [3.3]paracyclophane.

Differences between para- and meta-substituted benzene bridges in organic mixed valence systems were studied by many different research groups. Veciana and collaborators investigated the influence of bridge topology using *p*- and *m*-divinylbenzene spacers between polychlorinated triphenylmethyl units (**23**, **110**) (Chart 39).^{120,121} In their charge-neutral forms, these molecules

are stable diradicals, and mixed valence species are obtained upon one-electron reduction. The through-bond distances between the radical α -carbons in **23** and **110** differ marginally (24.1 Å versus 22.7 Å), but only **23⁻** displays an intervalence absorption band from which an electronic coupling of 121 cm^{-1} can be estimated. EPR spectroscopy reveals that at a temperature of 200 K the para isomer (**23⁻**) is a charge-localized system with the entire density of the unpaired spin on half of the molecule (slow exchange limit), whereas at 300 K the unpaired electron couples with two equivalent ^1H nuclei, indicating that the fast exchange limit for thermal charge transfer is attained at this temperature. The meta isomer (**110⁻**) exhibits EPR spectra consistent with the slow exchange limit at all temperatures between 200 and 300 K. These findings are in line with the differences between Kekulé- and non-Kekulé-substituted dinitroaromatic radical anions reported above.

The radical cation of bis(triarylamine) **111** (Chart 40) is essentially a topological isomer of **35⁺** with two additional methyl groups at the bridging benzene unit. In the para-substituted phenylenediamine **35**, the first two one-electron oxidations are 410 mV apart, but in the meta-substituted compound **111** the difference is only 160 mV.¹²² In the latter, the two redox units are in fact so effectively decoupled from one another that the biradical form (**111²⁺**) becomes stable in solution at -78°C . An analogous comparative study was performed with the carbanions of **112** and **113**.⁵³ Compound **112⁻** turned out to be a delocalized system on the EPR time scale, whereas in **113⁻** the unpaired electron is localized on one side of the molecule.

Lambert and Nöll explored the radical cations of the topological isomers **114** and **115** (Chart 41) as well as polymeric mixed valence compounds resulting from electrochemical polymerization

Chart 38

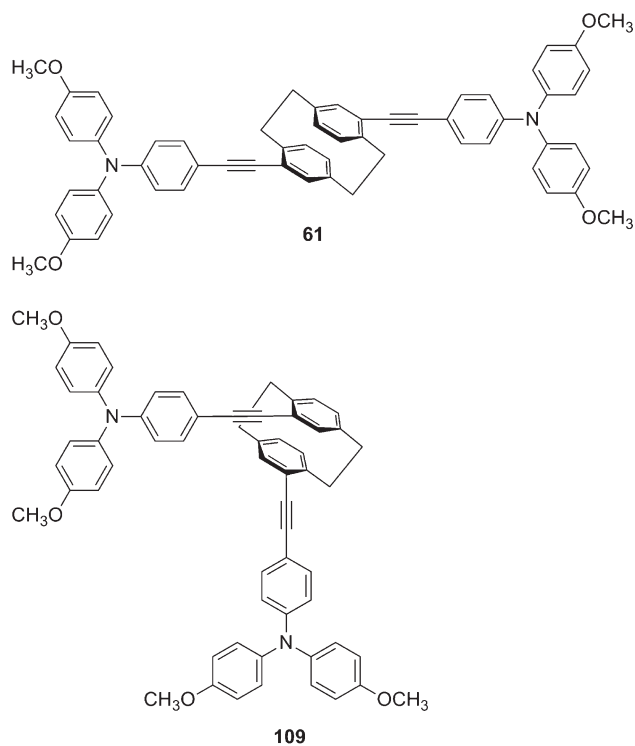
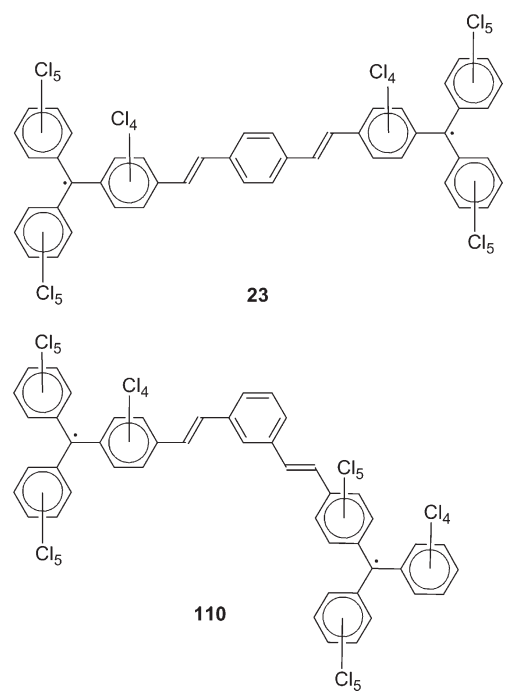


Chart 39



of the monomers **114** and **115**.⁷⁶ Contrary to most other triarylamine systems discussed herein, the terminal phenyl rings of **114** and **115** bear no substituents in the para position to the nitrogen atom, and this makes them susceptible to polymerization under application of oxidative potentials. The monomer **114**⁺ and its polymeric forms exhibit spectroscopic properties

Chart 40

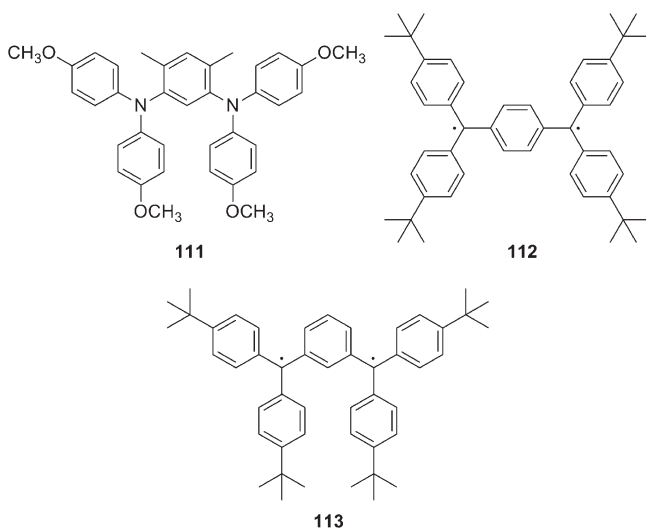
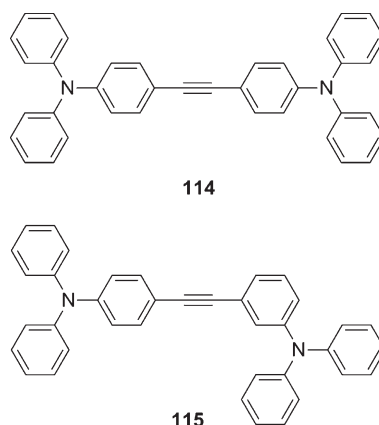


Chart 41



that are consistent with significantly stronger electronic coupling between individual redox units than in **115**⁺ and its polymeric forms. However, difficulties in determining extinction coefficients impede quantitative evaluation of the electronic coupling matrix elements in the polymers.

Lahil et al. investigated a series of extended tetrathiafulvalene molecules, among them the radical cations of **116** and **117** (Chart 42) in which two TTF units are fused to different sides of a benzene bridge.⁵⁹ The regiosomerism distinguishing **116** from **117** is reminiscent of the isomerism between para- and meta-substituted benzenes, and optical absorption spectra also reflect this structural analogy: **116**⁺ exhibits a broad intervalence absorption band centered around 1700 nm indicative of class II mixed valence behavior, while **117**⁺ appears to be a fully localized system without any electronic near-infrared absorptions. Structurally similar bis(tetrathiafulvalene) molecules with silicon or germanium double bridges and their mixed valence states have been investigated by Geoffroy and co-workers (section 3.3).¹²³

The issue of electronic coupling and π -conjugation across *p*-phenylene bridges as a function of twist angles has received considerable attention in research on charge and energy transfer.^{81,82}

Chart 42

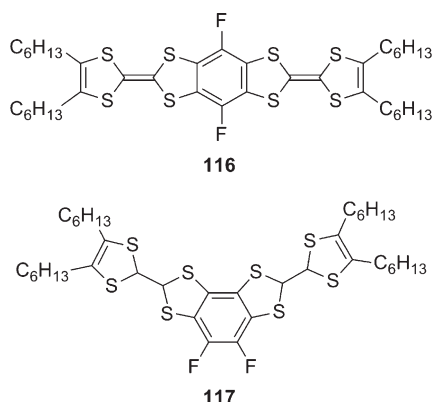
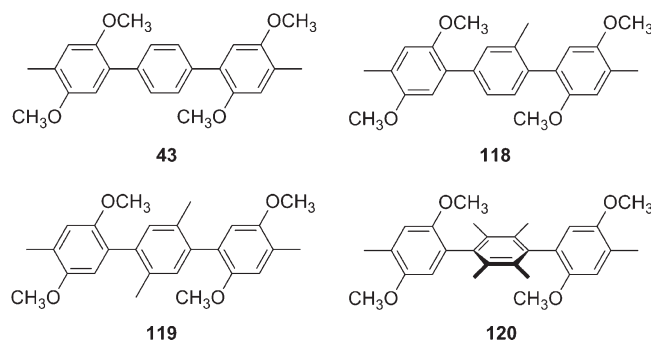


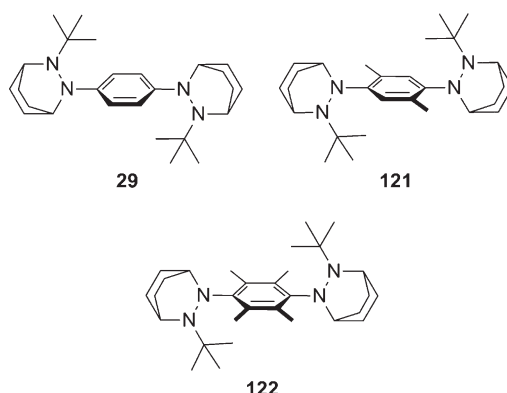
Chart 43



Among the many studies that were conducted in this context are several on organic mixed valence systems. Kochi and co-workers investigated conformation effects on electronic coupling between *p*-phenylene-bridged 2,5-dimethoxy-4-methylphenyl redox centers. Specifically, they compared four radical cations (**43**⁺, **118**⁺–**120**⁺, Chart 43) that have between 0 and 4 methyl substituents attached to a single bridging phenyl unit.⁸⁹ At a constant center-to-center distance of 8.6 Å between redox centers, Mulliken–Hush analysis of intervalence absorption data yields electronic coupling matrix elements of 760 cm^{−1} (**43**⁺), 377 cm^{−1} (**118**⁺), 325 cm^{−1} (**119**⁺), and 170 cm^{−1} (**120**⁺). In **43**⁺, a comparatively low torsion angle of ~30° between the individual phenylene planes enables a reasonably efficient π -conjugation pathway. In an X-ray crystal structure of the charge-neutral form of **120**, the torsion angle between the durene bridge and the two attached redox partners is 81.3°, which means that the π -conjugation pathway is essentially blocked.⁹⁰ EPR line broadening experiments show that this entails a decrease of the rate for thermal electron transfer at −100 °C from ~10¹⁰ s^{−1} in **43**⁺ to less than 3 × 10⁶ s^{−1} in **120**⁺.⁸⁹

Nelsen et al. performed a similar study on *p*-phenylene-bridged bis(hydrazine) radical cations (**29**⁺, **121**⁺, **122**⁺, Chart 44).^{40,124} Investigation of these molecules is somewhat complicated by the fact that they occur as a mixture of diastereomers and rotational conformers. X-ray crystallographic work shows that the twist angle between the phenylene spacer and the two attached redox units increases from 48 to 66° when going from **29**⁺ to **122**⁺. From intervalence absorption data, the electronic coupling is calculated to decrease from 2510 cm^{−1}

Chart 44



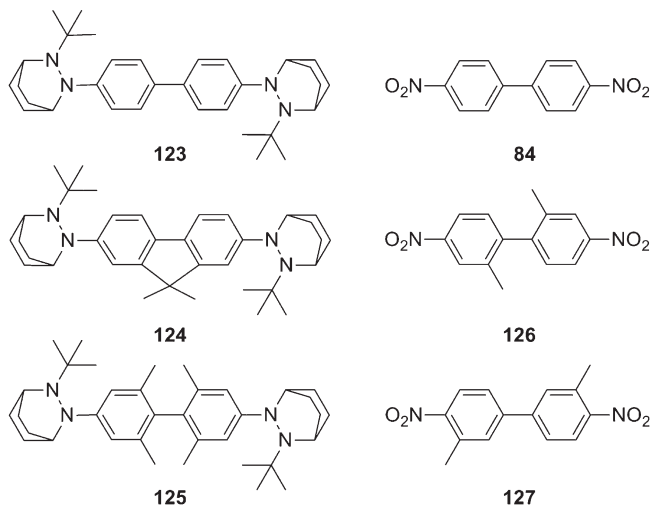
in **29**⁺ to 1710 cm^{−1} in **121**⁺ and 1150 cm^{−1} in **122**⁺. This factor of ~2 decrease upon exchange of an unsubstituted phenylene unit by a durene spacer is significantly less dramatic than the factor of ~5 decrease observed between **43**⁺ and **120**⁺ by Kochi and co-workers.⁸⁹ Nelsen et al. pointed out that the effective distance between redox centers is influenced by charge delocalization into the bridge,¹²⁴ and this may introduce errors in the calculation of electronic coupling matrix elements from intervalence absorption data. The electronic couplings in the hydrazine radical cations **29**⁺, **121**⁺, and **122**⁺ are remarkably insensitive to temperature changes, indicating that the average torsion angle is not much affected by temperature.¹²⁵ In **29**⁺, intramolecular electron transfer is too fast to measure by EPR spectroscopy, but thanks to decoupling of the two redox active units by bridge methylation, such measurements can be used to determine the rates for thermal electron transfer in **121**⁺ and **122**⁺. In dichloromethane at 200 K, $k_{ET} = 3.4 \times 10^7$ s^{−1} for **121**⁺ and $k_{ET} = 1.05 \times 10^7$ s^{−1} for **122**⁺.

A twist around a central phenylene bridging unit is also held (at least partly) responsible for the markedly different electronic structures of bis(hydrazine) **29**⁺ and diamine **33**⁺.⁷⁴ The former is a class II and the latter a class III system. The hydrazine groups are considerably more twisted relative to the phenylene bridge than the amines, and this makes H_{AB} significantly smaller in **29**⁺ than in **33**⁺. Together with the much larger inner-sphere reorganization energy in the bis(hydrazine) system, this accounts for the strongly different mixed valence properties of **29**⁺ and **33**⁺. Regarding electronic coupling strength, the *p*-phenylene-bridged bis(dioxaborine) system **20**[−] lies exactly between **29**⁺ and **33**⁺.⁴⁵

Molecules with biphenyl bridges have also proven useful for investigations of conformational effects on organic mixed valence. Nelsen et al. studied the radical cations of bis(hydrazines) **123**–**125** (Chart 45) by variable-temperature EPR spectroscopy and found that for **123**⁺ and **124**⁺ there is good agreement between the estimates of H_{AB} from optical spectroscopic and EPR data.¹²⁵ For the strongly twisted tetramethylbiphenyl-bridged compound (**125**⁺), no intervalence absorption band could be detected and EPR spectroscopy failed to provide an accurate estimate of k_{ET} . A comparative study of dinitro-substituted biphenyls yields similar results: The electronic coupling matrix element for **84**[−] amounts to 1100 cm^{−1}, while for **126**[−] $H_{AB} = 710$ cm^{−1} and for **127**[−] $H_{AB} = 540$ cm^{−1}.¹²⁶

Insight into the importance of twist angles in TMPD-related molecules was obtained by Yamamoto and co-workers in a

Chart 45



comparative study of the radical cations of molecules 128–133 (Chart 46).¹²⁷ The time scale for electron transfer in these strongly coupled class III systems reaches picoseconds, and hence infrared spectroscopy monitoring the N–H stretching absorption proved useful for investigation of intramolecular electron transfer in these radical cations. At temperatures below ~ 200 K two separate N–H vibration bands due to neutral and cationic nitrogen centers were observable, while at higher temperature there was coalescence to a single signal.^{127,128} Analysis of the infrared data with Bloch-type equations gave results that were consistent with those obtained from analysis of intervalence absorption data in the framework of Marcus–Hush theory. Rates for thermal electron transfer were found to vary between $3.9 \times 10^{10} \text{ s}^{-1}$ for 130^+ to $2.4 \times 10^{11} \text{ s}^{-1}$ for 128^+ , and optical absorption spectroscopy gave electronic coupling matrix elements that varied from 3440 cm^{-1} (130^+) to 3780 cm^{-1} (128^+).¹²⁷

An extreme case of twisting was obtained in the spiro-fused bis(triarylamine) compound 134 (Chart 47) from Hirao et al.¹²⁹ In this molecule, two redox active triarylamine-based π -systems are linked perpendicularly to one another through a spiro Si atom. The first two one-electron oxidation waves for this molecule are 160 mV apart, indicating that, despite their orthogonal geometry, there is significant electronic coupling between the two triarylamine moieties. EPR measurements on 134^+ in the temperature range between 203 and 324 K demonstrate that a thermally activated intramolecular electron transfer is active at room temperature ($k_{\text{ET}} = 4.2 \times 10^9 \text{ s}^{-1}$), but an intervalence absorption band could not be detected.

A similarly large twist angle (close to 90°) is predicted by computational work for the two bicyclooctyl-substituted amines in molecule 135 (Chart 48).¹³⁰ Yet, an intervalence absorption band for 135^+ is easily detectable, and this was attributed to the ease of twisting about the oxygen–aryl bonds. It was estimated that the energetic cost associated with torsion from 90 to 70° is only ~ 0.26 kcal/mol for this particular linkage.

Conformational effects also play a role in the tetra- and hexacyclic bis(hydrazine) compounds 136–139 (Chart 49) from the Nelsen group.¹³¹ In the methylated molecules (136 and 137), the intervalence absorption bands are observed at substantially lower energies than for analogous molecules with

bulkier substituents (138 and 139). Sterically more demanding substituents hinder flattening at the nitrogen centers following oxidation, and hence the inner-sphere reorganization energy associated with intervalence electron transfer is increased in $138^+/139^+$ with respect to $136^+/137^+$. In addition, the tetra-cyclic radical cations 136^+ and 138^+ have detectably smaller electronic couplings than the hexacyclic analogues 137^+ and 139^+ , despite the presence of very similar double 4- σ -bond pathways connecting the two dinitrogen units. However, it has not been possible to identify any single structural factor that is responsible for this.

3.3. Influence of the Bridge Redox States

When substituents are attached to conjugated bridges, they may not only induce changes in the bridge conformation but also affect the redox potentials of the bridge. This in turn can have an important influence on the electronic coupling that is mediated by the bridge. There are several studies from the field of organic mixed valence that nicely illustrate this phenomenon. Building on their own prior work on bis(triarylamine) radical cations, Lambert and co-workers explored the influence of bridge redox states on electron transfer in a series of radicals that is based on prototype system 53^+ .¹³² The redox potential of the bridge was modulated through replacement of the central phenyl unit by naphthalene (140, Chart 50), anthracene (141), *p*-dimethoxybenzene (142), and benzo-15-crown (143) spacers. A three-state model, involving the one-electron oxidized states of the bridge, had to be employed for analysis of the intervalence absorptions of the radical cationic forms of these species. Electronic coupling between the bridge and the triarylamine redox centers was found to be particularly strong for 141^+ and 142^+ which have central anthracene and *p*-dimethoxybenzene units. This was attributed to the comparatively low oxidation potentials of these two particular bridge units, and the resulting small energy gap between the one-electron oxidized state of the bridge and those of the triarylamine centers.^{132,133} According to superexchange theory,²⁰ this is beneficial for hole tunneling (section 1.2).²² In the case of 141^+ and 142^+ this energy gap may even be sufficiently small in order for a hopping mechanism to become active.¹³² Complexation of Ca^{2+} into the benzocrown of 143^+ decreases the triarylamine-bridge coupling from 950 to 480 cm^{-1} . It was left open whether this is due to a field effect caused by the dipositive charge of the calcium cation or induced by conformational changes of the crown ether that entail modification of the overlap between oxygen lone pairs with the phenylene ring.

These results are in line with the observation of accelerated (photoinduced) hole transfer in donor–bridge–acceptor systems that incorporate anthracene and dimethoxybenzene bridging units,^{134–138} and they are similar to the findings reported by Nelsen et al. for related bis(hydrazine) mixed valence species. Specifically, Nelsen and Ismagilov found the rate of intramolecular electron transfer in the *p*-xylene bridged bis(hydrazine) cation 121^+ to be measurable by EPR spectroscopy, while the structurally very similar *p*-dimethoxybenzene bridged radical cation 144^+ (Chart 51) exhibited a rate beyond the EPR time scale.¹¹³ For the anthracene-bridged bis(hydrazine) system 145, molecule 122 with its durene spacer is the best reference point, because of similar twist angles between the bridge and the two attached redox units in these two cases. Variable-temperature EPR spectroscopy shows that the barrier to thermal electron transfer is 29% (1.7 kcal/mol) lower in 145^+ than in 122^+ .¹³⁹

Chart 46

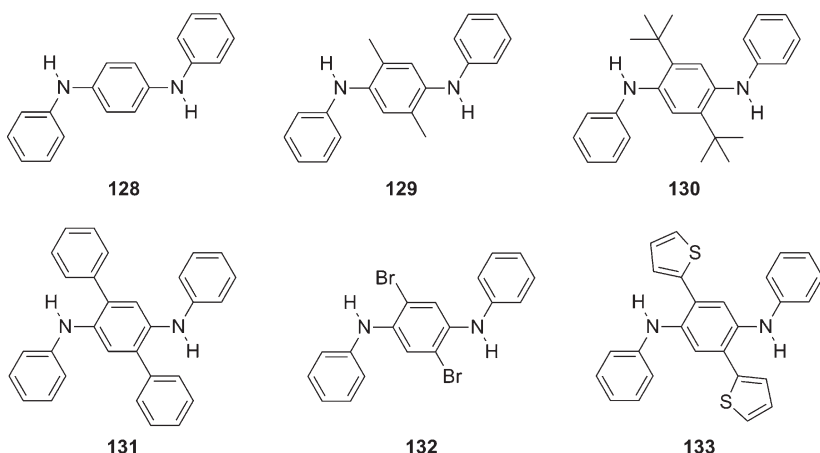


Chart 47

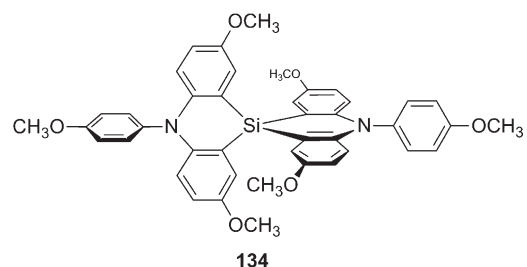


Chart 48

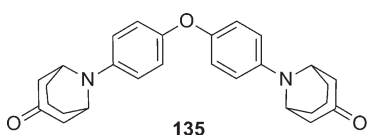
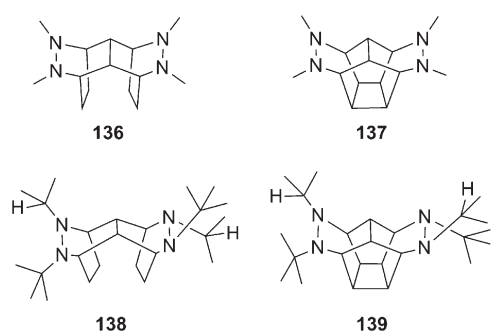


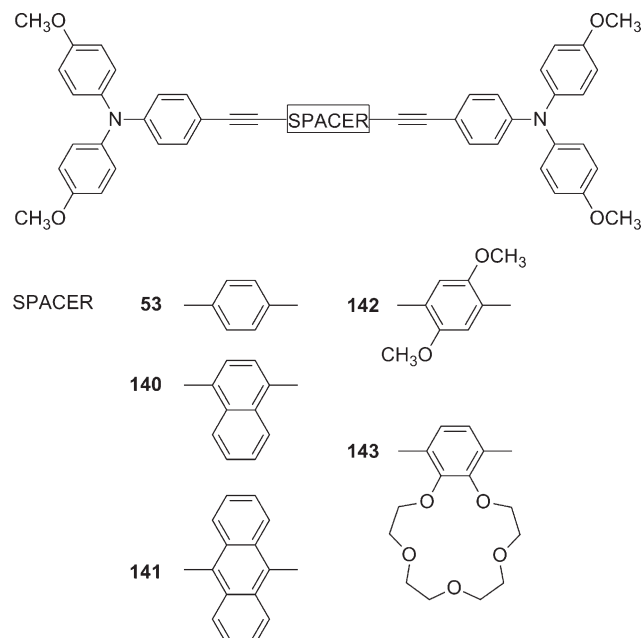
Chart 49



This was attributed to an energetically low lying oxidized state of the bridge.

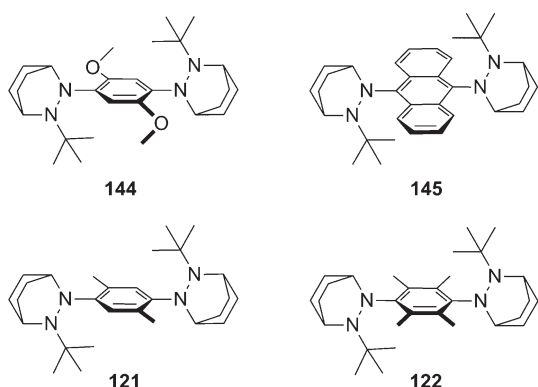
Lambert's bis(triarylamine) molecules 35 (Chart 52), 146, and 147 are analogues of 53, 140, and 141 without ethynyl linkers.¹⁴⁰ Asymmetric, weakly solvent-dependent intervalence absorption bands point toward assignment of 146⁺ and 147⁺ to

Chart 50



class III or at least to class III/class II borderline. Analysis of intervalence absorption spectra and electronic structure calculations (calibrated by experimental photoelectron spectroscopy data) concur that the electronic coupling between the two triarylamine units decreases by roughly a factor of 2 between the benzene- (35^+) and the anthracene-bridged system (147^+). The trend for electronic coupling in the benzene–naphthalene–anthracene series here is exactly opposite to that observed for the molecules with additional ethynyl linkers isolating the central bridge units (53^+ , 140^+ , and 141^+). Steric effects must be responsible for this behavior: In 35^+ , the bridging phenyl unit is twisted by 27° with respect to the plane formed by the two N–C_{anisyl} bonds, whereas in 147^+ a twist angle of 62° was calculated. The gain in electronic coupling obtained by decreasing the energy gap between the triarylamines and the bridge is thus outweighed by the loss caused through unfavorable mutual orientation. The presence of additional ethynyl linkers in 141^+

Chart 51



preserves effective π -coupling through the central anthracene unit because there is not enough steric strain that would impede coplanarity. The comparison of the benzene–naphthalene–anthracene systems with and without ethynyl linkers (53^+ , 140^+ , 141^+ versus 35^+ , 146^+ , 147^+) is a nice illustration of the fact that the magnitude of electronic coupling is governed by a subtle interplay of energetic and geometric factors, as predicted by superexchange theory.²⁰

Methyl-substitution of molecular phenylene bridge units does also strengthen the electronic coupling pathway for hole tunneling between triarylamine redox centers, but the effect is somewhat weaker than in the case of methoxyl groups. For the radical cation of **53** (Chart 53), the electronic coupling amounts to 990 cm^{-1} , whereas in **148**⁺ H_{AB} has increased to 1320 cm^{-1} . Interestingly, this appears to be accompanied by a $\sim 500\text{ cm}^{-1}$ increase in reorganization energy. Thus, there is plenty of evidence that substitution of phenylene bridges with electron-donating methoxyl- (**142**⁺, **144**⁺) or methyl groups (**148**⁺) enhances hole tunneling pathways. Electron-withdrawing cyano substituents have the opposite effect, as seen from the comparison of the radical cations of **55** and **149**.¹⁴¹ The room-temperature EPR spectrum of **149**⁺ exhibits a five-line pattern indicative of interaction of the unpaired spin with two nitrogen centers and full charge delocalization, while at 191 K a three-line spectrum shows that the odd electron is localized on one triarylamine unit on the EPR time scale. In the same temperature range, **55**⁺ remains in the fast exchange limit, and charge localization cannot be induced by cooling. Analysis of the intervalence absorption data is in line with faster electron transfer in **55**⁺ than in **149**⁺: The electronic coupling matrix elements calculated through evaluation of the transition dipole moments for the intervalence absorption bands are 700 cm^{-1} for **55**⁺ and 470 cm^{-1} for **149**⁺.^{98,141}

A different strategy to tune the energy gap between the bridge states and those of the attached redox centers is to vary the oxidizing (or reducing) power of the terminal redox units while leaving the bridge unaltered. This is relatively straightforward to accomplish for triarylaminies because their commonly used methoxyl para substituents can easily be replaced by other, less electron-donating substituents. An investigation of the radical cations of **51** (Chart 54) and **151**–**153** is relevant in this context.¹⁴² The energetic position of the intervalence absorption band in these four systems was found to vary linearly with the splitting between the first oxidation potentials of the two differently substituted triarylamine units. The somewhat surprising outcome of a two-state model analysis is a nearly constant

electronic coupling matrix element of $1020 \pm 50\text{ cm}^{-1}$ for all four radical cations, despite significant variations in the triarylamine-bridge energy gap.¹⁴²

Modulation of the energy gap between the redox sites and the connecting bridge also occurs when a biphenyl spacer is replaced by a fluorene unit.¹⁴³ The two types of bridges hold the redox centers at nearly identical distance, but oxidation of fluorene occurs at substantially lower potentials than oxidation of biphenyl. The presence of energetically low-lying one-electron oxidized bridge states strengthens the superexchange pathway for hole tunneling, in the same way as seen above for methoxyl or methyl substitution of simple phenylene units. However, this effect is superposed by increased electronic coupling due to lower torsion angles between the individual phenyl units in fluorene with respect to biphenyl. The combined effects of low-lying bridge energy levels and small twist angles lead to the observation of electronic coupling matrix elements of 630 cm^{-1} for the fluorene system **154**⁺ (Chart 55) compared to 430 cm^{-1} for the biphenyl system **44**⁺.⁸⁹ A similar observation is made for the bis(hydrazine) systems **123**⁺ and **124**⁺.¹²⁵ There, H_{AB} is a factor of 1.13 larger for the fluorene- than for the biphenyl-bridged system. Interestingly, for the dinitroaromatic radical anions **84**[–] and **85**[–] the opposite observation was made:^{17,126} The biphenyl-bridged system (**84**[–]) has a slightly stronger electronic coupling (3450 cm^{-1}) than the fluorene-bridged anion **85**[–] (3395 cm^{-1}), despite the obvious advantage of a flatter bridging geometry in the latter. However, by contrast to the hole-transfer systems **44**⁺ and **154**⁺ as well as **123**⁺ and **124**⁺, charge transfer in the dinitroaromatic radical anions **84**[–] and **85**[–] proceeds by an electron-transfer pathway.¹⁷ Thus, when the bridge becomes easier to oxidize but more difficult to reduce, this increases the energetic barrier for electron tunneling and decreases electronic coupling between the nitro groups.

Comparison of mixed valence molecules belonging to the violene and cyanine families of radical cations does also provide evidence for the importance of small energy gaps between the bridge and the terminal redox sites. Violene radicals have $2n + 3$ π electrons on $2n + 2$ sp^2 hybridized atoms, while cyanine radicals have $2n + 4$ π electrons on $2n + 3$ sp^2 hybridized atoms.⁹² The radical cations of molecules **28** (Chart 56), **33**, **47**, and **48** are examples of the violene family, while **155**⁺–**158**⁺ are examples of cyanine radicals.

The distance dependence of H_{AB} along the two different series comprised of four radicals is identical (Figure 9), and a distance decay constant of $\beta_n = 0.3$ was determined in both cases.⁶⁵ However, at equal number of σ -bonds between the nitrogens, the absolute values of the electronic coupling matrix elements in the cyanine radicals are nearly twice as large as in the violene systems. When extrapolated to van der Waals contact between redox centers, $H_{AB} = 74.4\text{ kcal/mol}$ for the cyanines and $H_{AB} = 41.8\text{ kcal/mol}$ for the violenes. This discrepancy can be attributed to smaller tunneling-energy gaps associated with hole transfer in the cyanines compared to violenes. Thus, the violene–cyanine comparison shows that, due to bridge redox effects, an entire family of molecules can be predestined to better electronic coupling than another one.

The use of five-membered aromatic rings as bridging groups between triarylamine redox centers does also lead to observations that illustrate the importance of the bridge redox states. Nöll et al. found that 1,3-azulene has the ability to mediate strong electronic coupling between triarylaminies because it has a very low first oxidation potential that leads to a small energy barrier for

Chart 52

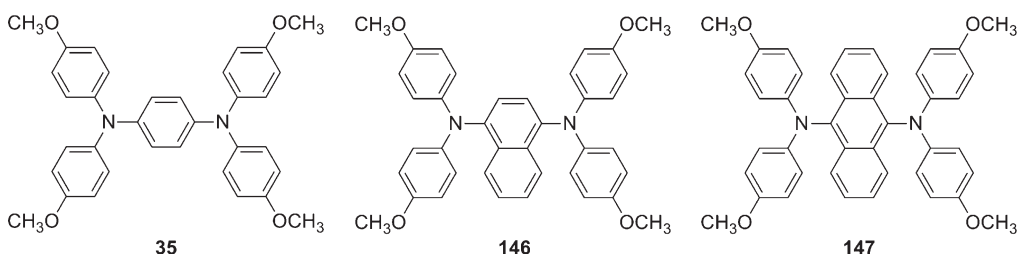


Chart 53

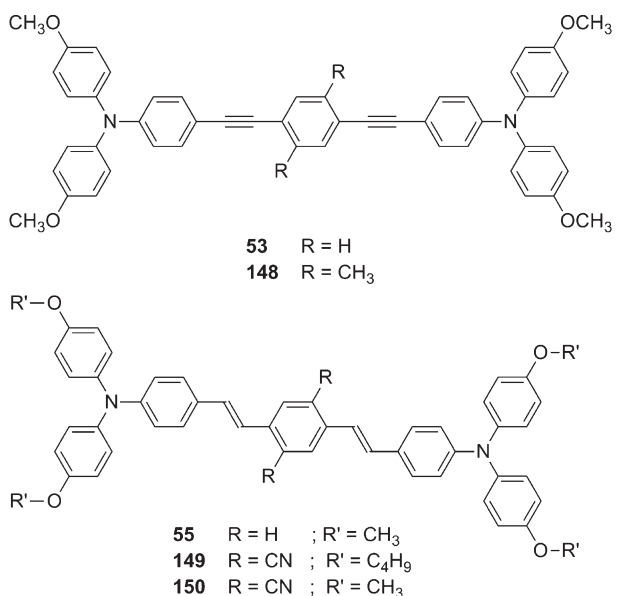
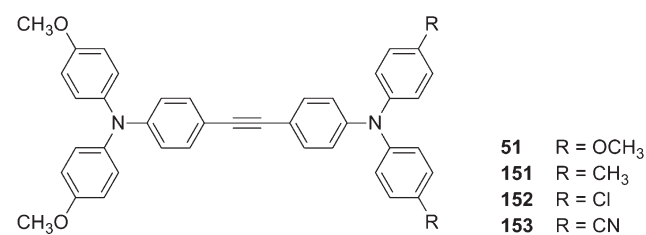


Chart 54



intramolecular hole transfer.¹⁴⁴ On the basis of intervalence absorption band analysis, the electronic coupling in the azulene-bridged radical cation of 159 (Chart 57) is almost equally as strong as that in the isomeric naphthalene-bridged system 146⁺ (3900 cm^{-1} versus 4000 cm^{-1}). At first glance, this is somewhat surprising because for 159⁺ one might expect the two amines to be only weakly coupled given the pseudo-meta topology resulting from 1,3-substitution of azulene. Apparently, this effect is compensated by the low oxidation potential of azulene. In molecule 160, tertiary amine redox units were attached to the 2- and 6-positions of azulene.¹⁴⁵ In this case, the bridge exerts a push-pull effect on the overall molecule: One redox unit is attached to the electron-rich five-membered ring and the other to the electron-poor seven-membered ring. This introduces a redox

asymmetry of about 1200 cm^{-1} into the overall system, while providing an electronic coupling $H_{AB} = 1140\text{ cm}^{-1}$ for optically induced hole transfer between the two slightly unequal redox centers.

Other five-membered rings that were used as bridges in bis(triarylamine) mixed valence systems are furan (161, Chart 58) and thiophene (162, 163).¹⁴⁶ While 161⁺ and 162⁺ are ordinary mixed valence radicals with intervalence absorption bands between 4000 and 8000 cm^{-1} , 163⁺ is to be considered a bridge-localized system with most of the charge density located at the 3,4-ethylenedioxythiophene unit. Thus, in the latter, the linker connecting the two triarylamines has such a low oxidation potential that it is no longer a simple bridge but has become the most redox active unit in the molecule.

In the radical cationic forms of the fused bis(tetrathiafulvalene) molecules 116 (Chart 59) and 164, the electronic structure of the bridge has a big influence on intervalence electron transfer between the two TTF moieties.¹⁵ Compound 116⁺ is a class II system with $H_{AB} \approx 1000\text{ cm}^{-1}$, but 164⁺ is a class III system with an electronic coupling twice as large. The replacement of the bridging (fluorinated) benzene spacer by a pyrazine unit causes a substantial stabilization of the bridge HOMO and LUMO. This leads to stronger superexchange interactions because the energy gap between the TTF and the bridge states becomes smaller. Molecules 165 and 166 with their central 1,4-disilicon and 1,4-digermanium six-membered rings are structurally similar bis(tetrathiafulvalene) systems. One might expect bridge redox effects to lead to different electronic couplings in 165⁺ and 166⁺, but it was merely reported that both radical cations appear to be fully delocalized systems on the EPR time scale, and precise values of H_{AB} were not determined.¹²³

In the context of TTF-containing organic mixed valence species it is worth noting that the tetrathiafulvalene motif has also been used as a bridging unit connecting other redox centers. For instance, in molecules 167 (Chart 60) and 168 a TTF unit bridges two benzoquinone or naphthoquinone moieties.¹⁴⁷ The radical anion of 167 is a true mixed valence species in which electron delocalization between the two quinones becomes thermally activated above 260 K, the activation energy being roughly 8 kcal/mol. It has been noted that TTF has such a small ionization potential that it is a very promising material for molecular wires that closely match the work function of metal layers on electrodes.¹⁴⁸

Differences between the redox states of the bridge and those of the attached benzoquinone or imide units also play an important role in Miller's early investigations of diquinone and diimide systems.^{50,87} The anthracene-bridged diquinone radical anion 14⁻ is a class II system, whereas the anthracene-bridged diimide radical anion 41⁻ belongs to class III. The reason for this is a

Chart 55

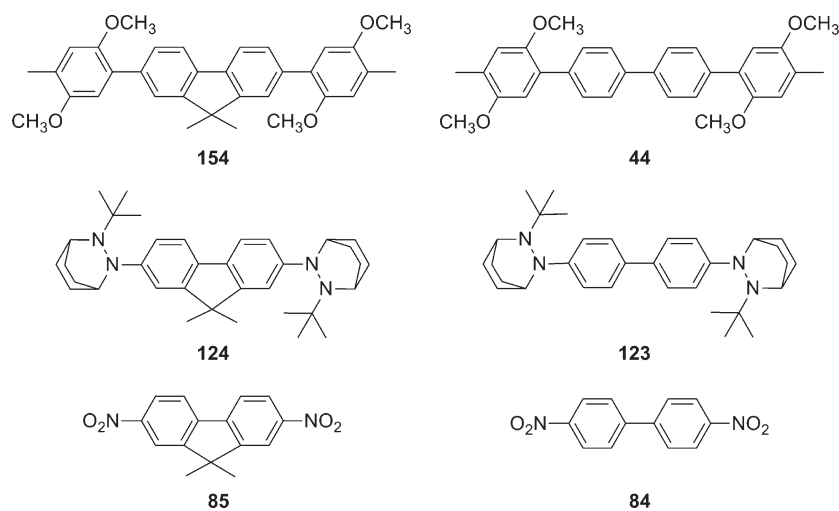


Chart 56

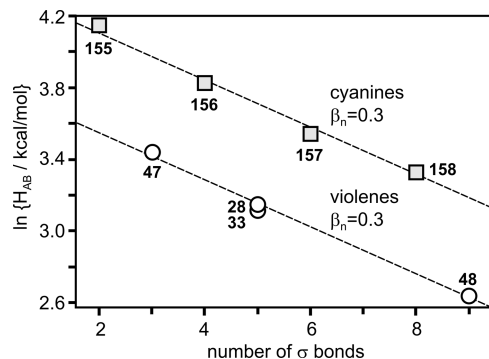
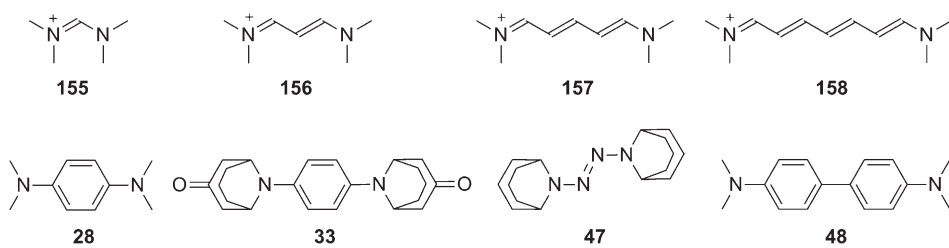


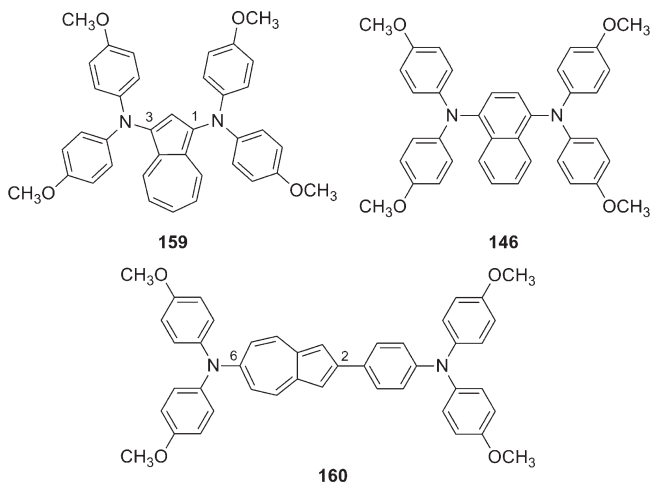
Figure 9. Distance dependence of H_{AB} along a series of four violene (open circles) and cyanine mixed valence compounds (gray filled squares).⁶⁵ The slopes of the linear regression fits (dashed lines) are -0.15 in both cases, yielding $\beta_n = 0.3$ for the electron-transfer rates. Adapted with permission from ref 65. Copyright 1998 American Chemical Society.

smaller energy gap between the one-electron reduced states of anthracene and the imide moieties than between anthracene and the quinone units.¹⁴⁹

4. MULTIDIMENSIONAL ORGANIC MIXED VALENCE

When more than two redox active units are arranged in nonlinear fashion, multidimensional mixed valence systems can be obtained. With purely organic systems, pioneering work in

Chart 57



this area was made by Bonvoisin, Launay, and Veciana. Both the one- and the two-electron reduced forms of the perchlorated species 169 (Chart 61) are mixed valence systems.¹⁵⁰ The charge-neutral form of 169 is a chemically and thermally stable organic triradical with a quartet ground state. It was anticipated that in its mono- and dianionic forms, intramolecular electron transfer between magnetically coupled redox centers could be observed. Indeed, 169^- exhibits an intervalence charge-transfer

Chart 58

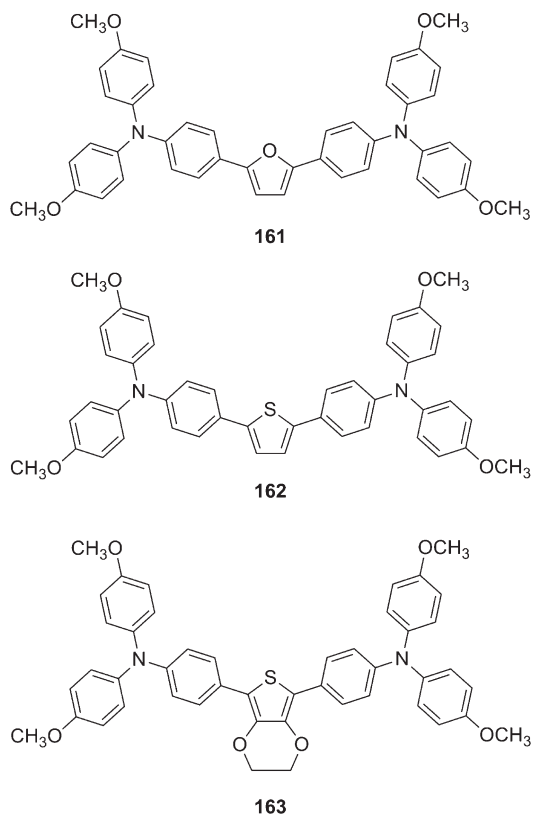
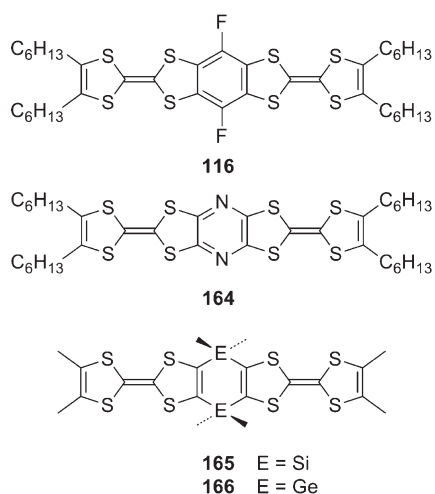


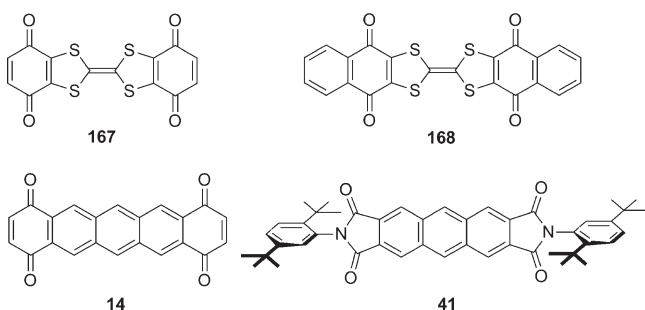
Chart 59



band around 2900 nm, and variable-temperature EPR spectroscopy established the presence of a triplet ground state. Thus, **169**[−] is a rare example of a purely organic mixed valence high-spin species. In the dianion, electronic coupling between the individual redox centers is somewhat larger than in the mono-anion (392 cm^{-1} versus 320 cm^{-1}).

Similar research was performed with triarylamine instead of polychlorinated phenyl redox units.¹⁵¹ Compounds **170**⁺ and **170**²⁺ are both class II mixed valence systems with electronic

Chart 60



couplings of 204 and 224 cm^{-1} based on intervalence band analysis.¹⁵² These rather small couplings reflect the meta topology of the central phenyl unit. The intervalence absorption bands of the mono- and dications of **170** are nearly identical. Therefore, a situation in which two electrons move toward a hole cannot easily be distinguished from a situation in which one electron can move toward two holes (Figure 10).

In molecule **171** (Chart 62) the 3-fold symmetry is lost, and in its mixed valence mono- and dicationic forms there are now two distinguishable pathways for electron transfer: One that formally occurs between nitrogen centers separated by two phenyl spacers and one in which the nitrogens are three phenyl rings apart. The intervalence absorption bands caused by these two electron transfers cannot be resolved completely, yet based on a two-dimensional Hush analysis, electronic coupling matrix elements of 387 and 230 cm^{-1} for the shorter and longer pathways in **171**⁺ were estimated.¹⁵³

EPR investigations of the radical monocation of the C_3 -symmetrical tris(diarylaminobenzene species **172** suggested that at $-78\text{ }^\circ\text{C}$ the unpaired spin is delocalized equally over all three nitrogen centers, but detailed investigations of intervalence absorptions were not undertaken.¹⁵⁴ At higher temperatures, **172**⁺ and **172**²⁺ as well as related 1,3,5-tris(diarylaminobenzene radicals with para substituents other than *tert*-butyl appear to be unstable.

Ito and co-workers investigated a more complicated system (**173**) that is based on the same central structural motif as molecule **172** but has additional diarylamine units attached at the periphery of each of the three branches of the star-shaped molecule.¹⁵⁵ To elucidate the electronic structure of its cationic forms, simultaneous investigation of a reference molecule (**174**) turned out to be useful. Molecule **174** represents a substructure of **173**, and its cyclic voltammogram exhibits three well-separated and reversible one-electron oxidation waves. However, in the voltammogram of the star-shaped molecule **173**, there are not simply three reversible three-electron waves as could be expected for the superposition of three mutually independent molecular subunits of type **174**, but there are at least five individual oxidation waves. This is a manifestation of electronic coupling among the peripherally substituted triarylamines via the central 1,3,5-substituted phenyl unit. However, EPR spectroscopy shows that these couplings are weak: Between 203 and 293 K the monocation of reference molecule **174** is a fully delocalized system, but in **173**⁺ the hole is localized on one of the three identical branches. Thus, as expected from the results presented in section 3.2, the para-disubstituted phenyls within the subunit **174** mediate much stronger electronic coupling than the meta linkages of the central phenyl unit in **173** that interconnects the

Chart 61

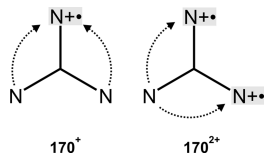
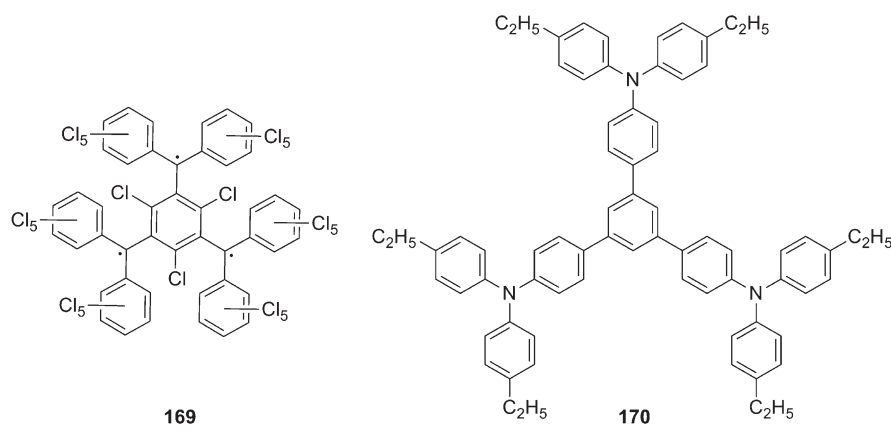


Figure 10. Possibilities for electron transfer (dashed arrows) in the mixed valence monocation (left) and dication (right) of a star-shaped triarylamine compound.¹⁵¹

three individual branches. Consequently, in optical absorption spectra of 173^+ only the intervalence absorption band due to charge transfer *within* a given branch can be observed, whereas intervalence charge transfer between adjacent branches remains undetected.

A pseudo-tetrahedral organic mixed valence system was reported by Lambert and co-workers.¹⁵⁶ The phosphonium cation 175^+ (Chart 63) provides an elegant way of connecting four triarylamine redox centers in a highly symmetrical three-dimensional structure. Compound 175^+ can be reversibly oxidized up to the pentacationic form, and all five redox species have an intense absorption around 800 nm, but only 175^{2+} , 175^{3+} , and 175^{4+} show an additional broad band occurring as a weak shoulder at 850 nm. This weak band was assigned to intervalence charge transfer and analyzed in the framework of a four-dimensional Marcus–Hush approach. This leads to the conclusion that $H_{AB} = 260 \text{ cm}^{-1}$ for all three mixed valence species, a value that is close to the electronic couplings typically observed for *m*-phenylene-bridged triarylamines with comparable N–N distances. The question of possible pathways for electron transfer is particularly interesting in these tetrahedral systems: It is conceivable that electron transfer does not proceed along the backbone and the central phosphorus atom of the tetrahedron, but that it is mediated by solvent molecules that are located between its four legs. Investigations of photoinduced electron transfer have demonstrated that solvent mediated electron tunneling can be an efficient alternative to tunneling across rather insulating bridges.^{23,157} An additional interesting aspect of the tetrahedral system is the dimensionality of the electron transfer pathway in the different mixed valence forms: While in 175^{2+} and 175^{4+} the thermal electron-transfer pathway is one-dimensional, there exist two possibilities for 175^{3+} , namely, a concerted two-dimensional process and a

two-step one-dimensional way. Theoretical analysis indicates that the latter process is more probable.¹⁵⁶

The hexakis(triarylamine) system **176** (Chart 64) is accessible using the tolane molecule **51** as a starting material for Hagihara cross-coupling.¹⁵⁸ The cyclic voltammogram of **176** shows only one unresolved oxidation wave that involves six electrons and leads to 176^{6+} . In the course of oxidation, a near-infrared absorption band becomes observable, and since it is impossible to control experimentally the precise oxidation state of **176**, this band was attributed to intervalence charge transfer in the trication of **176** for which the intervalence band should be most intense. Computational work suggests that 176^{3+} has a ${}^4\text{A}_2$ ground state, but there is also a ${}^2\text{E}$ state that is energetically so close that it is populated at room temperature. Since there are ${}^4\text{E}$ as well as ${}^2\text{E}$ and ${}^2\text{A}$ excited states, there is a multitude of spin-allowed transitions that may contribute to the observed intervalence absorption band, and thus its detailed analysis becomes very difficult.

A nearly identical system (**177**) was investigated by Kochi and co-workers.¹⁵⁹ Compound **177** differs from **176** only in the presence of ethyl groups at the place of anisyl moieties. The important physical difference to **176** is that the cyclic voltammogram of **177** displays four discernible waves, namely, three one-electron oxidations all separated by at least 100 mV followed by one three-electron oxidation. This allows the selective formation of the monocation of **177** and in-depth investigation of its intervalence absorption band. For this purpose, the two-state model was extended to include six equivalent redox centers, taking into account only equivalent interactions between neighboring redox units. This analysis leads to $H_{AB} = 1600 \text{ cm}^{-1}$ and $\lambda = 5400 \text{ cm}^{-1}$, indicating that 177^+ is close to the class II/class III borderline with almost complete toroidal charge delocalization.

To overcome the problem of selective formation of one specific redox state in a hexakis(triarylamine) species, Lambert and Nöll reverted to molecule **178** which has three nitrogens substituted with *p*-anisyl groups and three nitrogens with *p*-tolyl substituents.¹⁶⁰ This leads to voltammograms comprised of two well-separated three-electron waves, corresponding to consecutive oxidation of the three anisyl nitrogens prior to the three less electron-rich tolyl nitrogens. Consequently, selective formation of 178^{3+} is possible, and its intervalence absorption can be analyzed in the framework of a multidimensional Mulliken–Hush formalism. There are 20 diabatic states that need to be

Chart 62

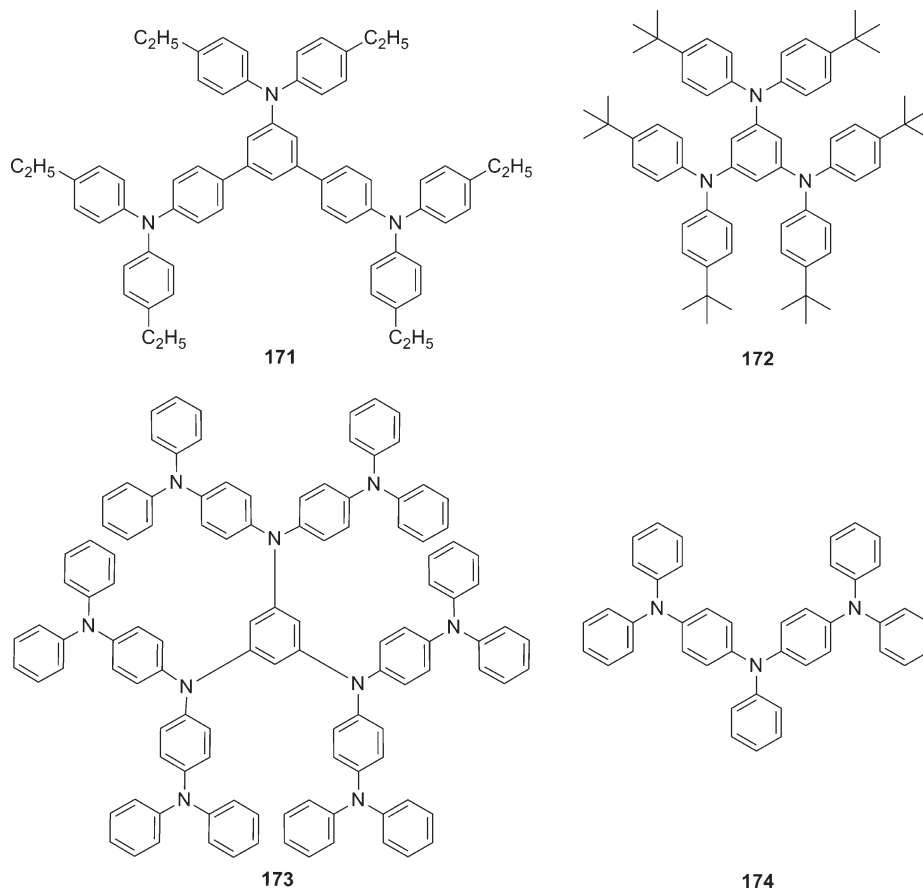
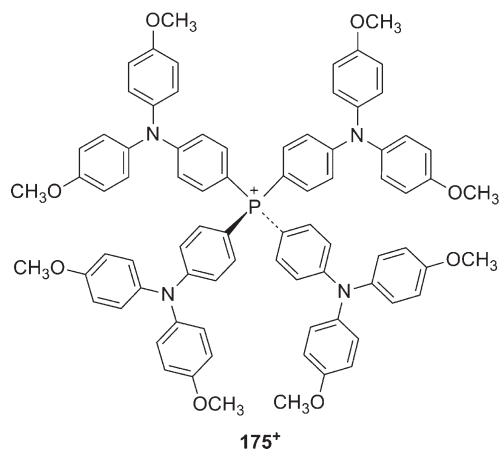
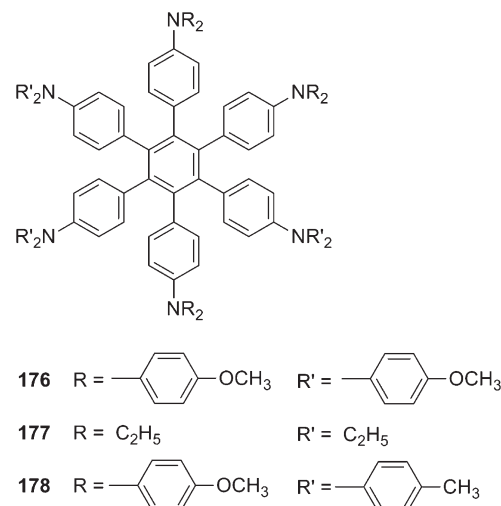


Chart 63



taken into account, and in order to simplify the problem, only electronic couplings between adjacent triarylamine branches (substituted in the *ortho* position at the central phenyl unit) were taken into account. An electronic coupling matrix element of 460 cm⁻¹ was found for 178³⁺. This value is almost a factor of 3 smaller than that found for the tolane monomer 51⁺ ($H_{AB} = 1200 \text{ cm}^{-1}$) in which there is an equal number of bonds between the two nitrogen centers. Twisting of the connecting aryl units in the sterically crowded 178³⁺ is likely

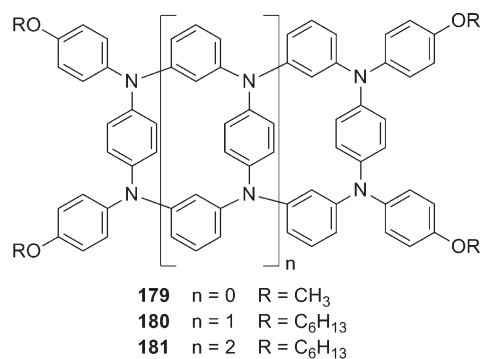
Chart 64



to be one of the main reasons for this strongly diminished electronic coupling.

Thanks to advances in palladium-catalyzed amination reactions, it has become possible to synthesize well-defined ladder materials comprised of several triarylamine units.¹⁶¹ Molecules 179–181 (Chart 65) may be regarded as oligomers of

Chart 65



tetraaryl-*p*-phenylenediamine. The smallest member of this series (**179**) has four clearly distinguishable one-electron oxidation waves, but for **180** and **181** the cyclic voltammograms become less straightforward to interpret. Chemical oxidation of **179**–**181** with 1 equiv of Pb(OAc)₄ leads to the formation of EPR active species that exhibit intervalence absorptions. On the basis of the through-space distance (4.8 Å) between two phenylenediamine units in **181**, the two-state Hush model yields $H_{AB} \approx 2350 \text{ cm}^{-1}$ for coupling between two rungs of the ladder-type molecule, while on the basis of the through-bond distance (10.5 Å) $H_{AB} \approx 1100 \text{ cm}^{-1}$ was estimated.¹⁶¹ Which one of the two pathways is more important is not clear, but it is interesting to note that a crystal structure of **180** shows that the three individual *p*-phenylenediamine units are canted from the plane formed by the nitrogens and the *m*-phenylene units. This may be beneficial for through-space interaction between individual (and almost coplanar) *p*-phenylenediamine units.

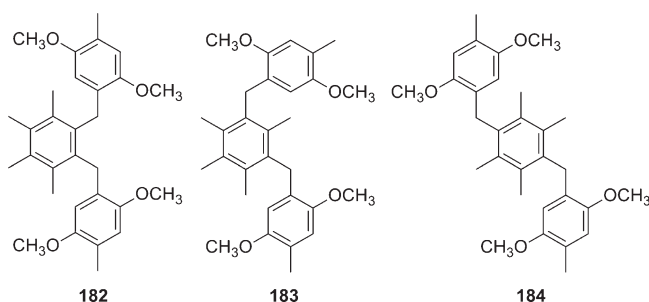
Müllen and co-workers investigated a series of hexa-peri-hexabenzocoronenes which, when oxidized to their radical cationic forms, represent multidimensional organic mixed valence systems.¹⁶² While these are spectacular molecules, relatively little information regarding intramolecular electronic coupling between the individual redox units was extracted from these systems. So far, the focus of this work seems to have been on intermolecular charge carrier mobility along columnar stacks of these molecules.

5. INTERVALENCE CHARGE TRANSFER ACROSS NONCOVALENT PATHWAYS

This subchapter reviews systems in which an *intramolecular* charge transfer between organic redox sites is mediated by noncovalent pathways. Intermolecular charge transfer in so-called pimers and related systems in which there is an attracting, noncovalent interaction between two organic redox centers are also considered. However, the many examples of simple bimolecular self-exchange reactions between organic molecules and their oxidized or reduced forms cannot be reviewed here.^{163–165}

Several of the above-mentioned examples of organic mixed valence systems were suspected to permit charge-transfer pathways that do not proceed along covalent bonds. For instance, a through-space pathway was believed to be activated in the radical cation of tetraanisyl-*p*-phenylenediamine (**36**⁺) due to direct interaction of the two nitrogen lone-pair orbitals.⁸⁰ Paracyclophane bridging units in **62**⁺ and **63**⁺ were investigated with the expectation to find evidence for through-space coupling between the two π-faces of a given paracyclophane unit, but surprisingly similar couplings were found for [2.2]paracyclophane and

Chart 66



[3.3]paracyclophane.¹⁰² Solvent-mediated electron transfer between the four individual branches of the tetrahedral tetrakis(triarylamine) species **175**⁺ was regarded as a viable alternative to electron transfer across the insulating phosphorus atom,¹⁵⁶ and through-space charge transfer was discussed as a possibility in macrocycles **38**–**40** and ladder-type molecules **179**–**181**.^{84–86,161}

One of the most convincing pieces of evidence for efficient through-space coupling in organic mixed valence systems is provided by the radical cation of **182** (Chart 66).¹⁶⁶ The *o*-xylylene bridge of this molecule imparts conformational flexibility, and the X-ray crystal structure of the charge-neutral form shows that there is an anti conformation between the two redox active 2,5-dimethoxy-4-methylphenyl units of a given molecule. By contrast, in the hexachloroantimonate salt of **182**⁺, the two units are in syn conformation with nearly coplanar π-systems that are separated by 3.2 Å, suggesting that there is significant electronic interaction between them. This is supported by electrochemical investigations which show that the first two oxidations of **182** are one-electron processes that are separated by a potential difference of 160 mV, while in the *m*- (**183**⁺) and *p*-xylylene isomers (**184**⁺) the two redox units are oxidized simultaneously at the same electrochemical potential. EPR investigations provide further evidence for stronger electronic coupling in **182**⁺ compared to **183**⁺ and **184**⁺: While EPR spectra of the latter can be simulated with the unpaired spin located on one redox unit, the spectrum of **182**⁺ is consistent with spin delocalization. An intervalence absorption band could be observed exclusively for **182**⁺, and on the basis of Hush theory $H_{AB} = 400 \text{ cm}^{-1}$ was obtained. It appears plausible that this relatively large value is attained mostly thanks to through-space interaction between the two 2,5-dimethoxy-4-methylphenyl units.

In a closely related study, the same research group used phenothiazine redox units in lieu of 2,5-dimethoxy-4-methylphenyl moieties.¹⁶⁷ The *o*-xylylene-bridged system **185** (Chart 67) was compared to an *o*-phenylene-bridged diphenothiazine molecule (**186**) and a system with a *p*-phenylene spacer (**187**). Remarkably, electronic coupling between the two phenothiazine units was found to be stronger for the *o*-xylylene system ($H_{AB} = 530 \text{ cm}^{-1}$) than for the *p*-phenylene-bridged system ($H_{AB} = 400 \text{ cm}^{-1}$). However, the greatest interaction was found for the *o*-phenylene molecule ($H_{AB} = 1280 \text{ cm}^{-1}$), presumably thanks to nearly cofacial arrangement of the redox units with a center-to-center distance of only 3.3 Å in the charge-neutral form of **186**. A crystal structure of **185**⁺ shows that its two phenothiazine units are not arranged in the same type of cofacial arrangement as the 2,5-dimethoxy-4-methylphenyl units in the *o*-xylylene analogue **182**⁺.

Chart 67

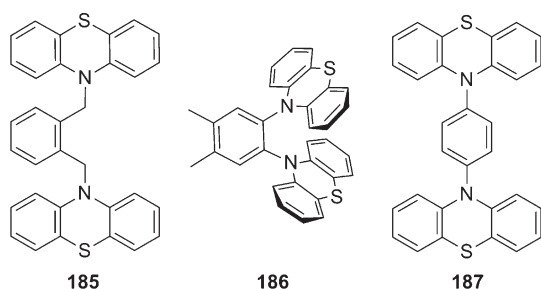
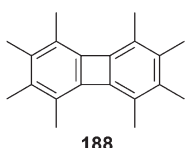


Chart 68



When phenothiazine and its radical cation are present at sufficiently high concentration in dichloromethane, the two types of species form a dimer radical cation through intermolecular π -association.¹⁶⁷ The resulting molecular ensemble, called pimer, was found to exhibit an intervalence absorption band between 1100 and 2400 nm that can be analyzed using Hush theory.¹⁶⁷ This yields $H_{AB} = 660 \text{ cm}^{-1}$ for the pimer, a value that is comparable to that found for the *o*-xylylene-bridged radical cation **185**⁺. Thus it seems that intimate mutual cofacial arrangement of phenothiazine units provides an efficient electronic coupling pathway.

In addition to the phenothiazine pimer, Kochi and co-workers also investigated several other radical cation pimers with a view to evaluating electronic couplings and other factors that are important for intervalence charge transfer in such molecular ensembles. The octamethylbiphenylene molecule **188** (Chart 68) turned out to be particularly well suited for this purpose.¹⁶⁸ In the solid state, **188** and **188**⁺ stack on each other with an intermolecular distance of 3.4 Å,¹⁶⁹ and in dichloromethane solution they aggregate with an association constant of 350 M^{-1} ,¹⁶⁸ that is a value roughly 70 times larger than that measured for the phenothiazine pimer from above.¹⁶⁷

The EPR spectrum of the pimer formed by **188** and **188**⁺ at -78°C is distinctly different from that of the **188**⁺ monomer and can be simulated by assuming delocalization of the unpaired spin over the entire bimolecular ensemble. Moreover, an intervalence absorption band is observed exclusively for the pimer, but not for the monomer. Kochi and co-workers pointed out that the nature of the electronic interaction within such mixed valence pimers is similar to the interaction within charge-transfer complexes formed through π -stacking of electron-rich with electron-poor arenes (Figure 11).^{170,171} Thus, there is a close analogy between charge-transfer transitions in the latter and intervalence transitions in pimers.

As illustrated by the example of tetracyanoethylene (TCNE), pimer formation can also occur with anionic species.¹⁷² The association constant between TCNE and TCNE^- in CH_2Cl_2 is only 4.5 M^{-1} , but the intervalence absorption band of the resulting anionic ensemble can easily be detected. The $(\text{TCNE})_2^-$ pimer

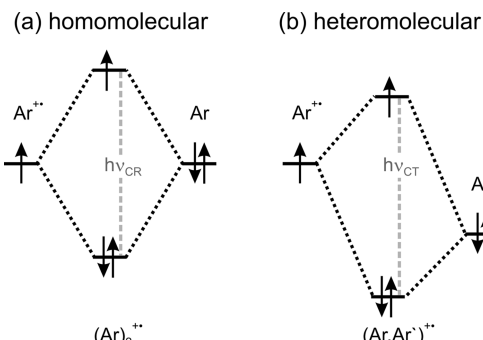


Figure 11. Molecular orbital diagrams for pimer formation between two identical arene (Ar) units of differing oxidation state (left) and for the formation of charge transfer complexes (right) between two different arene units (Ar and Ar'). The dashed vertical arrows represent charge resonance (CR) and charge transfer (CT) transitions. Reprinted with permission from ref 170. Copyright 2001 The Royal Society of Chemistry. Adapted with permission from ref 171. Copyright 2000 American Chemical Society.

is considered an important encounter complex for electron self-exchange between TCNE and TCNE^- , and it is found to represent a class II mixed valence system with $H_{AB} \approx 1000 \text{ cm}^{-1}$ and $\lambda \approx 7000 \text{ cm}^{-1}$.

The tetrathiafulvalene molecule has received particular attention with respect to pimer formation and associated mixed valence phenomena. Critical for π -complex formation in this case is the choice of a very weakly coordinating anion (e.g., dodecamethylcarboranate) and a weakly polar solvent (e.g., CH_2Cl_2) to minimize cation–anion pairing.¹⁷³ Under these conditions, TTF and TTF^+ associate with an equilibrium constant $K_a = 6 \text{ M}^{-1}$, and a strongly solvent-dependent intervalence absorption band becomes observable. Its analysis yields $H_{AB} = 1600 \text{ cm}^{-1}$ and $\lambda = 4800 \text{ cm}^{-1}$. Taken together, these facts suggest that the TTF/TTF⁺ π -complex is a class II mixed valence species, and this assignment is supported by computational work.

Spanggaard et al. searched for *intramolecular* pimer formation in bis(tetrathiafulvalene) molecules in which two TTF moieties are linked covalently to one another through two or more flexible linkers.¹⁷⁴ Despite considerable efforts on a series of molecules, the rigid system **189** (Chart 69) was the only one for which an intervalence absorption band due to pimer formation could be observed unambiguously. However, the intervalence band in this case originates from *intermolecular* pimer formation between **189** and **189**⁺ rather than being caused by an *intramolecular* π -complex. Similar intermolecular pimers were obtained with molecular clips that contain two TTF units attached to a glycoluril backbone.¹⁷⁵

Intramolecular formation of a TTF/TTF⁺ π -complex could be achieved by using a calix[4]arene unit with two TTF units attached to it in a face-to-face fashion (**190**).¹⁷⁶ While in the charge-neutral form there are no short contacts between the two redox active units, one-electron oxidation and subsequent addition of Na^+ give rise to the formation of a species that exhibits an intervalence absorption band. Rigidification of the calix[4]arene cone through binding of sodium is crucial for the formation of this particular intramolecular pimer.

Two recent studies attempted to make use of supramolecular chemistry for the formation of the TTF/TTF⁺ π -complex in dilute solution. Kim and co-workers used a cucurbit[8]uril molecule to encapsulate two TTF molecules in its hydrophobic

Chart 69

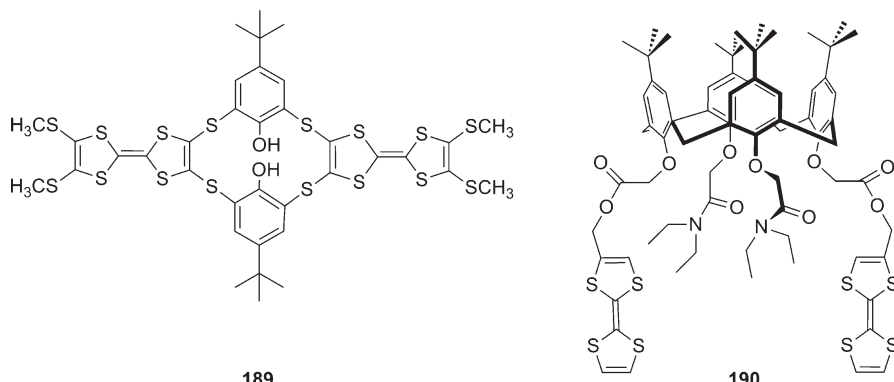
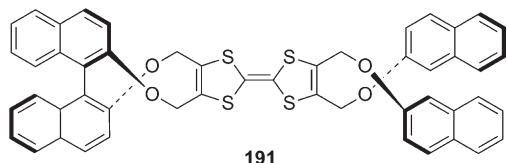


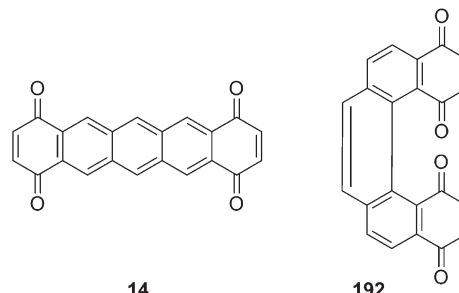
Chart 70



cavity, but only managed to observe the cation radical dimer $[(\text{TTF})_2]^{2+}$.¹⁷⁷ Fujita and co-workers employ a molecular cage comprised of two tris(4-pyridyl)triazine ligands held at an interplane separation of $\sim 10 \text{ \AA}$ through six palladium ions and three 4,4'-bipyridine ligands.¹⁷⁸ Two TTF molecules can be enclosed in the rather electron-deficient cavity of this self-assembled triangular coordination cage. The cyclic voltammogram of this molecular ensemble shows that the first oxidation of the two enclosed TTF molecules occurs at electrochemical potentials differing by 152 mV, thereby indicating substantial mutual electronic communication between them. The mixed valence dimer $[(\text{TTF})_2]^+$ exhibits an intervalence band in the near-infrared and is found to be stable with a half-life of approximately one day. Only upon further oxidation to the dicationic state, TTF is liberated rapidly from the cage.

An unusual way of forming $[(\text{TTF})_2]^+$ pimers in dilute solution was discovered by Fourmig   and co-workers.¹⁷⁹ In molecule 191 (Chart 70) a TTF molecule was substituted with two 1,1'-binaphthol units, and it was possible to obtain enantiopure RR, SS, and meso isomers. Oxidation of enantiopure solutions of RR-191 or SS-191 initially leads to the formation of a species that absorbs around 2000 nm. The absorbance of this band maximizes after addition of 0.5 equiv of oxidizing agent, suggesting that it might be due to intervalence charge transfer between a neutral and an oxidized molecule in a primer. Cyclic voltammetry supports this interpretation because a splitting of the first oxidation of TTF into two separate waves can be observed for sufficiently concentrated solutions. Importantly, these experimental observations are made exclusively for enantiopure solutions of the RR- and SS-forms, but not for the meso isomer. Molecular models offer an explanation for this peculiar behavior: In the RR- and SS-forms the two naphthol arms are oriented parallel to one another and leave enough open space between them for accommodation of a TTF unit from a second identical molecule. This may result in self-association of two TTF

Chart 71

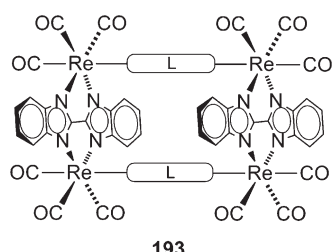


units with their long axes almost perpendicular to each other, which is beneficial for overlap between their HOMOs. In the meso form such aggregation is precluded by the unfavorable mutual orientation of the naphthol substituents, and mixed valence pimers do not form.

Evidence for through-space interactions in organic mixed valence species has also been found by Miller and co-workers in their early work on diquinone molecules.^{180,181} On the basis of optical absorption and EPR investigations, the radical anions of the isomeric molecules 192 (Chart 71) and 14 were assigned to different mixed valence classes. Whereas 192^- was identified as a fully delocalized system, 14^- was assigned to class II. X-ray crystal structure analysis shows that the carbonyl groups at the inside of the helical structure of 192 can approach each other to a distance of 2.85 \AA . It is believed that thanks to this transannular overlap of carbonyl groups, delocalization of the odd electron in 192^- can occur not only around the covalent phenanthrene backbone of the helix but also across the gap between the two ends of the molecule.

Through-space communication between organic moieties that gives rise to interesting mixed valence properties has also been observed in Hupp's molecular squares with the generalized structure 193 (Chart 72).^{182,183} Formally, these molecules are coordination compounds, but the rhenium(I) tricarbonyl complexes are only structural elements (forming the corners of the squares), and the mixed valence properties are due to stacked organic ligands L that are held together in relatively close contact ($\sim 3.8 \text{ \AA}$) by the metal centers. Ligand L can be a reducible dipyrindyl or diazine ligand, for example 4,4'-dipyrindyl or 2,7-diazapryrene. Spectroscopic studies of these molecules indicate that direct orbital overlap between the two ligands L is more

Chart 72



important than superexchange coupling through the rectangle framework. In the case of $L = 4,4'$ -dipyridyl, an electronic coupling matrix element as large as 1000 cm^{-1} was estimated. Recently, a similar type of mixed valence species in which two redox active tri(4-pyridyl)-1,3,5-triazine units are held together in close cofacial contact ($\sim 3.3 \text{ \AA}$) by six corner-building rhodium complexes was reported by the same researchers.¹⁸⁴ Through-space interactions between the two triazine units are believed to be of key importance in the highly coupled ($H_{AB} = 2800 \text{ cm}^{-1}$) mixed valence form of this triangular prism.

6. USE OF EPR SPECTROSCOPY AS A DIRECT TEST FOR HUSH THEORY

Already several of the earliest studies of purely organic mixed valence systems made use of EPR spectroscopy to assess the extent of spin delocalization. This includes for example Mazur's diketone 8^- ,¹⁸⁵ or Miller's diquinone radical anions ($12^- - 14^-$).⁸⁷ The Nelsen group noted that the rates for intramolecular electron transfer in certain carefully selected organic mixed valence systems could be sufficiently slow in order to be measurable by EPR spectroscopy, while at the same time their intervalence absorption bands remain intense enough to stay easily detectable. This favorable scenario should permit direct comparison of electron-transfer rates measured by EPR spectroscopy with rates estimated from Hush analysis of optical absorption spectra, thereby providing a significant test of Hush theory. This test is difficult to perform with metal-centered mixed valence compounds because the electron-transfer rates in such systems are frequently (but not always)¹⁸⁶ beyond the EPR time scale.

The crux is that the intensity of the intervalence absorption band and the rate for electron transfer are both proportional to H_{AB}^2 .^{3,6,24} Hence, if electronic coupling is strong and intervalence bands are easy to detect, electron-transfer rates are usually too fast to be measurable by EPR spectroscopy. The solution to this problem is to decelerate electron transfer by using molecules that undergo redox chemistry only with large reorganization energies.

The Nelsen group found that several bis(hydrazine) radical cations fulfill this requirement.⁴⁰⁻⁴² The slowness of electron transfer in these systems is due to the fact that electron loss by a hydrazine unit is associated with an unusually large geometry change, which makes the inner-sphere reorganization energy very large. This geometry change involves rearrangement of the two nitrogen lone pair orbital axes from perpendicular in the charge-neutral molecule to coplanar in the cationic form (Figure 12), and a simultaneous shortening of the N–N bond distance by about 0.1 \AA .^{113,187} In simple N,N' -dialkylated bis(hydrazine) molecules the torsion angle between the N and N' lone pairs is indeed close to 90° in the neutral form, but when

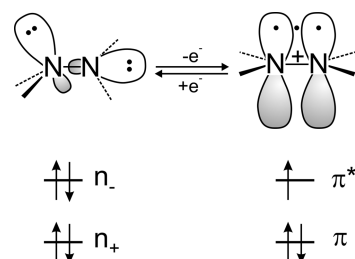
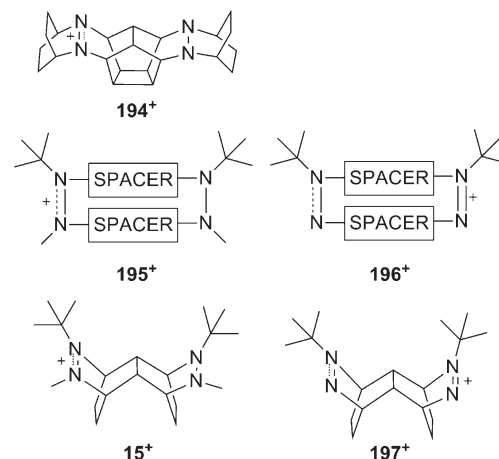


Figure 12. Illustration of the geometry and bonding changes associated with the oxidation of hydrazine units. Reprinted with permission from ref 113. Copyright 2006 Elsevier.

Chart 73

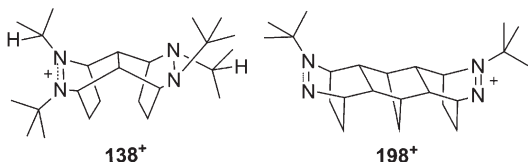


using N,N' -bicyclic substituents (such as the case for example in molecule 194^+), this twist angle deviates from 90° , and this provides a means of tuning the magnitude of the inner-sphere reorganization energy.¹¹³ Estimates of the λ_{in} -values are accessible either through investigation of *intramolecular* charge transfer in bis(hydrazine) radical cations, or alternatively from studies of *intermolecular* electron transfer between monohydrazine analogues,^{113,188} and from calculations.^{189,190}

The first mixed valence system for which precise measurement of the rate for intramolecular electron transfer by EPR spectroscopy and detection of the intervalence absorption band was possible is the radical cation of molecule 194 (Chart 73).¹⁹¹ This molecule is the result of a most impressive synthetic effort that consumed over 15 person-years.¹¹³ The EPR spectrum of 194^+ in butyronitrile at -67°C shows the quintet expected for interaction of the unpaired spin with only two nitrogen atoms, while at 107°C the nine-line signal expected for delocalization over four nitrogens is observed. An electron-transfer rate of $1.32 \times 10^8 \text{ s}^{-1}$ was interpolated for a temperature of 25°C , and this translates into a barrier-crossing frequency of 1295 cm^{-1} . However, analysis of the intervalence absorption band using Hush theory yields a barrier-crossing frequency of only 700 cm^{-1} . The rather large discrepancy between the two values likely arises from the fact that more than one single frequency is coupled to the intramolecular electron transfer.¹⁹¹

Comparison of bis(hydrazine) and bis(hydrazyl) radical cations (with the generic structures 195^+ and 196^+ , respectively) underscores the importance of large reorganization energies for direct measurement of the rate for intramolecular electron

Chart 74



transfer with EPR spectroscopy.⁴¹ In both types of radical cations, the spin-bearing dinitrogen units are structurally similar with the unpaired electron located in an N–N π -antibonding orbital. However, their diamagnetic dinitrogen units are very different: In 195^+ the charge-neutral hydrazine unit has pyramidal nitrogens and a long N–N (single) bond, while the cationic diazenium unit in 196^+ has a planar (*tert*-butylated) nitrogen atom and a short N–N (double) bond. Thus, the geometry changes associated with intramolecular electron transfer are expected to be significantly larger in bis(hydrazine) than in bis(hydrazone) radical cations. Comparison of 15^+ with 197^+ shows that this expectation is indeed fulfilled:⁴¹ Intramolecular electron transfer was found to be slow on the EPR time scale for the bis(hydrazine) and fast for the bis(hydrazone) radical cation, and inner-sphere reorganization energies of 45.8 kcal/mol (15^+) and 16.9 kcal/mol (197^+) were estimated.⁴¹

In bis(hydrazone) radical cations, the rate for intramolecular electron transfer reaches the EPR time scale only when the distance between the two hydrazone units is increased from four (as is the case in 197^+ , Chart 73) to six connecting σ -bonds (as is the case in 198^+ , Chart 74).^{113,192} Interestingly, for 198^+ the agreement between the EPR data and optical absorption data was far better than for 4- σ -bonded bis(hydrazine) systems. In the specific case of the 6- σ -bonded bis(hydrazone) radical cation 198^+ the electron-transfer rate determined from EPR spectroscopy was roughly a factor of 5 larger than that estimated from intervalence band analysis,¹⁹² while in the case of the 4- σ -bonded bis(hydrazine) radical cation 138^+ the difference amounts to a factor of 36.¹³¹ It has been suggested that this is due to stronger vibronic coupling in the bis(hydrazine) systems with respect to bis(hydrayls). In a series of bis(hydrazine) systems the vibronic coupling constants $S = \lambda_{\text{in}}/\hbar\nu_{\text{in}}$ were found to be consistently larger ($S = 13.6$ –17.5) than in a series of bis(hydrazone) cations ($S = 6.5$ –7.6).¹⁹² Any anharmonicity that might be present in the electron-transfer potential wells (Figure 1) can therefore be expected to introduce a greater error in Hush analysis of hydrazine intervalence absorption bands than in the case of hydrazone data.

Synthesis of molecules with carbon frameworks such as those in radicals 198^+ and 138^+ requires many individual steps, and the final molecules are usually produced as syn and anti isomers that are difficult or even impossible to separate.^{113,192} The synthesis of *p*-phenylene-bridged bis(hydrazine) molecules such as 29 is considerably more straightforward, but some difficulties associated with diastereomerism and rotational isomerism do also occur for such simpler systems.¹²⁴ Be that as it may, the prior sections of this review have already shown that various EPR investigations of bis(hydrazine) and bis(hydrazone) radical cations provided valuable insight into the influence of distance,^{110,125} bridge topology,¹¹⁰ bridge redox levels,¹³⁹ and conformational effects¹²⁴ on intervalence charge transfer.

The usefulness of EPR spectroscopy for investigation of intramolecular electron transfer in organic mixed valence systems

is by far not limited to bis(hydrazine) and bis(hydrazone) systems. A recent study by Lancaster et al. reports on measurement of intramolecular electron-transfer rates in bis(triarylamine) radical cations by variable-temperature EPR spectroscopy and comparison with optical absorption data.¹⁴¹ Indeed, the radical cations of 53 and 150 are the first triarylamine mixed valence species for which EPR spectra were found to exhibit a temperature-induced transition from the slow exchange limit (with electron localization on one triarylamine unit) to the fast exchange regime (with spin delocalization over the two nitrogens) and in which optical and thermal electron transfer have been observed and correlated. When the barriers for thermal electron transfer are compared to those extracted from analysis of the intervalence absorption bands, one arrives at the important conclusion that the two sets of data are only compatible with one another if one assumes a charge-transfer distance that is only about 40% of the N–N distance.¹⁴¹ As discussed already in prior sections of this review, several other studies concur with the finding that the N–N distance can be a bad measure for the electron-transfer distance in bis(triarylamine) systems or in dinitroaromatic radical anions—particularly in fully delocalized (class III) systems.^{17,65,98}

EPR spectroscopy was also used to estimate the rates or barriers for intramolecular electron transfer in bis(triarylamine) radical cations by Kattnig et al. (e.g., 53^+ , $60^+ - 62^+$),¹⁰² and by Hirao et al. (134^+ , 174^+).^{129,155} Other types of organic mixed valence systems to which EPR spectroscopy has been applied include dinitroaromatic radical anions (81^- , 83^- , 101^-),^{17,118} polychlorinated triphenylmethyl radicals (23^- , 110^-),^{51,120,121} dimethoxytolyl radical cations ($43^+ - 46^+$, $118^+ - 120^+$),^{89,166} viologens (25^+),⁵⁶ and diquinone radical anions ($12^- - 14^-$).^{87,147,148}

7. SOLVENT AND ION PAIRING EFFECTS

A spectacular case of solvent-dependent mixed valence behavior is provided by the dinitroaromatic radical anions 88^- and 89^- that were introduced already in section 3.1.¹¹¹ In these 11- σ -bond bridged species the distance between the two nitro groups is sufficiently large for the solvent contribution to the total reorganization energy (λ_{out}) to play a dominant role over inner-sphere contributions (λ_{in}). In hexamethylphosphoramide (HMPA, Chart 75) and the cyclic urea DMPU, 88^- and 89^- are class III species, whereas in acetonitrile they exhibit broad and unstructured near-infrared absorption bands that are typical for class II compounds. It appears plausible that the high cation-solvating power of HMPA and DMPU lead to particularly small λ_{out} -values, allowing full charge delocalization in the mixed valence anions. A similar crossover from class II to class III upon solvent variation was observed for dinitroaromatic radical anions with biphenyl bridges (84^- , 126^- , 127^-),¹²⁶ fluorene (85^-), or phenanthrene spacers (102^-),¹²⁶ and for the paracyclophane-bridged radical anions 107^- and 108^- .¹¹⁹

A big impetus for understanding the solvent dependence of intervalence absorption bands comes from the interest in separating the inner- and outer-sphere parts of the total reorganization energy. This is necessary for application of modern vibronic coupling theory to electron transfer in mixed valence compounds. A detailed study of bis(hydrazine) mixed valence radical cations bridged by saturated ($199^+ - 201^+$, Chart 76) or aromatic spacers ($29^+, 122^+, 123^+, 202^+, 203^+$) demonstrated that modeling λ_{out} for these systems is highly nontrivial.^{110,113,193} Indeed, λ_{out} was found to correlate not at all with the distance between the redox active units as would be expected on the basis

Chart 75

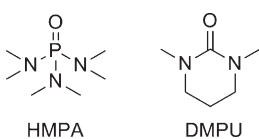


Chart 76

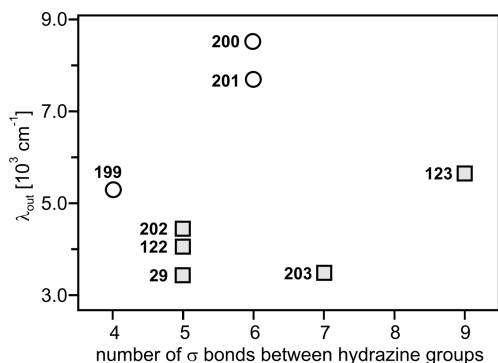
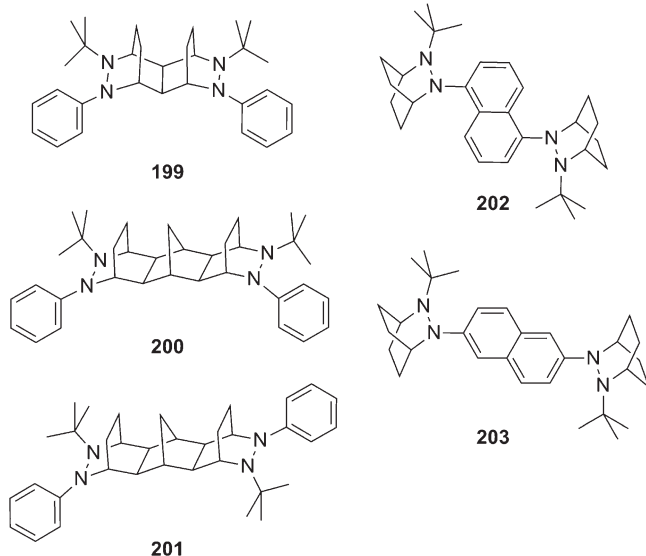
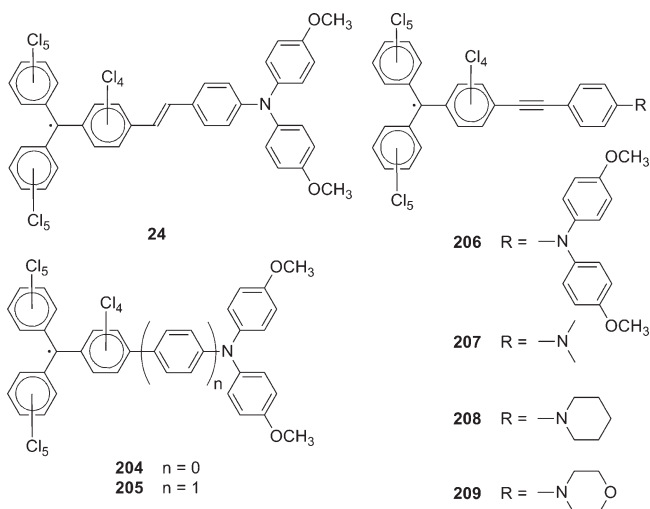


Figure 13. Plot of the outer-sphere reorganization energies (λ_{out}) associated with intervalence charge transfer in bis(hydrazine) radical cations versus the number of σ -bonds between hydrazine groups. The open circles represent molecules with saturated alkyl bridges, while the gray filled squares represent systems with unsaturated aryl spacers. Reprinted with permission from ref 113. Copyright 2006 Elsevier.

of dielectric continuum theory (Figure 13). This theory assumes that the bridge affects λ_{out} merely through the distance that it sets between the two redox active moieties. However, saturated bridges tend to produce larger λ_{out} values than unsaturated ones (circles versus squares in Figure 13). This suggests that solvation of the molecular bridge plays in fact an important role.^{110,113,193}

This becomes particularly problematic when attempting to model the solvent dependence of mixed valence species in which the molecular bridge is involved more or less directly in the intramolecular electron-transfer process, rather than simply

Chart 77



being a completely redox inert spacer. This is the case for example in the bis(triarylamine) radical cations 35^+ and $50^+–52^+$ for which electronic structure calculations indicate that charge transfer from one triarylamine unit to the other is accompanied by a charge shift from the terminal anisyl rings toward the molecular bridges.⁷⁸

The intervalence absorptions of class III mixed valence species generally exhibit a much weaker dependence on solvent than class II compounds. Indeed, weak solvent dependence is frequently used as one of the arguments to assign a mixed valence species to class III. In the fully delocalized systems 29^+ and 34^+ , the intervalence bands shift by about 100 cm^{-1} when going from apolar (chloroform) to polar solvents (acetonitrile).¹⁹⁴ By treating the solvent merely as a dielectric continuum, the energy of the intervalence absorption (E_{op}) in 11 different solvents cannot be modeled satisfactorily for these two radical cations. It was found that besides the refractive index of the solvent, the so-called solvent donicity, as measured by Gutmann's solvent donicity numbers,¹⁹⁵ has an important influence.¹⁹⁴ This is a nondielectric continuum effect, and the importance of solvent donicity depends strongly on the nature of the mixed valence compound that is studied. For dinitro aromatic radical anions solvent donicity has an opposite effect on λ_{out} than for bis(triarylamine) radical cations: For the radical anions λ_{out} increases in better electron-accepting solvents, but for radical cations λ_{out} increases in better electron-donating solvents.¹¹¹

Solvent dependence studies are frequently plagued by poor solubilities of the mixed valence species in apolar solvents because they are usually charged. This problem was overcome by the recent development of a new family of charge-neutral mixed valence compounds with molecule 24 (Chart 77) as the prototype system.^{52,196} In these molecules, a triarylamine unit is connected to a perchlorinated triarylmethyl radical center. Intramolecular electron transfer formally occurs from the triarylamine nitrogen to the trisubstituted carbon center, thereby producing a zwitterionic excited state from an apolar ground state.⁵² Molecule 24 and its analogues 204–209 are soluble even in *n*-hexane, and this allowed investigation of the intervalence absorption in 13 different solvents. Interestingly, the intervalence band maximum (E_{op}) of 24 shows a very weak and superficially nonsystematic dependence on solvent polarity varying only

from $12\,300\text{ cm}^{-1}$ in *n*-hexane to $12\,600\text{ cm}^{-1}$ in acetonitrile.⁵² This remarkably weak solvent dependence can be explained by the occurrence of two opposing effects: The solvent reorganization energy increases with increasing solvent polarity, but the energy difference between diabatic ground- and excited-state potential surfaces decreases concomitantly. The latter effect is due to the fact that the excited state is zwitterionic while the ground state is apolar.⁵² Investigation of molecules **204–209** leads to the same principal conclusion.¹⁹⁶

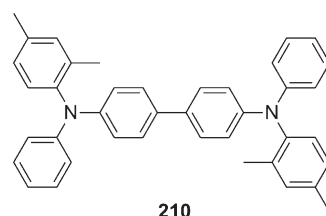
Solvent effects did also play an important role in a rather unusual study of a mixed valence phenomenon. Investigation of bis(triarylamine) molecules **61**, **141**, and **148** by pump/probe spectroscopy revealed that the first excited states of these charge-neutral species are similar to the ground states of their radical cation forms.¹⁹⁷ In other words, while the neutral bis(triarylamine) molecules are in their first excited states, they behave like mixed valence species. This conclusion was based, *inter alia*, on great similarities between the solvent dependences of the excited-state absorption spectrum of neutral **141** and the ground-state absorption spectrum of **141⁺**.

Ion pairing can have a big influence on mixed valence. When reducing dinitroaromatics or quinones with sodium metal, addition of cryptand **79** greatly increases the rates for intramolecular electron transfer in the resulting mixed valence radical anions because the sodium cation is encapsulated and, in consequence, can interact much less tightly with the anion.^{47,111} For a given dinitroaromatic radical anion, the rate for intramolecular electron transfer can be increased by an order of magnitude when compared to using tetrabutylammonium as a counterion.¹⁹⁸

In bis(hydrazine) radical cations **29⁺**, **123⁺**, and **124⁺**, ion pairing effects were observed in two different types of experiments:¹⁹⁹ First, variation of the bis(hydrazine) radical concentration from ~ 0.1 to $\sim 10\text{ mM}$ in dichloromethane induces blue shifts of the intervalence absorption bands on the order of 500 cm^{-1} . Second, addition of an inert salt such as tetrabutylammonium hexafluorophosphate to a $\sim 0.1\text{ mM}$ solution of these species in dichloromethane leads to similar blue shifts. On the basis of titration experiments, ion pairing equilibrium constants of 3100 M^{-1} (**29⁺**, **123⁺**) and 6100 M^{-1} (**124⁺**) were determined, and the ion pair energies were found to be in the range from -4.6 to -5.3 kcal/mol .¹¹³ EPR measurements of these radical cations have to occur at concentrations at which already a substantial amount ($\sim 30\%$) of ions is paired while optical absorption experiments can be performed at lower concentrations. It has been pointed out that this is one source of uncertainty that accompanies the comparison of electron-transfer rates determined from EPR and optical absorption spectroscopy. In the specific case of the molecules considered here, this comparison is rather favorable with a difference of only a factor of 2.5 between k_{ET} values determined by the two different methods.

An interesting question that has been addressed by Nelsen et al. concerns the influence of ion pairing and “effective polarity” on intervalence charge transfer in the solid state. These researchers investigated the intervalence absorptions of two bis(hydrazine) radical cations (**29⁺**, **122⁺**) in solvents ranging in polarity from dichloromethane to dimethylformamide and compared these solution data to diffuse reflectance spectra measured on various solid supports (Al_2O_3 , LiCl , BaSO_4 , and KBr).²⁰⁰ While increasing the solvent polarity induces a blue shift of the intervalence bands due to an increase of the solvent

Chart 78



reorganization energy (λ_{out}), the nature of the solid support has a minor influence. The solid-state transition energies are higher than those in solution, which is interpreted as a manifestation of ion pairing. On the basis of intervalence band energies, the “effective polarity” of the crystalline material seems to be comparable to that of liquid acetonitrile.²⁰⁰

8. CRYSTALLOGRAPHIC STUDIES

Obtaining X-ray crystal structures of class II mixed valence complexes can be difficult because many of them disproportionate upon crystallization.⁴ The same problem has been encountered for organic mixed valence compounds,⁴² and consequently there exist more crystal structures of class III organic mixed valence systems than on class II compounds. In terms of determining distances between the redox active centers of organic mixed valence compounds, X-ray crystallography is of limited use because the electron-transfer distance can in many instances not be related directly to interatomic distances. However, structural analyses of organic mixed valence compounds are useful, for example, to elucidate molecular distortions that affect orbital overlaps and π -conjugation. Care must be taken when attempting to make a classification of mixed valence species on the basis of X-ray structural data alone. The situation in the solid state is fundamentally different from that in solution, where time and density fluctuations of the solvent may affect the degree of delocalization in the mixed valence species. Moreover, an apparently fully centrosymmetric solid-state structure may actually be slightly asymmetric due to static or dynamic disorder in the crystal, or the symmetry of the radical cation in the crystal might be induced by a counterion placed right above or below the cation.⁷³ Particularly useful are comparative structural studies of charge-neutral (closed-shell) molecules and their oxidized or reduced (mixed-valence) forms. This has been possible for the vinylene-bridged bis(triarylamine) molecule **54**.⁹⁹ Upon oxidation, its $\text{N}-\text{C}_{\text{stilbene}}$ bonds shorten slightly, and there occur pronounced differences between the $\text{N}-\text{C}_{\text{stilbene}}$ and $\text{N}-\text{C}_{\text{anisyl}}$ bond lengths. The same bond length changes occur on both triarylamine units. In addition, there is a symmetrical quinonoidal pattern of bond length alteration in the two benzene rings of the connecting stilbene moiety that occurs in the cationic form but not in the neutral molecule. While all of these observations are consistent with assignment of **54⁺** to class III, the crystallographic data cannot exclude the possibility of a class II species with only slight asymmetry or in which asymmetry is masked by static or dynamic disorder.⁹⁹

Among the many bis(triarylamine) systems that were investigated in the context of mixed valence, molecule **210** (Chart 78) is one of the few that could be crystallized in both its neutral and its cationic form.²⁰¹ The most significant change in structure following oxidation is the decrease in the biphenyl torsion angle from 37.1° in neutral **210** to 4.1° in **210⁺** SbCl_6^- . The fact that

the N–N distance is virtually unaffected by oxidation (9.981(6) Å versus 9.89(1) Å) may reflect delocalization of the HOMO over the entire N–C₆H₄–C₆H₄–N framework, as predicted by DFT calculations. Thus, it appears that the fraction of electronic charge lost upon oxidation is divided over all the atoms in the benzidine framework, and the molecular bridge cannot be considered a redox inert spacer that merely sets the distance between the two triarylamines.²⁰¹

The radical cation of bis(hydrazine) molecule **29** is one of the rare class II organic mixed valence systems that could be crystallized.⁴² In this case, the N–N distance shortens considerably upon oxidation (from 1.461 Å in the neutral species to 1.359 Å in the tetraphenylborate (BPh₄⁻) salt), and the two hydrazine units undergo significant structural changes (Figure 12) that are in line with the very large inner-sphere reorganization energies commonly observed for this family of mixed valence compounds. The twist angle between the lone pair of the aryl-connected nitrogen and the aryl π system increases upon oxidation from 37.5 to 47.6° in the phenyl-bridged molecule **29**,⁴² and from 50.2 to 66.7° in the durene-bridged analogue **122**.^{124,139} In the crystal structure of the phenyl-bridged system (**29**⁺), the BPh₄⁻ counterion is closer to the cation, and it is less symmetrically placed with respect to the center of the cation than in the durene-bridged analogue (**122**⁺BPh₄⁻).²⁰⁰ These differences in ion pairing provide an explanation for the experimental observation of stronger intervalence absorption changes associated with the transition from solution to the solid state in the case of **29**⁺ compared to **122**⁺.

The 2,5-dimethoxy-4-methylphenyl (DMP) redox units used by the Kochi group (e.g., in **42**–**46**) undergo relatively large structural changes upon oxidation, and there have been several X-ray structural studies on such systems.^{88,90} The quinonoidal distortion of these redox units has been used as a geometric measure of their degree of oxidation. In the X-ray crystal structure of **42**⁺SbCl₆⁻, the structure of each of the two directly connected redox units is exactly intermediate between the geometry of neutral DMP and DMP⁺. In **43**⁺SbCl₆⁻ the two redox units are separated by a *p*-phenylene spacer, and the two DMP units are structurally different from each other: One of them is closer to the neutral structure, while the other has a structure that resembles that of DMP⁺. On the basis exclusively of these structural data, one arrives at the conclusion that there is an asymmetric charge distribution of 20–80% between the two redox sites in **43**⁺. Indeed, **42**⁺ and **43**⁺ represent cases in which the X-ray structures accurately reflect the electronic structures of mixed valence species in solution: Spectroscopic studies demonstrated that **42**⁺ is a class III and **43**⁺ a class II mixed valence system.^{88,89} In the biphenyl-bridged system **44**⁺, the structures of the two DMP units are such that they suggest complete charge localization, i.e., class I behavior, while spectroscopic studies show that **44**⁺ is a class II system in solution.^{88,90} It is noteworthy that there exists a linear correlation between the observed splitting in electrochemical potential between the first two oxidations in molecules **42**–**44** and the amount of positive charge that is delocalized in the crystal structures of their radical cations (Figure 14).⁹⁰

The crystal structures of the biphenyl-bridged system **44**⁺ (Chart 79) and its fluorene-bridged analogue **211**⁺ provide structural evidence for the fact that fluorene mediates stronger electronic coupling than biphenyl. While the structure of **44**⁺ is indicative of complete charge localization, **211**⁺ exhibits an X-ray crystal structure that is in line with class II mixed valence behavior

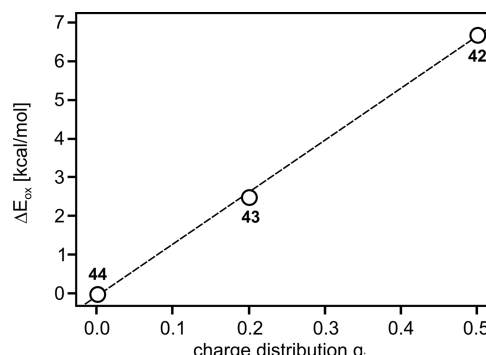
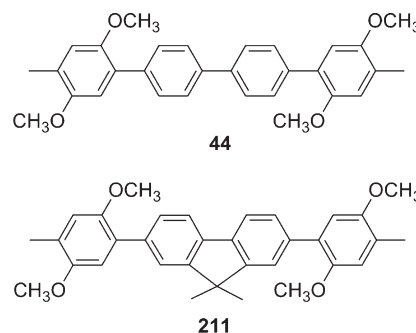


Figure 14. Linear correlation between the observed splitting in electrochemical potential between the first two oxidations in molecules **42**–**44** and the distribution of positive charge (q_i) over the two redox sites in the crystal structures of their radical cations;⁹⁰ $q_i = 0$ represents full charge localization on a single redox site, and $q_i = 0.5$ represents complete charge delocalization over both redox sites. Reproduced with permission from ref 90. Copyright 2001 The Royal Society of Chemistry.

Chart 79



with 35% of the excess positive charge on one DMP unit and 20% on the other. As discussed on the examples of biphenyl- and fluorene-bridged dinitro (**84**, **85**⁺) and bis(hydrazine) mixed valence species (**123**⁺, **124**⁺), electronic coupling differences between the two types of bridges may have two origins, namely, lower torsion angles between the two phenyl rings (here, 16.9° in **44**⁺ versus 5.7° in **211**⁺) and greater ease of bridge oxidation.²² The fact that 45% of the excess positive charge in the crystal structure of **211**⁺ does not appear to reside on the terminal DMP units suggests that bridge oxidation is indeed very important.

While **42**⁺–**44**⁺ and **211**⁺ are rigid rodlike molecules, the DMP units in the systems **182**⁺–**184**⁺ are linked through methylene groups that impart much greater structural flexibility. In consequence, two types of structural changes are associated with oxidation of molecule **182**.¹⁶⁶ First, the charge-neutral form has its two redox centers in anti conformation and hence relatively far apart, while in the cationic form they are in syn conformation with a cofacial separation of only 3.2 Å. Second, a quinonoidal distortion of the redox centers occurs upon oxidation. The extent of charge delocalization can be assessed in the same way as for the rigid systems, but in the particular instance of **182**⁺, the structural distortions associated with charge localization are found to be strongly anion dependent: The crystal structure of **182**⁺Pf₆⁻ suggests complete delocalization, while that of **182**⁺SbCl₆⁻ is consistent with a 90:10 charge distribution between the two DMP units.¹⁶⁶ This example

underscores the importance of ion pairing effects in mixed valence chemistry.

9. CONCLUDING REMARKS

One of the motivations for research on organic mixed valence comes from the interest in organic molecular wires.⁷⁷ Electron flow over long distances will likely have to occur by the hopping mechanism in order to be efficient,^{202,203} and therefore it is important to know the size of the molecular hopping stations over which an electron can be delocalized. Molecules with organic redox sites are particularly favorable in this respect because charge tends to be more delocalized in these systems than in metal-based mixed valence compounds. Indeed, determination of the adiabatic electron-transfer distance in organic mixed valence compounds is often a challenging task.^{113,124,204,205}

For fundamental investigations of the mixed valence phenomenon, molecules with purely organic redox centers offer several advantages over coordination compounds. The intervalence absorption bands of many organic mixed valence systems tend to have higher extinction coefficients than those of metal-based mixed valence species. Because of their weakness and great width, these near-infrared absorptions can be difficult to even detect in coordination compounds; moreover, they may be overlapped by absorptions caused by other (e.g., ligand-to-metal charge transfer) transitions.¹⁹⁴ In many organic mixed valence systems, these difficulties are not encountered to the same extent. What is more, certain organic mixed valence systems combine strong electronic coupling with large reorganization energies, thereby allowing easy detection of intervalence absorption bands *and* direct measurement of electron-transfer rates by EPR spectroscopy. This provides the basis for a direct test of Hush theory, which is difficult, albeit not impossible to perform with coordination compounds.

By far not all organic mixed valence systems can be analyzed within Hush's framework of a two-state model. To class II systems, it is only applicable when the one-electron oxidized or one-electron reduced states of the bridge are high enough in energy. For certain class III systems it appears to be completely inappropriate,¹¹³ but neighboring orbital models can be useful for analysis of electronic coupling in such cases.¹⁹ Dielectric continuum theory fails to describe the effect of solvent on the reorganization energy in many organic mixed valence compounds, and solvent donicity has to be taken into account.^{111,194,195}

The families of organic mixed valence systems that have been best explored to date include bis(triarylamine) radical cations, bis(hydrazine) and bis(hydrazone) radical cations, dinitroaromatic and diquinone radical anions, and bis(tetrathiafulvalene) radical cations. Given the important role played by methylviologen and its numerous derivatives in bimolecular electron-transfer chemistry, surprisingly few studies were specifically geared at understanding the electronic coupling between the two redox sites in the one-electron reduced forms of these compounds. The same is true for diimide radical anions, despite the fact that they currently receive much attention in electron-transfer chemistry and other contexts.⁵⁷ It is possible that many researchers quite simply do not perceive these radicals as mixed valence species.

The future challenges in the field of organic mixed valence are similar to those recently formulated by Keene in a more general review on the subject of intervalence compounds.⁸ These challenges include for example the identification of mode-specific

contributions to electron-transfer barriers by IR and resonance Raman experiments, determination of adiabatic electron-transfer distances by electroabsorption experiments that exploit the Stark effect, and the development of appropriate theoretical models describing ion pairing and solvent donicity effects.

AUTHOR INFORMATION

Corresponding Author

*E-mail: oliver.wenger@chemie.uni-goettingen.de.

BIOGRAPHIES



Jihane Hankache, born 1984 in Baskinta, Lebanon, received her master degree in chemistry from the Lebanese University in 2005. From 2006 to 2008 she studied in France and obtained a diploma in materials engineering from ESIREM-Dijon and a master degree in nanotechnology from Université de Bourgogne. After a brief research stay at EMPA in Thun, Switzerland, she began her Ph.D. thesis under the supervision of Oliver Wenger at the University of Geneva and then moved with him to Göttingen.



Oliver S. Wenger did his Ph.D. thesis between 1999 and 2002 under the supervision of Hans U. Güdel at the University of Bern in Switzerland. After postdoctoral work at the California Institute of Technology with Harry B. Gray from 2002 to 2004 and at Université Louis Pasteur in Strasbourg with Jean-Pierre Sauvage from 2004 to 2006, he started independent research as an assistant professor at the University of Geneva. In 2009, he moved to the University of Göttingen, where he now has a tenured position as an associate professor.

ACKNOWLEDGMENT

Financial support from the Swiss National Science Foundation through Grant No. 200021-117578 is acknowledged.

REFERENCES

- (1) Creutz, C.; Taube, H. *J. Am. Chem. Soc.* **1969**, *91*, 3988.
- (2) Creutz, C.; Taube, H. *J. Am. Chem. Soc.* **1973**, *95*, 1086.
- (3) Demadis, K. D.; Hartshorn, C. M.; Meyer, T. *J. Chem. Rev.* **2001**, *101*, 2655.
- (4) Creutz, C. *Prog. Inorg. Chem.* **1983**, *30*, 1.
- (5) Kaim, W.; Klein, A.; Glöckle, M. *Acc. Chem. Res.* **2000**, *33*, 755.
- (6) Brunschwig, B. S.; Creutz, C.; Sutin, N. *Chem. Soc. Rev.* **2002**, *31*, 168.
- (7) Brunschwig, B. S.; Sutin, N. *Coord. Chem. Rev.* **1999**, *187*, 233.
- (8) D'Alessandro, D. M.; Keene, F. R. *Chem. Soc. Rev.* **2006**, *35*, 424.
- (9) D'Alessandro, D. M.; Keene, F. R. *Chem. Rev.* **2006**, *106*, 2270.
- (10) Launay, J.-P. *Chem. Soc. Rev.* **2001**, *30*, 386.
- (11) Ward, M. D. *Chem. Soc. Rev.* **1995**, *24*, 121.
- (12) Cowan, D. O.; LeVanda, C.; Park, J.; Kaufman, F. *Acc. Chem. Res.* **1973**, *6*, 1.
- (13) Richardson, D. E.; Taube, H. *Coord. Chem. Rev.* **1984**, *60*, 107.
- (14) Robin, M. B.; Day, P. *Adv. Inorg. Chem. Radiochem.* **1967**, *10*, 247.
- (15) Nelsen, S. F. *Chem.—Eur. J.* **2000**, *6*, 581.
- (16) Hush, N. S. *Prog. Inorg. Chem.* **1967**, *8*, 391.
- (17) Nelsen, S. F.; Konradsson, A. E.; Weaver, M. N.; Telo, J. P. *J. Am. Chem. Soc.* **2003**, *125*, 12493.
- (18) Nelsen, S. F.; Weaver, M. N.; Zink, J. I.; Telo, J. P. *J. Am. Chem. Soc.* **2005**, *127*, 10611.
- (19) Nelsen, S. F.; Weaver, M. N.; Luo, Y.; Lockard, J. V.; Zink, J. I. *Chem. Phys.* **2006**, *324*, 195.
- (20) McConnell, H. M. *J. Chem. Phys.* **1961**, *35*, 508.
- (21) Creutz, C.; Newton, M. D.; Sutin, N. *J. Photochem.* **1994**, *82*, 47.
- (22) Wenger, O. S. *Acc. Chem. Res.* **2011**, *44*, 25.
- (23) Wenger, O. S. *Chem. Soc. Rev.* **2011**, doi: 10.1039/c1cs15044h.
- (24) Marcus, R. A.; Sutin, N. *Biochim. Biophys. Acta* **1985**, *811*, 265.
- (25) Chen, P. Y.; Meyer, T. J. *Chem. Rev.* **1998**, *98*, 1439.
- (26) Wudl, F.; Wobschal, D.; Hufnagel, E. *J. J. Am. Chem. Soc.* **1972**, *94*, 670.
- (27) Kaufman, F.; Cowan, D. O. *J. Am. Chem. Soc.* **1970**, *92*, 6198.
- (28) Shimada, K.; Shimozato, Y.; Szwarc, M. *J. Am. Chem. Soc.* **1975**, *97*, 5834.
- (29) Kosower, E. M.; Teuerstein, A. *J. Am. Chem. Soc.* **1976**, *98*, 1586.
- (30) Melby, L. R.; Mahler, W.; Mochel, W. E.; Harder, R. J.; Hertler, W. R.; Benson, R. E. *J. Am. Chem. Soc.* **1962**, *84*, 3374.
- (31) Mazur, S.; Sreekumar, C.; Schroeder, A. H. *J. Am. Chem. Soc.* **1976**, *98*, 6713.
- (32) Schroeder, A. H.; Mazur, S. *J. Am. Chem. Soc.* **1978**, *100*, 7339.
- (33) Huber, W.; Müllen, K. *Acc. Chem. Res.* **1986**, *19*, 300.
- (34) Gerson, F.; Wellauer, T.; Oliver, A. M.; Paddon-Row, M. N. *Helv. Chim. Acta* **1990**, *73*, 1586.
- (35) Gerson, F.; Huber, W.; Martin, W. B.; Caluwe, P.; Pepper, T.; Szwarc, M. *Helv. Chim. Acta* **1984**, *67*, 416.
- (36) Jozefiak, T. H.; Miller, L. L. *J. Am. Chem. Soc.* **1987**, *109*, 6560.
- (37) Miller, L. L.; Liberko, C. A. *Chem. Mater.* **1990**, *2*, 339.
- (38) Almlöf, J. E.; Feyereisen, M. W.; Jozefiak, T. H.; Miller, L. L. *J. Am. Chem. Soc.* **1990**, *112*, 1206.
- (39) Jozefiak, T. H.; Almlöf, J. E.; Feyereisen, M. W.; Miller, L. L. *J. Am. Chem. Soc.* **1989**, *111*, 4105.
- (40) Nelsen, S. F.; Ismagilov, R. F.; Trieber, D. A. *Science* **1997**, *278*, 846.
- (41) Nelsen, S. F.; Chang, H.; Wolff, J. J.; Adamus, J. *J. Am. Chem. Soc.* **1993**, *115*, 12276.
- (42) Nelsen, S. F.; Ismagilov, R. F.; Powell, D. R. *J. Am. Chem. Soc.* **1996**, *118*, 6313.
- (43) Nelsen, S. F.; Weaver, M. N.; Telo, J. P.; Lucht, B. L.; Barlow, S. *J. Org. Chem.* **2005**, *70*, 9326.
- (44) Kaim, W.; Schulz, A. *Angew. Chem., Int. Ed.* **1984**, *23*, 615.
- (45) Risko, C.; Barlow, S.; Coropceanu, V.; Halik, M.; Brédas, J. L.; Marder, S. R. *Chem. Commun.* **2003**, 194.
- (46) Zális, S.; Kaim, W. *Main Group Chem.* **2006**, *5*, 267.
- (47) Nelsen, S. F.; Weaver, M. N.; Telo, J. P. *J. Phys. Chem. A* **2007**, *111*, 10993.
- (48) Hoekstra, R. M.; Zink, J. I.; Telo, J. P.; Nelsen, S. F. *J. Phys. Org. Chem.* **2009**, *22*, 522.
- (49) Michaelis, L. *Chem. Rev.* **1935**, *16*, 243.
- (50) Rak, S. F.; Jozefiak, T. H.; Miller, L. L. *J. Org. Chem.* **1990**, *55*, 4794.
- (51) Bonvoisin, J.; Launay, J.-P.; Rovira, C.; Veciana, J. *Angew. Chem., Int. Ed.* **1994**, *33*, 2106.
- (52) Heckmann, A.; Lambert, C.; Goebel, M.; Wortmann, R. *Angew. Chem., Int. Ed.* **2004**, *43*, 5851.
- (53) Utamapanya, S.; Rajca, A. *J. Am. Chem. Soc.* **1991**, *113*, 9242.
- (54) Braterman, P. S.; Song, J. I. *J. Org. Chem.* **1991**, *56*, 4678.
- (55) Kosower, E. M.; Cotter, J. L. *J. Am. Chem. Soc.* **1964**, *86*, 5524.
- (56) Funston, A.; Kirby, J. P.; Miller, J. R.; Pospíšil, L.; Fiedler, J.; Hromadová, M.; Gál, M.; Pecka, J.; Valášek, M.; Zawada, Z.; Rempala, P.; Michl, J. *J. Phys. Chem. A* **2005**, *109*, 10862.
- (57) Würthner, F. *Chem. Commun.* **2004**, 1564.
- (58) Gosztola, D.; Niemczyk, M. P.; Svec, W.; Lukas, A. S.; Wasielewski, M. R. *J. Phys. Chem. A* **2000**, *104*, 6545.
- (59) Lahllil, K.; Moradpour, A.; Bowlas, C.; Menou, F.; Cassoux, P.; Bonvoisin, J.; Launay, J.-P.; Dive, G.; Dehareng, D. *J. Am. Chem. Soc.* **1995**, *117*, 9995.
- (60) Iyoda, M.; Hasegawa, M.; Miyake, Y. *Chem. Rev.* **2004**, *104*, 5085.
- (61) Roth, H. D. *Tetrahedron* **1986**, *42*, 6097.
- (62) Wurster, C. *Chem. Ber.* **1879**, *12*, 522.
- (63) Weitz, E. Z. *Elektrochem.* **1928**, *34*, 538.
- (64) Bruce, C. R.; Norberg, R. E.; Weissman, S. I. *J. Chem. Phys.* **1956**, *24*, 473.
- (65) Nelsen, S. F.; Tran, H. Q.; Nagy, M. A. *J. Am. Chem. Soc.* **1998**, *120*, 298.
- (66) De Boer, J. L.; Vos, A. *Acta Crystallogr.* **1972**, *B28*, 835.
- (67) Brouwer, A. M. *J. Phys. Chem. A* **1997**, *101*, 3626.
- (68) Cadogan, K. D.; Albrecht, A. C. *J. Phys. Chem.* **1969**, *73*, 1868.
- (69) Heller, E. *J. Acc. Chem. Res.* **1981**, *14*, 368.
- (70) Telo, J. P.; Nelsen, S. F.; Zhao, Y. *J. Phys. Chem. A* **2009**, *113*, 7730.
- (71) Nelsen, S. F.; Yunta, M. J. R. *J. Phys. Org. Chem.* **1994**, *7*, 55.
- (72) Grampp, G.; Jaenicke, W. *Ber. Bunsen-Ges. Phys. Chem.* **1991**, *95*, 904.
- (73) Szeghalmi, A. V.; Erdmann, M.; Engel, V.; Schmitt, M.; Amthor, S.; Kriegisch, V.; Nöll, G.; Stahl, R.; Lambert, C.; Leusser, D.; Stalke, D.; Zabel, M.; Popp, J. *J. Am. Chem. Soc.* **2004**, *126*, 7834.
- (74) Bailey, S. E.; Zink, J. I.; Nelsen, S. F. *J. Am. Chem. Soc.* **2003**, *125*, 5939.
- (75) Tutt, L.; Tannor, D.; Schindler, J.; Heller, E. J.; Zink, J. I. *J. Phys. Chem.* **1983**, *87*, 3017.
- (76) Lambert, C.; Nöll, G. *Synth. Met.* **2003**, *139*, 57.
- (77) Lambert, C.; Nöll, G. *J. Am. Chem. Soc.* **1999**, *121*, 8434.
- (78) Coropceanu, V.; Malagoli, M.; André, J. M.; Brédas, J. L. *J. Am. Chem. Soc.* **2002**, *124*, 10519.
- (79) Coropceanu, V.; Gruhn, N. E.; Barlow, S.; Lambert, C.; Durivage, J. C.; Bill, T. G.; Nöll, G.; Marder, S. R.; Brédas, J. L. *J. Am. Chem. Soc.* **2004**, *126*, 2727.
- (80) Nöll, G.; Avola, M. *J. Phys. Org. Chem.* **2006**, *19*, 238.
- (81) Benniston, A. C.; Harriman, A. *Chem. Soc. Rev.* **2006**, *35*, 169.
- (82) Hanss, D.; Wenger, O. S. *Eur. J. Inorg. Chem.* **2009**, 3778.
- (83) Ito, A.; Nakano, Y.; Urabe, M.; Kato, T.; Tanaka, K. *J. Am. Chem. Soc.* **2006**, *128*, 2948.
- (84) Nelsen, S. F.; Li, G.; Schultz, K. P.; Tran, H. Q.; Guzei, I. A.; Evans, D. H. *J. Am. Chem. Soc.* **2008**, *130*, 11620.

- (85) Jalilov, A. S.; Li, G. Q.; Nelsen, S. F.; Guzei, I. A.; Wu, Q. *J. Am. Chem. Soc.* **2010**, *132*, 6176.
- (86) Rosspeintner, A.; Griesser, M.; Matsumoto, I.; Teki, Y.; Li, G. Q.; Nelsen, S. F.; Gescheidt, G. *J. Phys. Chem. A* **2010**, *114*, 6487.
- (87) Rak, S. F.; Miller, L. L. *J. Am. Chem. Soc.* **1992**, *114*, 1388.
- (88) Lindeman, S. V.; Rosokha, S. V.; Sun, D.; Kochi, J. K. *J. Am. Chem. Soc.* **2002**, *124*, 843.
- (89) Rosokha, S. V.; Sun, D.-L.; Kochi, J. K. *J. Phys. Chem. A* **2002**, *106*, 2283.
- (90) Sun, D. L.; Lindeman, S. V.; Rathore, R.; Kochi, J. K. *J. Chem. Soc., Perkin Trans. 2* **2001**, 1585.
- (91) Weiss, E. A.; Ahrens, M. J.; Sinks, L. E.; Gusev, A. V.; Ratner, M. A.; Wasielewski, M. R. *J. Am. Chem. Soc.* **2004**, *126*, 5577.
- (92) Hüning, S.; Berenth, H. *Top. Curr. Chem.* **1980**, *92*, 1.
- (93) Paddon-Row, M. N.; Oliver, A. M.; Warman, J. M.; Smit, K. J.; Dehaas, M. P.; Oevering, H.; Verhoeven, J. W. *J. Phys. Chem.* **1988**, *92*, 6958.
- (94) Reimers, J. R.; Hush, N. S. *Inorg. Chem.* **1990**, *29*, 3686.
- (95) Coropceanu, V.; Lambert, C.; Nöll, G.; Brédas, J. L. *Chem. Phys. Lett.* **2003**, *373*, 153.
- (96) Davis, W. B.; Svec, W. A.; Ratner, M. A.; Wasielewski, M. R. *Nature* **1998**, *396*, 60.
- (97) Giacalone, F.; Segura, J. L.; Martín, N.; Guldi, D. M. *J. Am. Chem. Soc.* **2004**, *126*, 5340.
- (98) Barlow, S.; Risko, C.; Chung, S. J.; Tucker, N. M.; Coropceanu, V.; Jones, S. C.; Levi, Z.; Brédas, J. L.; Marder, S. R. *J. Am. Chem. Soc.* **2005**, *127*, 16900.
- (99) Barlow, S.; Risko, C.; Coropceanu, V.; Tucker, N. M.; Jones, S. C.; Levi, Z.; Khrustalev, V. N.; Antipin, M. Y.; Kinnibrugh, T. L.; Timofeeva, T.; Marder, S. R.; Brédas, J. L. *Chem. Commun.* **2005**, 764.
- (100) Heckmann, A.; Amthor, S.; Lambert, C. *Chem. Commun.* **2006**, 2959.
- (101) Amthor, S.; Lambert, C. *J. Phys. Chem. A* **2006**, *110*, 1177.
- (102) Kattnig, D. R.; Mladenova, B.; Grampp, G.; Kaiser, C.; Heckmann, A.; Lambert, C. *J. Phys. Chem. C* **2009**, *113*, 2983.
- (103) Zhou, G.; Baumgarten, M.; Müllen, K. *J. Am. Chem. Soc.* **2007**, *129*, 12211.
- (104) Zhou, G.; Baumgarten, M.; Müllen, K. *J. Am. Chem. Soc.* **2008**, *130*, 12477.
- (105) Roncali, J. *Chem. Rev.* **1992**, *92*, 711.
- (106) Lacroix, J. C.; Chane-Ching, K. I.; Maquère, F.; Maurel, F. *J. Am. Chem. Soc.* **2006**, *128*, 7264.
- (107) Odom, S. A.; Lancaster, K.; Beverina, L.; Lefler, K. M.; Thompson, N. J.; Coropceanu, V.; Brédas, J. L.; Marder, S. R.; Barlow, S. *Chem.—Eur. J.* **2007**, *13*, 9637.
- (108) Holzapfel, M.; Lambert, C.; Selinka, C.; Stalke, D. *J. Chem. Soc., Perkin Trans. 2* **2002**, 1553.
- (109) Knorr, A.; Daub, J. *Angew. Chem., Int. Ed.* **1997**, *36*, 2817.
- (110) Nelsen, S. F.; Konradsson, A. E.; Teki, Y. *J. Am. Chem. Soc.* **2006**, *128*, 2902.
- (111) Nelsen, S. F.; Weaver, M. N.; Telo, J. P. *J. Am. Chem. Soc.* **2007**, *129*, 7036.
- (112) Pettersson, K.; Wiberg, J.; Ljungdahl, T.; Mårtensson, J.; Albinsson, B. *J. Phys. Chem. A* **2006**, *110*, 319.
- (113) Nelsen, S. F. *Adv. Phys. Org. Chem.* **2006**, *41*, 183.
- (114) Manner, V. W.; Markle, T. F.; Freudenthal, J. H.; Roth, J. P.; Mayer, J. M. *Chem. Commun.* **2008**, 256.
- (115) Jones, S. C.; Coropceanu, V.; Barlow, S.; Kinnibrugh, T.; Timofeeva, T.; Brédas, J. L.; Marder, S. R. *J. Am. Chem. Soc.* **2004**, *126*, 11782.
- (116) Schull, T. L.; Kushmerick, J. G.; Patterson, C. H.; George, C.; Moore, M. H.; Pollack, S. K.; Shashidhar, R. *J. Am. Chem. Soc.* **2003**, *125*, 3202.
- (117) Mayor, M.; Buschel, M.; Fromm, K. M.; Lehn, J. M.; Daub, J. *Chem.—Eur. J.* **2001**, *7*, 1266.
- (118) Nelsen, S. F.; Weaver, M. N.; Konradsson, A. E.; Telo, J. P.; Clark, T. *J. Am. Chem. Soc.* **2004**, *126*, 15431.
- (119) Nelsen, S. F.; Konradsson, A. E.; Telo, J. P. *J. Am. Chem. Soc.* **2005**, *127*, 920.
- (120) Rovira, C.; Ruiz-Molina, D.; Elsner, O.; Vidal-Gancedo, J.; Bonvoisin, J.; Launay, J.-P.; Veciana, J. *Chem.—Eur. J.* **2001**, *7*, 240.
- (121) Lloveras, V.; Vidal-Gancedo, J.; Ruiz-Molina, D.; Figueira-Duarte, T. M.; Nierengarten, J.-F.; Veciana, J.; Rovira, C. *Faraday Discuss.* **2006**, *131*, 291.
- (122) Yano, M.; Aoyama, K.; Ishida, Y.; Tatsumi, M.; Sato, K.; Shiomi, D.; Takui, T. *Polyhedron* **2003**, *22*, 2003.
- (123) Biaso, F.; Geoffroy, M.; Canadell, E.; Auban-Senzier, P.; Levillain, E.; Fourmigué, M.; Avarvari, N. *Chem.—Eur. J.* **2007**, *13*, 5394.
- (124) Nelsen, S. F.; Ismagilov, R. F.; Powell, D. R. *J. Am. Chem. Soc.* **1997**, *119*, 10213.
- (125) Nelsen, S. F.; Ismagilov, R. F.; Gentile, K. E.; Powell, D. R. *J. Am. Chem. Soc.* **1999**, *121*, 7108.
- (126) Nelsen, S. F.; Schultz, K. P.; Telo, J. P. *J. Phys. Chem. A* **2008**, *112*, 12622.
- (127) Nishiumi, T.; Nomura, Y.; Chimoto, Y.; Higuchi, M.; Yamamoto, K. *J. Phys. Chem. B* **2004**, *108*, 7992.
- (128) Nishiumi, T.; Nomura, Y.; Higuchi, M.; Yamamoto, K. *Chem. Phys. Lett.* **2003**, *378*, 18.
- (129) Hirao, Y.; Urabe, M.; Ito, A.; Tanaka, K. *Angew. Chem., Int. Ed.* **2007**, *46*, 3300.
- (130) Nelsen, S. F.; Li, G. Q.; Konradsson, A. *Org. Lett.* **2001**, *3*, 1583.
- (131) Nelsen, S. F.; Ramm, M. T.; Wolff, J. J.; Powell, D. R. *J. Am. Chem. Soc.* **1997**, *119*, 6863.
- (132) Lambert, C.; Nöll, G.; Schelter, J. *Nat. Mater.* **2002**, *1*, 69.
- (133) Lambert, C.; Amthor, S.; Schelter, J. *J. Phys. Chem. A* **2004**, *108*, 6474.
- (134) Walther, M. E.; Wenger, O. S. *ChemPhysChem* **2009**, *10*, 1203.
- (135) Kilså, K.; Kajanus, J.; Macpherson, A. N.; Mårtensson, J.; Albinsson, B. *J. Am. Chem. Soc.* **2001**, *123*, 3069.
- (136) Miller, S. E.; Lukas, A. S.; Marsh, E.; Bushard, P.; Wasielewski, M. R. *J. Am. Chem. Soc.* **2000**, *122*, 7802.
- (137) Albinsson, B.; Eng, M. P.; Pettersson, K.; Winters, M. U. *Phys. Chem. Chem. Phys.* **2007**, *9*, 5847.
- (138) Hanss, D.; Walther, M. E.; Wenger, O. S. *Chem. Commun.* **2010**, *46*, 7034.
- (139) Nelsen, S. F.; Ismagilov, R. F.; Powell, D. R. *J. Am. Chem. Soc.* **1998**, *120*, 1924.
- (140) Lambert, C.; Risko, C.; Coropceanu, V.; Schelter, J.; Amthor, S.; Gruhn, N. E.; Durivage, J. C.; Brédas, J. L. *J. Am. Chem. Soc.* **2005**, *127*, 8508.
- (141) Lancaster, K.; Odom, S. A.; Jones, S. C.; Thayumanavan, S.; Marder, S. R.; Brédas, J. L.; Coropceanu, V.; Barlow, S. *J. Am. Chem. Soc.* **2009**, *131*, 1717.
- (142) Lambert, C.; Nöll, G. *J. Chem. Soc., Perkin Trans. 2* **2002**, 2039.
- (143) Walther, M. E.; Grilj, J.; Hanss, D.; Vauthey, E.; Wenger, O. S. *Eur. J. Inorg. Chem.* **2010**, 4843.
- (144) Nöll, G.; Amthor, S.; Avola, M.; Lambert, C.; Daub, J. *J. Phys. Chem. C* **2007**, *111*, 3512.
- (145) Lambert, C.; Nöll, G.; Zabel, M.; Hampel, F.; Schmälzlin, E.; Bräuchle, C.; Meerholz, K. *Chem.—Eur. J.* **2003**, *9*, 4232.
- (146) Nöll, G.; Avola, M.; Lynch, M.; Daub, J. *J. Phys. Chem. C* **2007**, *111*, 3197.
- (147) Dumur, F.; Gautier, N.; Gallego-Planas, N.; Sahin, Y.; Levillain, E.; Mercier, N.; Hudhomme, P.; Masino, M.; Girlando, A.; Lloveras, V.; Vidal-Gancedo, J.; Veciana, J.; Rovira, C. *J. Org. Chem.* **2004**, *69*, 2164.
- (148) Gautier, N.; Dumur, F.; Lloveras, V.; Vidal-Gancedo, J.; Veciana, J.; Rovira, C.; Hudhomme, P. *Angew. Chem., Int. Ed.* **2003**, *42*, 2765.
- (149) Liberko, C. A.; Rak, S. F.; Miller, L. L. *J. Org. Chem.* **1992**, *57*, 1379.
- (150) Sedó, J.; Ruiz, D.; Vidal-Gancedo, J.; Rovira, C.; Bonvoisin, J.; Launay, J.-P.; Veciana, J. *Adv. Mater.* **1996**, *8*, 748.
- (151) Bonvoisin, J.; Launay, J.-P.; Van der Auweraer, M.; De Schryver, F. C. *J. Phys. Chem.* **1994**, *98*, 5052.

- (152) Bonvoisin, J.; Launay, J.-P.; Van der Auweraer, M.; De Schryver, F. C. *J. Phys. Chem.* **1996**, *100*, 18006.
- (153) Bonvoisin, J.; Launay, J.-P.; Verbouwe, W.; Van der Auweraer, M.; De Schryver, F. C. *J. Phys. Chem.* **1996**, *100*, 17079.
- (154) Stickley, K. R.; Blackstock, S. C. *Tetrahedron Lett.* **1995**, *36*, 1585.
- (155) Hirao, Y.; Ito, A.; Tanaka, K. *J. Phys. Chem. A* **2007**, *111*, 2951.
- (156) Lambert, C.; Nöll, G.; Hampel, F. *J. Phys. Chem. A* **2001**, *105*, 7751.
- (157) Kumar, K.; Lin, Z.; Waldeck, D. H.; Zimmt, M. B. *J. Am. Chem. Soc.* **1996**, *118*, 243.
- (158) Lambert, C.; Nöll, G. *Angew. Chem., Int. Ed.* **1998**, *37*, 2107.
- (159) Sun, D.; Rosokha, S. V.; Kochi, J. K. *Angew. Chem., Int. Ed.* **2005**, *44*, 5133.
- (160) Lambert, C.; Nöll, G. *Chem.—Eur. J.* **2002**, *8*, 3467.
- (161) Yan, X. Z.; Pawlas, J.; Goodson, T.; Hartwig, J. F. *J. Am. Chem. Soc.* **2005**, *127*, 9105.
- (162) Wu, J. S.; Baumgarten, M.; Debije, M. G.; Warman, J. M.; Müllen, K. *Angew. Chem., Int. Ed.* **2004**, *43*, 5331.
- (163) Nelsen, S. F.; Pladziewicz, J. R. *Acc. Chem. Res.* **2002**, *35*, 247.
- (164) Nelsen, S. F.; Trieber, D. A.; Nagy, M. A.; Konradsson, A.; Halfen, D. T.; Splan, K. A.; Pladziewicz, J. R. *J. Am. Chem. Soc.* **2000**, *122*, 5940.
- (165) Nelsen, S. F.; Weaver, M. N.; Pladziewicz, J. R.; Ausman, L. K.; Jentzsch, T. L.; O'Konek, J. J. *J. Phys. Chem. A* **2006**, *110*, 11665.
- (166) Sun, D.-L.; Rosokha, S. V.; Lindeman, S. V.; Kochi, J. K. *J. Am. Chem. Soc.* **2003**, *125*, 15950.
- (167) Sun, D.; Rosokha, S. V.; Kochi, J. K. *J. Am. Chem. Soc.* **2004**, *126*, 1388.
- (168) Kochi, J. K.; Rathore, R.; Le Maguères, P. *J. Org. Chem.* **2000**, *65*, 6826.
- (169) Rathore, R.; Kumar, A. S.; Lindeman, S. V.; Kochi, J. K. *J. Org. Chem.* **1998**, *63*, 5847.
- (170) Le Maguères, P.; Lindeman, S. V.; Kochi, J. K. *J. Chem. Soc., Perkin Trans. 2* **2001**, 1180.
- (171) Le Maguerès, P.; Lindeman, S. V.; Kochi, J. K. *Org. Lett.* **2000**, *2*, 3567.
- (172) Rosokha, S. V.; Newton, M. D.; Head-Gordon, M.; Kochi, J. K. *Chem. Phys.* **2006**, *324*, 117.
- (173) Rosokha, S. V.; Kochi, J. K. *J. Am. Chem. Soc.* **2007**, *129*, 828.
- (174) Spanggaard, H.; Prehn, J.; Nielsen, M. B.; Levillain, E.; Allain, M.; Becher, J. *J. Am. Chem. Soc.* **2000**, *122*, 9486.
- (175) Chiang, P.-T.; Chen, N.-C.; Lai, C.-C.; Chiu, S.-H. *Chem.—Eur. J.* **2008**, *14*, 6546.
- (176) Lyskawa, J.; Sallé, M.; Balandier, J. Y.; Le Derf, F.; Levillain, E.; Allain, M.; Viel, P.; Palacin, S. *Chem. Commun.* **2006**, 2233.
- (177) Ziganshina, A. Y.; Ko, Y. H.; Jeon, W. S.; Kim, K. *Chem. Commun.* **2004**, 806.
- (178) Yoshizawa, M.; Kumazawa, K.; Fujita, M. *J. Am. Chem. Soc.* **2005**, *127*, 13456.
- (179) Saad, A.; Barrière, F.; Levillain, E.; Vanthuyne, N.; Jeannin, O.; Fourmigüé, M. *Chem.—Eur. J.* **2010**, *16*, 8020.
- (180) Liberko, C. A.; Miller, L. L.; Katz, T. J.; Liu, L. B. *J. Am. Chem. Soc.* **1993**, *115*, 2478.
- (181) Yang, B. W.; Liu, L. B.; Katz, T. J.; Liberko, C. A.; Miller, L. L. *J. Am. Chem. Soc.* **1991**, *113*, 8993.
- (182) Dinolfo, P. H.; Williams, M. E.; Stern, C. L.; Hupp, J. T. *J. Am. Chem. Soc.* **2004**, *126*, 12989.
- (183) Dinolfo, P. H.; Hupp, J. T. *J. Am. Chem. Soc.* **2004**, *126*, 16814.
- (184) Dinolfo, P. H.; Coropceanu, V.; Brédas, J. L.; Hupp, J. T. *J. Am. Chem. Soc.* **2006**, *128*, 12592.
- (185) Fürderer, P.; Gerson, F.; Heinzer, J.; Mazur, S.; Ohya-Nishiguchi, H.; Schroeder, A. H. *J. Am. Chem. Soc.* **1979**, *101*, 2275.
- (186) Elliott, C. M.; Derr, D. L.; Matyushov, D. V.; Newton, M. D. *J. Am. Chem. Soc.* **1998**, *120*, 11714.
- (187) Nelsen, S. F.; Blackstock, S. C.; Haller, K. J. *Tetrahedron* **1986**, *42*, 6101.
- (188) Nelsen, S. F.; Chen, L. J.; Ramm, M. T.; Voy, G. T.; Powell, D. R.; Accola, M. A.; Seehafer, T. R.; Sabelko, J. J.; Pladziewicz, J. R. *J. Org. Chem.* **1996**, *61*, 1405.
- (189) Nelsen, S. F.; Blackstock, S. C.; Kim, Y. *J. Am. Chem. Soc.* **1987**, *109*, 677.
- (190) Nelsen, S. F. *J. Am. Chem. Soc.* **1996**, *118*, 2047.
- (191) Nelsen, S. F.; Adamus, J.; Wolff, J. J. *J. Am. Chem. Soc.* **1994**, *116*, 1589.
- (192) Nelsen, S. F.; Trieber, D. A.; Wolff, J. J.; Powell, D. R.; Rogers-Crowley, S. *J. Am. Chem. Soc.* **1997**, *119*, 6873.
- (193) Nelsen, S. F.; Trieber, D. A.; Ismagilov, R. F.; Teki, Y. *J. Am. Chem. Soc.* **2001**, *123*, 5684.
- (194) Nelsen, S. F.; Tran, H. Q. *J. Phys. Chem. A* **1999**, *103*, 8139.
- (195) Gutmann, V. *Coord. Chem. Rev.* **1976**, *18*, 225.
- (196) Heckmann, A.; Lambert, C. *J. Am. Chem. Soc.* **2007**, *129*, 5515.
- (197) Amthor, S.; Lambert, C.; Dümmler, S.; Fischer, I.; Schelter, J. *J. Phys. Chem. A* **2006**, *110*, 5204.
- (198) Hosoi, H.; Mori, Y.; Masuda, Y. *Chem. Lett.* **1998**, 177.
- (199) Nelsen, S. F.; Ismagilov, R. F. *J. Phys. Chem. A* **1999**, *103*, 5373.
- (200) Nelsen, S. F.; Konradsson, A. E.; Clennan, E. L.; Singleton, J. *Org. Lett.* **2004**, *6*, 285.
- (201) Low, P. J.; Paterson, M. A. J.; Puschmann, H.; Goeta, A. E.; Howard, J. A. K.; Lambert, C.; Cherryman, J. C.; Tackley, D. R.; Leeming, S.; Brown, B. *Chem.—Eur. J.* **2004**, *10*, 83.
- (202) Cordes, M.; Giese, B. *Chem. Soc. Rev.* **2009**, *38*, 892.
- (203) Gray, H. B.; Winkler, J. R. *Proc. Natl. Acad. Sci. U. S. A.* **2005**, *102*, 3534.
- (204) Bublitz, G. U.; Boxer, S. G. *Annu. Rev. Phys. Chem.* **1997**, *48*, 213.
- (205) Nelsen, S. F.; Newton, M. D. *J. Phys. Chem. A* **2000**, *104*, 10023.